Vol. 123 Nos. 1-6

November-December 1958

PROCEEDINGS OF THE ACADEMY OF SCIENCES

OF THE USSR

(DOKLADY AKADEMII NAUK SSSR)

Physical Chemistry Section

A publication of the Academy of Sciences of the USSR

IN ENGLISH TRANSLATION

Year and issue of first translation:
Vol. 112, Nos. 1-6 Jan.-Feb. 1957

Annual subscription	*$160.00*
Single issue	*35.00*

Copyright 1959

CONSULTANTS BUREAU INC.
227 W. 17th ST., NEW YORK 11, N. Y.

A complete copy of any paper in this issue may be purchased from the publisher for $5.00

Note: The sale of photostatic copies of any portion of this copyright translation is expressly prohibited by the copyright owners.

Printed in the United States of America

PROCEEDINGS OF THE ACADEMY OF SCIENCES OF THE USSR

Physical Chemistry Section

Volume 123, Numbers 1-6 November-December 1958

CONTENTS

	PAGE	RUSS. ISSUE	RUSS. PAGE
A Study of the Reactions Involved in the Formation of Hydrogen Peroxide by the Oxidation of 2-Ethylhydroquinone and Isopropanol Using an Isotope Method. A. I. Brodskii, V. I. Franchuk, M. M. Aleksanskii and V. A. Lunenok-Burmakina	765	1	117
The Mass Spectra of Large Molecules. M. V. Gur'ev, M. V. Tikhomirov and N. N. Tunitskii	769	1	120
The Rate of Degenerative Chain Branching in the Oxidation of n-Decane. D. G. Knorre, Z. K. Maizus and N. M. Emanuel'	773	1	123
The Radiation Vulcanization of Polyamides (Anide G-669). S. A. Pavlova, S. R. Rafikov and B. L. Tsetlin	777	1	127
The Structure of Water. I. Z. Fisher and V. K. Prokhorenko	781	1	131
The Molecular Orbitals of Radicals with Nonalternating Rings. M. E. Diatkina, S. N. Dobriakov and E. M. Shustorovich	783	2	308
Polarography at High Pressures. S. G. Mairanovskii, M. G. Gonikberg and A. A. Opekunov	787	2	312
The Adsorption of Hydrocarbons at Raised Temperatures. I. V. Smirnova and K. V. Topchieva	791	2	316
The Extraction of Sulfide Inclusions from Molten Slags by Means of an Electric Field. V. V. Khlynov and O. A. Esin	795	2	320
The Part Played by the Emulsifier in the Oxidation-Reduction Initiation of Emulsion Polymerization. A. I. Iurzhenko, N. Ia. Ivanova and V. D. Enal'ev	799	2	324
The Distribution of Impurity in a Monocrystal of Metallic Zinc Possessing a Honeycomb-Like Substructure. M. Voloukh and I. B. Borovskii	803	3	490
The Behavior of the Antimonides of Aluminum, Gallium and Indium in the Liquid State. V. M. Glazov and A. A. Vertman	805	3	492
Theory of the Fluctuations in Crystal Sensitivity in Nuclear Photographic Emulsions. G. I. Zel'tser and A. L. Kartuzhanskii	809	3	495
The Relationship Between the Chemisorptive Properties of Metals and the Structure of the Specimens. N. N. Kavtaradze	813	3	498
The Role of Chain Branching and Rupture in Thermal Chain Flame Propagation. L. A. Lovachev	817	3	501

CONTENTS (continued)

	PAGE	RUSS. ISSUE	RUSS. PAGE
Concerning Certain Solubilization Rules for Albuminous Systems. V. A. Pchelin, V. N. Izmailova and K. T. Ochurova	821	3	505
Details of the Kinetics of Supersaturation in Aqueous Calcium Oxide Suspensions. E. E. Segalova, S. I. Kontorovich and P. A. Rebinder	825	3	509
An Experimental Investigation of the Stress Distribution During Rupture of Polymers. V. E. Gul' and I. M. Chernin	829	4	713
The Dehydration and Rehydration of Quartz Surfaces. S. P. Zhdanov	833	4	716
The Relation Between the Surface Structures and the Phase Compositions of Electrolytic Deposits of Alloys. Iu. M. Polukarov and V. V. Bondar'	837	4	720
The Effect of the Radioactivity of Barium Sulfate on its Sorptional Properties. Vikt. I. Spitsyn and V. V. Gromov	841	4	722
The Solubility of Finely Pulverized Quartz in Water. G. S. Khodakov and E. R. Plutsis	845	4	725
Thermodynamic Properties of Alloys of Copper and Palladium. A. A. Vecher and Ia. I. Gerasimov	849	5	868
Formation of Free Radicals in Bimolecular Reactions. Reaction Between Triphenylchloromethane and Ethyllithium. F. S. D'iachkovskii, N. N. Bubnov and A. E. Shilov	851	5	870
Retention of Latent Image and Sensitivity in Granular Photographic Emulsions Stabilized with Triethanolamine. A. P. Zhdanov, A. L. Kartuzhanskii, I. V. Ryzhkova and L. I. Shur	855	5	874
The Effects of Electronegative Elements on the Catalytic Action of Silver on the Oxidation of Ethylene. A. I. Kurilenko, N. V. Kul'kova, V. E. Ostrovskii and M. I. Temkin	859	5	878
Investigation of Free Radicals Formed in Solid Bodies in the Process of Irradiation with Fast Electrons. Iu. N. Molin, A. T. Koritskii, N. Ia. Buben and V. V. Voevodskii	863	5	882
Oxidation of Divalent Vanadium at a Germanium Anode. Iu. V. Pleskov and B. N. Kabanov	865	5	884
The Problem of the Semiconductive Properties of Iron-Copper Synthesis Catalysts and Activation by the Action of Alkaline Promoters. I. B. Rapoport and V. N. Kulakov	869	5	887
The Nature of the Acidity of Aluminosilicate Cracking Catalysts. K. V. Topchieva and I. F. Moskovskaia	873	5	891
The Effects of Ions of Tetravalent Titanium on the Electrochemical Properties and Corrosion Behavior of Titanium. V. V. Andreeva and V. I. Kazarin	877	6	1048
Effect of Calcium Chloride on the Process of Structure Formation in Aqueous Suspensions of Tricalcium Aluminates. E. P. Andreeva, E. E. Segalova and E. E. Volynets	881	6	1052

CONTENTS (continued)

	PAGE	RUSS. ISSUE	RUSS. PAGE
Kinetics of the Oxidation of Coal with Nitric Acid. V. S. Veselovskii and G. L. Orleanskaia	885	6	1056
Differential Heats of Adsorption of Water Vapor on Silica Gels of Different Degrees of Hydration. T. S. Egorova, V. F. Kiselev and K. G. Krasil'nikov	889	6	1060
Measurement of the Vapor Pressures of Cobalt and Nickel. An. N. Nesmeianov and De Dyk Man	893	6	1064
The Surface Activities of Liquid Metallic Coatings and their Effects on the Strengths of Metals. N. V. Pertsov and P. A. Rebinder	897	6	1068
Investigation of the Saturation Vapor Pressures of Some Thallium Compounds. M. G. Shakhtakhtinskii and A. A. Kuliev	901	6	1071
Spontaneous Thinning of Thin Double-Sided Liquid Films. A. Sheludko	905	6	1074
Tables of Contents for Volumes 118-123, 1958	911		
Author Index for Volumes 118-123, 1958	926		

A STUDY OF THE REACTIONS INVOLVED IN THE FORMATION OF HYDROGEN PEROXIDE BY THE OXIDATION OF 2-ETHYLHYDROQUINONE AND ISOPROPANOL USING AN ISOTOPE METHOD

Corresponding Member AN SSSR A. I. Brodskii, V. I. Franchuk, M. M. Aleksanskii and V. A. Lunenok-Burmakina

No study has as yet been made of the mechanism of the reactions which form the basis of industrial methods for the preparation of hydrogen peroxide by the oxidation of 2-ethylanthrahydroquinone (or its derivatives) and isopropyl alcohol with elementary oxygen [1]. In order to throw some light on this problem, we have made a study of the reaction using an isotope method.

1. The oxidation of 2-ethylanthrahydroquinone and tetrahydro-2-ethylanthrahydroquinone was carried out in conditions similar to those employed in industry. The quinone sample was introduced into a vessel with a mixture of benzene and octyl alcohol to which Raney nickel had been added. Dry hydrogen, free from oxygen, was passed with constant shaking through the mixture for 20-40 minutes. When hydrogenation was complete the solution had a pale-yellow color with a faint opalescence. The solution was filtered under excess pressure of H_2 to remove the catalyst and collected in a similar evacuated vessel, through which oxygen, enriched with the heavy isotope O^{18}, was passed with shaking for 30-40 minutes. When oxidation was complete the hydrogen peroxide was extracted from the homogeneous solution with water and decomposed with potassium permanganate in vacuo. The isotopic composition of the oxygen liberated in this process was determined using a mass-spectrometer.

The results of experiments with 2-ethylanthraquinone, tetrahydro-2-ethylanthrahydroquinone and a mixture (1:1) of both (working mixture) are given in Table 1. It can be seen from this Table that the oxygen in the hydrogen peroxide formed comes entirely from the elementary oxygen used for the oxidation and not from the oxygen of the hydroxyl groups in the anthrahydroquinone or the alcohol.

From the effect of the pH on oxidation kinetics, Weissberger and co-workers [2] concluded that similar reactions involving hydroquinone derivatives take place with transfer of electrons from the hydroquinone anion to oxygen, for example in the case of durohydroquinone:

$$(CH_3)_4C_6(OH)_2 \rightleftharpoons (CH_3)_4C_6O_2^{\cdot\cdot} \xrightarrow{+O_2} (CH_3)_4C_6O_2 + O_2^{\cdot\cdot}.$$

In the case of the reactions which we have studied, such a mechanism is unlikely, since the reactions proceed readily in a neutral medium, and also is the nonionizing solvent benzene. The intermediate forma- of trans-annular peroxides must also be excluded, since the fairly high stability of these compounds [3] excludes the observed rapid course of the reaction. The data which we have obtained are compatible with mechanisms involving the intermediate formation of hydroperoxides or radicals with the removal of a proton from the hydroxyl group of the anthrahydroquinone.

In order to examine still further the mechanism of the reactions under study, we introduced deuterium into the hydroxyl groups of the 2-ethylanthrahydroquinone by exchange with methyl alcohol CH_3OD, in which the deuterium content in the hydroxyl was equivalent to an excess density of water of 12450 γ (approximately 11.6% D). The alcohol was distilled off and 0.8 g of the dry, heavy 2-ethylanthrahydroquinone in 25 ml benzene (which does not exchange hydrogen with anthrahydroquinone) oxidized for 5 hours by the passage of oxygen

TABLE 1

Substance	Weight of sample in g	Solvent		O^{18} content as % excess above natural O	
		benzene	octanol	in the original O_2	in the O_2 liberated from the H_2O_2
2-Ethylanthrahydroquinone (I)	1,8	25	25	0,966	1,04
Tetrahydro-2-ethylanthrahydroquinone (II)	1,8	25	30	0,966	0,956
Mixture of (I) and (II)	3,2	40	50	0,936	0,936
2-Ethylanthrahydroquinone*	1,8	25	25	0	0
Isopropyl alcohol	3,2	—	—	0,936	0,936

*In this experiment 2 ml of water containing 3 mole % O^{18} was added to the reaction mixture before the oxidation.

containing no excess O^{18}. The hydrogen peroxide formed was extracted with 1.5 g water, with which it exchanges its deuterium very rapidly. After purification this water had an excess density of 448 γ, which, taking into account the dilution, corresponds to a deuterium content in the hydrogen peroxide equivalent to 11580 γ (or 10.8% D). The benzene was distilled off and the dry anthraquinone ignited to yield water with an excess density of 18 γ, i.e., it was practically free from deuterium. Thus the hydrogen in the hydrogen peroxide obtained is derived entirely from the hydroxyl groups of the 2-ethylanthrahydroquinone. These data also enable us to exclude the intermediate formation of hydroperoxides with the peroxide group attached in any position other than the 9 or 10 positions, since such a mechanism would lead to the transfer of deuterium into the nucleus and to the transfer of only 50% of the hydroxyl deuterium to the peroxide formed, for example:

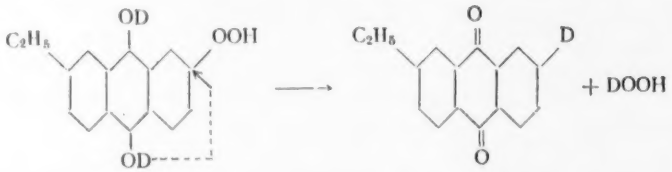

The formation of hydroperoxides in positions 9 and 10 does not contradict our observations. Taking into account the available data on the mechanism of other reactions of peroxide compounds which have been studied in detail [1], we consider that the most probable mechanism involves the formation of radicals according to the scheme:

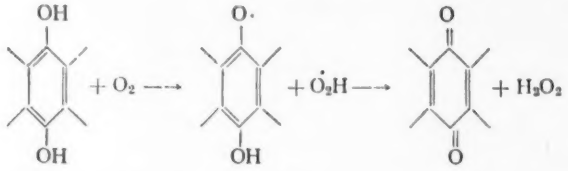

with the possible intermediate formation of the 9- or 10-hydroperoxide:

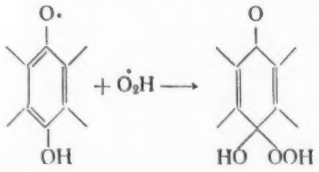

Geake and Lemon [4] have shown by potentiometric titration that the oxidation of anthraquinone and its derivatives by iron ferricyanide takes place in two stages with the intermediate formation of the semiquinone. In this study, however, the oxidation was carried out in alkaline medium.

At our request, V. V. Voevodskii, together with N. N. Bubnov and N. I. Tikhomirova, recorded the electron paramagnetic resonance spectrum of the 2-ethylanthrahydroquinone solution during its oxidation. The semiquinone radical was not detected, which is possibly explained by its low stationary concentration. At high concentrations in alkaline medium a clearly defined semiquinone radical-ion spectrum was obtained. In this case, however, its formation may also be ascribed to the reaction:

$$C_2H_5C_{14}H_7O_2'' + C_2H_5C_{14}H_7O_2 \rightleftharpoons 2C_2H_5C_{14}H_7\dot{O}_2''.$$

The study of the paramagnetic resonance spectra of the reacting systems being considered in this work will be continued.

2. It is known that a number of secondary alcohols are readily oxidized by elementary oxygen with the formation of ketones and hydrogen peroxide in good yield. One practical method for preparing the latter is by the oxidation of isopropyl alcohol in this way [5]. We carried out this reaction with 3.2 g of alcohol, distilled into an evacuated ampoule of molybdenum glass which had been given a prolonged treatment beforehand with boric acid and perhydrol. The ampoule was filled up with oxygen, enriched with O^{18}, at one atmosphere and heated to 100° for 20 hours. The yield of hydrogen peroxide amounted to 48%. Its isotopic composition is given in Table 1. In this case also, all the oxygen of the hydrogen peroxide is derived from the elementary oxygen and not from the oxygen of the alcoholic hydroxyl. The mechanism of this reaction is evidently analogous to that outlined above for the oxidation of anthrahydroquinone, involving O_2H radicals.

Some further indications of the course of the reactions involved in the oxidation of isopropyl alcohol are given by the work of Westheimer and Nicolaides [6]. They studied the oxidation of this alcohol with chromic acid and found a considerable kinetic isotopic effect when the secondary hydrogen was replaced by deuterium. It follows from this that in the slow stage of the reaction, removal of the secondary hydrogen atom takes place, and not removal of the hydroxyl hydrogen. All the data given above agree with the following two-stages mechanism:

$$(CH_3)_2CH(OH) + O_2 \rightarrow (CH_3)_2\dot{C} - OH + \dot{O}_2H \rightarrow (CH_3)_2C = O + H_2O.$$

with the possible intermediate formation of a hydroxy-hydroperoxide.

LITERATURE CITED

[1] W. C. Schumb, C. N. Satterfield and R. L. Wentworth, Hydrogen Peroxide, N.Y. – London, 1955.

[2] T. H. James and R. B. Weissberger, J. Am. Chem. Soc. 60, 98 (1938).

[3] A. V. Tobolsky and R. B. Mesrobian, Organic Peroxides, N. Y. – London, 1954.

[4] A. Geake and J. T. Lemon, Trans. Farad. Soc. 38, 1409 (1938).

[5] C. R. Harris, US Pat. 2,479,111, 1946; N. V. de Bataafsche Petroleum Maatschappij. Brit. Pat. 709,339, 1954.

[6] F. H. Westheimer and N. Nicolaides, J. Am. Chem. Soc. 71, 25 (1949).

L. V. Pisarzhevskii Institute of Physical Chemistry,
Ukr.SSR Academy of Sciences

Received June 21, 1958

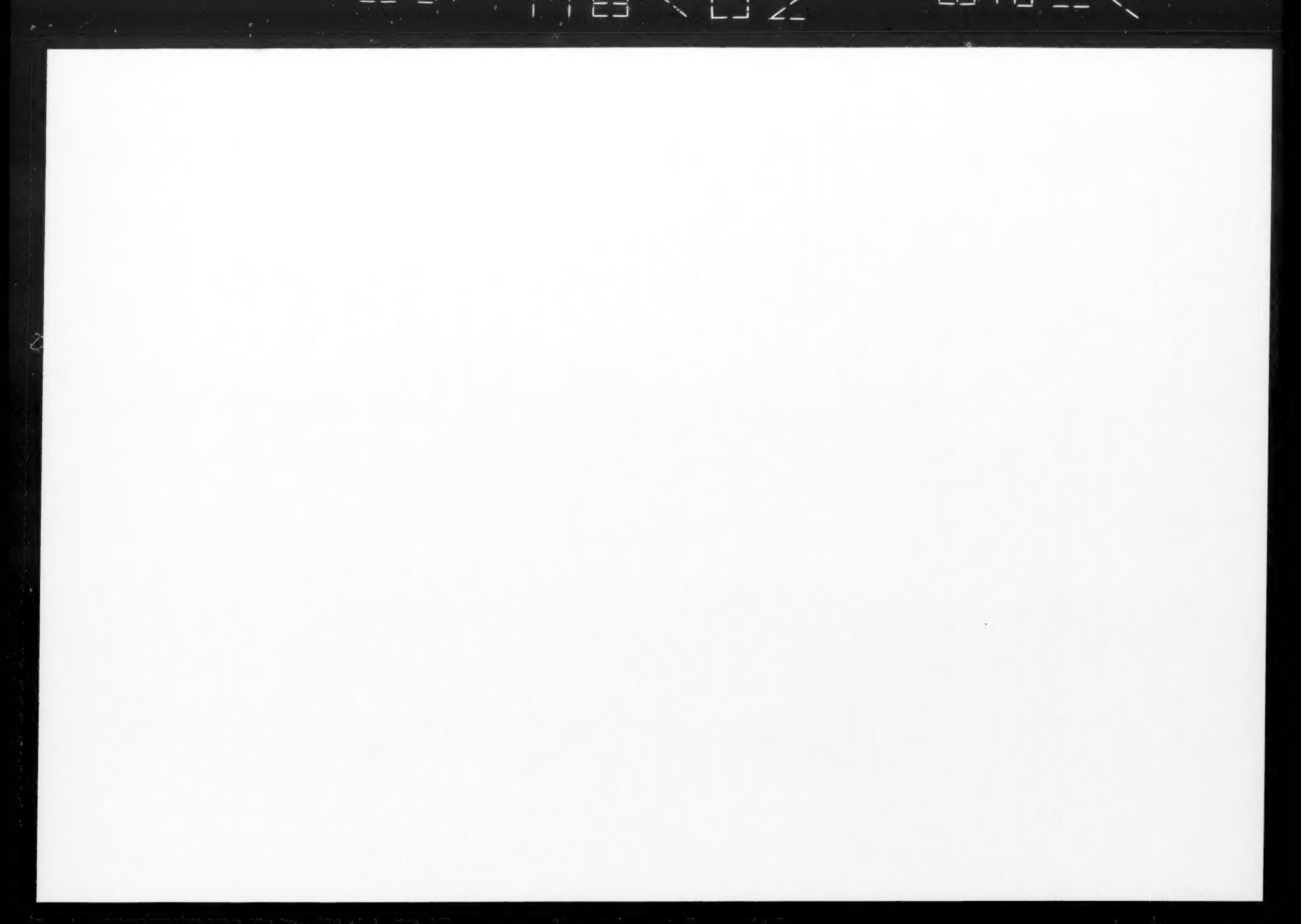

THE MASS SPECTRA OF LARGE MOLECULES

M. V. Gur'ev, M. V. Tikhomirov and N. N. Tunitskii

(Presented by Academician V. A. Kargin, June 6, 1958)

It is known that the bombardment of polyatomic molecules by electrons with energies of 50-100 ev is accompanied by ionization and dissociation of these molecules. At the present time it is generally accepted that in the process the molecule dissociates by simple rupture of the bonds [1]. An analysis of mass-spectral data, and particularly of data on the formation of "rearrangement" ions [3, 4], together with the study of the mass spectrum of deutero-octane, which we have carried out [5], lead to the conclusion that the above assumption in the general case is not accurate. This conclusion is confirmed, in particular, by the fact that in the mass spectrum of n-octane-2d_1 the ions $C_2H_5^+$ and $C_3H_7^+$ are labeled, not to the extent of 50%, as would have been expected in the case of simple rupture of the bonds, but to a considerably smaller extent – to approximately 30%. In order to explain this result it has been suggested that the fragment ions are formed with approximately equal probability from any part of the molecule with the capture of a hydrogen atom [5].

In order to reach a definite conclusion regarding the mechanism of the dissociation, we have synthesized n-nonane-5C^{13} and studied its mass spectrum. The synthesis was carried out using carbon monoxide containing 51% C^{13}. The scheme of the synthesis was as follows:

$$C^{13}O \xrightarrow[H_2SO_4]{NaOH} HC^{13}OOH \xrightarrow{C_4H_9OH} HC^{13}(=O)OC_4H_9 \xrightarrow{C_4H_9MgBr} C_4H_9-C^{13}H(OH)-C_4H_9 \longrightarrow$$

$$\xrightarrow{PBr_3} C_4H_9-C^{13}HBr-C_4H_9 \xrightarrow{Mg,H_2O} C_4H_9-C^{13}H_2-C_4H_9.$$

The mass spectra of n-nonane and n-nonane-5C^{13}, obtained under the usual conditions using an MI-1303 instrument and corrected for the natural C^{13} content, are given in Table 1.

Table 2 gives the fraction of ions containing C^{13} in ions of a given type, expressed as percentages.

If the n-nonane-5C^{13} molecule dissociated by the simple rupture of the bonds, then the ions of the type $C_2H_5^+$, $C_3H_5^+$, $C_4H_9^+$ would not contain carbon C^{13}. As can be seen from Table 2, however, between 14 and 46% of these ions contain C^{13}. The column headed "calculated" in Table 2 gives the percentages of ions of a given type containing C^{13}, calculated on the assumption that the formation of ions of the type $C_nH_{2n+1}^+$ ("terminal" ions) takes place with equal probability from any part of the molecule. From the central parts of the molecule, such ions are evidently formed with capture of a hydrogen atom. Fragment ions of other types $C_nH_m^+$ ($m < 2n + 1$), as we have already shown [5], are formed for the most part by the removal of hydrogen atoms from the "terminal" ions.

Preliminary studies of the relationship between the mass spectrum of n-nonane-5C^{13} and the energy of the electrons has shown that the mechanism of formation of the terminal ions $C_nH_{2n+1}^+$ remains practically unchanged right up to the appearance potential.

Thus in the general case the dissociation of large molecules by electron collision takes place as follows: first of all, with an even number of electrons terminal ions are formed with approximately equal probability from any part of the molecule with the capture of a hydrogen atom, after which some of these ions break down with removal of a hydrogen atom and produce the complete mass spectrum of the substance.

TABLE 1

m/e	Substance		m/e	Substance		m/e	Substance	
	n-nonane	n-nonane $5C^{13}$		n-nonane	n-nonane $5C^{13}$		n-nonane	n-nonane $5C^{13}$
13	0,034	0,043	48	0,003	0,002	77,7	—	0,085
14	0,081	0,089	49	0,012	0,007	79	0,038	0,026
15	0,383	0,406	50	0,085	0,049	80	0,008	0,036
15,5	0,006	0,002	51	0,175	0,127	81	0,028	0,075
16	0,070	0,102	52	0,085	0,143	82	0,017	0,045
21,7	0,044	0,002	53	0,593	0,316	83	0,063	0,038
22,7	—	0,024	54	0,308	0,513	84	1.335	0,112
24	0,025	0,026	55	3,053	1,424	85	4,85	1,310
25	0,090	0,082	56	3,55	4,44	86	—	4,74
26	0,786	0,666	57	15,20	9,02	91	0,013	0,012
27	6,71	5,98	58	—	6,55	92	0,003	0,012
28	1,534	2,23	61	0,002	0,001	93	0,004	—
29	8,51	7,73	62	0,009	0,004	94	0,002	0,005
29,5	0,014	0,06	63	0,029	0,014	95	0,008	0,028
30	0,026	1,173	64	0,007	0,027	96	0,009	0,044
			65	0,076	0,049	97	0,025	0,009
32,8	0,14	0,02	66	0,034	0,079	98	0,577	0,056
33,8	—	0,086	67	0,162	0,093	99	1,132	0,498
36	0,013	0,014	68	0,067	0,208	100	0,010	1,163
37	0,088	0,073	69	0,589	0,144	112	0,008	0,011
38	0,162	0,163	70	2,47	0,567	113	0,013	0,006
39	3,66	2,449	71	4,04	2,544	114	—	0,017
40	0,606	1,62	72	—	3,81	126	0,013	0,004
41	11,30	7,95				127	—	0,014
42	3,45	5,67				128	1,026	—
43	22,37	12,95	76,6	0,070	0,016	129	—	1,045
44	—	10,24					100,000	100,000

For example, in the case of one of the ways of forming an ion of the type $C_3H_7^+$ we have:

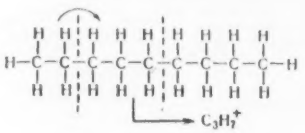

These facts are in accordance with the conclusions which can be drawn from an examination of the mass spectra of large molecules.

At the present time it is accepted that after the electron collision the excitation energy is redistributed over the whole molecule, which then dissociates in random fashion. Let us examine from this point of view two molecules of normal structure, for example n-hexane C_6H_{14} and n-tetratetracontane $C_{44}H_{90}$. It is reasonable to assume that the electron collides with approximately equal probability with any part of the molecule. The molecules under consideration consist for the most part of CH_2 groups with practically identical chemical and physical properties. It might therefore be thought that the mean excitation energies transferred to these molecules by the electron collison do not differ essentially from one another. From this it would be expected that molecular ions will be represented to a considerably greater extent in the mass spectrum of $C_{44}H_{90}$ than in that of C_6H_{14}. Experiment shows, however, that the larger the molecule (for the same structure) the smaller the fraction of molecular ions in its mass spectrum [6].

Thus,in order to explain the very fact that large molecules produce a mass spectrum, it is necessary to make the opposite assumption, namely that the energy given by the electron is not distributed throughout the whole molecule before its dissociation. This suggestion is in accordance with data obtained from the study of the initial regions of the ionization curves [7] and provides a ready explanation of the experimental results which we have obtained. In fact, if the electron falls with equal probability in any part of the molecule and the energy

TABLE 2

Ion	$C_2H_5^+$	$C_3H_7^+$	$C_4H_9^+$
Found	14	46	44
Calculated	25	43	67

which it gives up is distributed over only a small part of the molecule before dissociation, then that part will be the part which is "thrown out" of the molecule in the form of a fragment ion. The ions obtained in this way carry within themselves the greater part of the excitation energy and therefore subsequently readily dissociate with removal of hydrogen atoms.

From this is it follows in particular that molecules whose structure makes it possible for the excitation to be transferred along a chain of bonds will dissociate on electron collision to a slight extent. The fraction of molecular ions in the mass spectrum of such molecules will be large. One such example is the mass spectrum of benzene.

LITERATURE CITED

[1] M. Magat, Disc. Farad. Soc. No. 10, 113 (1951).

[2] Catalog of Mass-Spectral Data, Am. Petrol. Inst. Res. Project 44, Pittsburgh (1952-1955).

[3] A. Langer, J. Phys. Coll. Chem. 54, 618 (1950).

[4] F. L. Mohler, et al., J. Res. Nat. Bur. Stand. 44, 291 (1950).

[5] M. V. Gur'ev and M. V. Tikhomirov, J. Phys. Chem. 32, No. 12 (1958).

[6] International Petroleum Congress, 6, 1956, p. 298.

[7] L. Friedman, F. A. Long and M. Wolfsberg, J. Chem. Phys. 26, 714 (1957).

Received June 24, 1958

THE RATE OF DEGENERATIVE CHAIN BRANCHING IN THE OXIDATION OF n-DECANE

D. G. Knorre, Z. K. Maizus and N. M. Emanuel', Corresponding Member, Academy of Sciences USSR

According to modern theories, the retarding action of an inhibitor on a chain reaction is the result of interaction between the free radicals which are propagating the chain and the inhibitor molecules. Because of this interaction, the inhibitor is consumed and eventually disappears from the system. The disappearance of the inhibitor from the system results in a sharp increase in the rate of the chain process, i.e., the reaction then passes out of its induction period. The concentration of the radicals in the system determines the rate of consumption of the inhibitor and, consequently, fixes the duration of the induction period.

When it is a question of reaction in the liquid phase, where a second-power chain rupture predominates in the absence of an inhibitor, the concentration of radicals in the presence of the inhibitor I is covered by the equation

$$\frac{d[R]}{dt} = w_0 - ak_i[R][I] - k[R]^2,$$

in which ω_0 is the rate of generation of the free radicals, k_i is the rate constant for the interaction of these radicals with the molecules of the inhibitor, $\underline{k}$ is the rate constant for the recombination of the radicals, and $\underline{a}$ is a stoichiometric factor which gives the number of free radicals which are destroyed by one molecule of the inhibitor.

Supposing the radical concentration to be stationary, the following expression can be obtained for the rate of consumption of the inhibitor:

$$-\frac{d[I]}{dt} = \frac{k_i[I]}{2k}\left(\sqrt{a^2k_i^2[I]^2 + 4kw_0} - ak_i[I]\right). \qquad (1)$$

At sufficiently high inhibitor concentrations, $a^2k_i^2[I]^2 \gg 4kw_0$, and we find:

$$-\frac{d[I]}{dt} = \frac{w_0}{a}. \qquad (2)$$

Thus at these high inhibitor concentrations the consumption of the inhibitor proves to follow a zero-order reaction.

It has frequently been supposed that relation (2) is valid up to complete consumption of the inhibitor. If we start from the fact that the system passes out of its induction period once the inhibitor has been consumed, i.e., that $t = t_i$, when $[I] = 0$, t_i being the length of the induction period, integration of (2), then gives the relation

$$[I]_0 - \frac{w_0}{a}t_i = 0 \quad \text{or} \quad t_i = \frac{a[I]_0}{w_0}. \qquad (3)$$

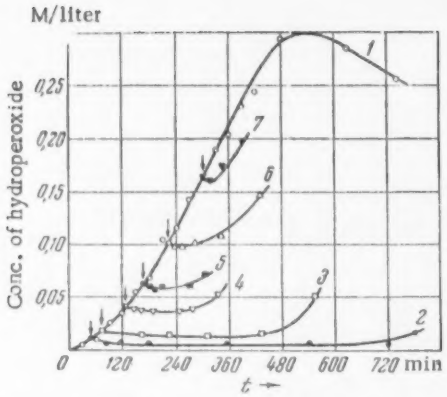

Fig. 1. Kinetic curves for the build-up of hydroperoxide in the oxidation of n-decane at 130°:
1) without an inhibitor, and 2–7 – in the presence of α-naphthol ($2 \cdot 10^{-6}$ M/ml) which was introduced at various times. The times of introduction of the inhibitor are indicated by arrows.

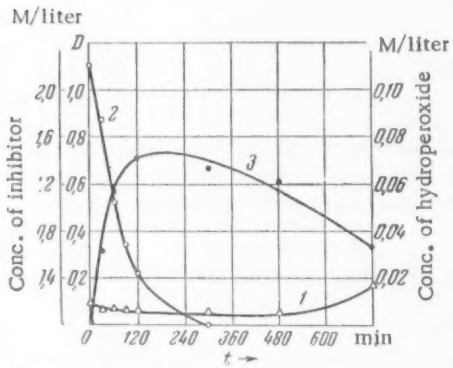

Fig. 2. The change in the concentration of hydroperoxide (1), the concentration of α-naphthol (2), and the optical density of the solution at λ = 420 mμ (3) for the introduction of α-naphthol ($2 \cdot 10^{-6}$ M/ml) into the oxidizing decane 50 minutes after the beginning of oxidation. Temperature, 130°.

Equations (2) and (3) are used for determining the rate of chain initiation [1-3]. A starting point here is found in the fact that chain initiation is an elementary reaction and that it must, accordingly, be unaltered by the introduction of small amounts of inhibitor into the system. When initiation is considered as an elementary process, the initiation rate should be proportional to the product of the concentration of the substances participating in the initiation process, and it is then possible to deduce the mechanism of the initiation process from the dependence of w_0 on the concentrations of the substances which are present in the system.

By making use of the customary procedure of introducing the inhibitor into the system initially, the measured rate of initiation can be referred to zero time.

On the other hand, by introducing the inhibitor during the course of the process, it becomes possible to obtain the rate of initiation at any stage of the reaction. For the oxidation processes, in which the basic mass of radicals for the developing process is obtained from the degenerative chain branching, it is of particular interest to attempt to obtain information about the rate and mechanism of the degenerative branching by the indicated method of inhibitors.

In the present work, the method of inhibitors has been applied for the measurement of the rate of degenerative chain branching in the liquid-phase oxidation of n-decane.

The n-decane was oxidized in an oxidation cell [4] by a current of oxygen, the rate of the oxidation being followed through the build-up of hydroperoxide, whose concentration was determined iodometrically. α-Naphthol was selected as the inhibitor, its concentration being measured spectrophotometrically after the compound which was present in a specimen had been extracted by 1 N NaOH and had been combined with phenyldiazonium chloride, the estimation being from the adsorption maximum in the resulting diazo substance (520 mμ).

In Fig. 1 there are given kinetic curves for the build-up of hydroperoxide in the course of the 130° oxidation of n-decane in the presence of α-naphthol at a concentration of $2 \cdot 10^{-6}$ M/ml, this α-naphthol having been introduced at various times. The corresponding curve for the case in which the inhibitor was introduced into the decane initially is not given since the induction period is extremely long in this instance. The period is 20 hours, even with an α-naphthol concentration of $0.5 \cdot 10^{-6}$ M/ml. This points to a sharp acceleration in the formation of the free radicals in the initial stage of the reaction. The induction period for the oxidation process proves to be the shorter, the later the inhibitor is introduced.

The introduction of α-napthol into the oxidizing n-decane results in a gradual yellowing of the solution. If the α-naphthol is introduced at a comparatively advanced stage, the formation of a brownish precipitate is also observed. The compound which is formed here has a characteristic spectrum in the visible region with an absorption maximum at 420 mμ. In Fig. 2 there is shown the alteration in: the concentration of the hydroper-

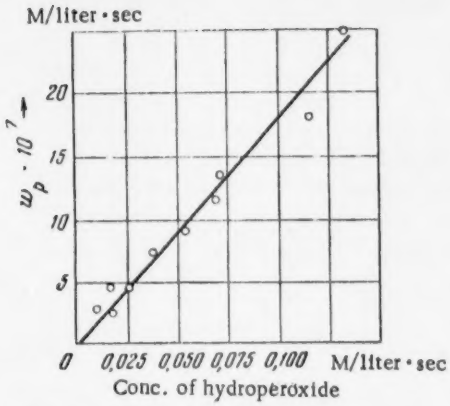

Fig. 3. The relation between the rate of branching and the concentration of hydroperoxide in the oxidation of n-decane at 130°.

oxide, the concentration of the α-naphthol, and the optical density of the solution at 420 mμ, for the introduction of $2 \cdot 10^{-6}$ M/ml of α-naphthol into the oxidizing decane 50 minutes after the beginning of oxidization. The value of the optical density passes through a maximum and then falls. This indicates that the color of the solution results from a certain intermediate compound which is formed from the α-naphthol. The introduction of a precipitate of this compound into fresh n-decane shows this intermediate substance to possess an inhibiting action.

The consumption of the α-naphthol follows a zero-order reaction, but only up to ~ 70% transformation, after which a distinct departure from a zero-order reaction is to be noted. It is possible that this is related to the fact that with decreasing inhibitor concentration, Equation (2) becomes inapplicable so that it is then necessary to use the more exact Equation (1); it is also true that some of the free radicals then begin to react with the new intermediate compound, rather than with the α-naphthol. In this connection Equation (3) proves to be inapplicable in our situation and calculation of the rate of branching was carried out only through Equation (2), the determination of $d[I]/dt$ being made from the linear portion of the curve showing the consumption of the inhibitor.

In the calculations it was assumed that $a = 2$, as is the case with the phenols, and with β-naphthol, for which this quantity has been experimentally evaluated [5]. Since degenerative branching leads to the formation of free radicals, it was considered that $w_0 = 2w_p$. From this it follows that

$$w_p = -d[I]/dt.$$

The rate of consumption of the inhibitor in the oxidation of n-decane, at 130° and at a hydroperoxide concentration of 0.02 M/l, proves to have the following values at the indicated inhibitor concentrations:

$[I]_0 \cdot 10^3$, M/l	1.1	1.7	3.1	4.4
$(d[I]/dt) \cdot 10^7$, M/l · sec	5.5	7.3	6.3	6.5

It is to be seen from these data that the value obtained for $d[I]/dt$ is independent of the inhibitor concentration. This shows that the inhibitor does not participate in the formation of the free radicals and is only an "instrument" for the measurement of the quantity w_p.

In Fig. 3 there is shown the relation between the rate of branching at 130°, as determined in this way, and the hydroperoxide concentration. It appears that the rate of branching is proportional to the hydroperoxide concentration. It has thus been directly proven that the hydroperoxide is the fundamental branching agent in the oxidation of n-decane. When evaluated from the relation between w_0 and the hydroperoxide concentration, the velocity constant for the branching reaction at 130° proves to be $1.9 \cdot 10^{-5}$ sec^{-1}. The energy of activation for the branching reaction, as determined from the temperature dependence of w_p is 24.8 kcal. The temperature dependence of the velocity constant can be described by

$$k = 6 \cdot 10^8 \exp(-24800/RT)\ sec^{-1}.$$

The value of the exponential multiplier is noteworthy, since it is unusually low for a process of thermal breakdown.

It is possible that this low value is to be explained by the fact that the degenerative chain branching proceeds, not through a monomolecular reaction, but through a bimolecular reaction with the hydrocarbon:

$$ROOH + HR \rightarrow RO\cdot + H_2O + R\cdot$$

From the energetic standpoint, such a reaction is more economical by 22 kcal (the difference between the energies of the OH bond in water and the C–H bond in n-decane) than is the direct rupture of the O–O bond.

The value which has been obtained for $\underline{k}$ deviates considerably from that which is given in the paper by Twigg [6] $8 \cdot 10^{11} \exp[(-31800/RT)]$. In this work measurement was made of the rate of breakdown of a mixture of the secondary decyl hydroperoxides, the velocity constant for the decomposition of the hydroperoxide being calculated by assuming the entire consumption of the latter at low concentrations to result from initial breakdown at the O–O bonds. Since our data have been obtained by a more direct method and gives a markedly different value for $\underline{k}$, it is possible that Twigg's reasoning is not correct.

LITERATURE CITED

[1] P. George, E. K. Rideal and A. Robertson, Proc. Roy. Soc., A, 185, 288 (1946).

[2] J. H. T. Brook and J. B. Matthews, Disc. Farad. Soc. 10, 291 (1951).

[3] C. E. H. Bawn, Disc. Farad. Soc. 14, 181 (1953).

[4] D. G. Knorre, Z. K. Maizus and N. M. Emanuel', J. Phys. Chem. 29, 710 (1955).

[5] Ch. E. Boozer, G. S. Hammond, Ch. E. Hamilton and J. N. Sen, J. Am. Chem. Soc. 77, 3233 (1955).

[6] G. H. Twigg, Disc. Farad. Soc. 14, 240 (1953).

The Institute of Chemical Physics of the
Academy of Sciences of the USSR

Received July 10, 1958

THE RADIATION VULCANIZATION OF POLYAMIDES (ANIDE G-669)

S. A. Pavlova, S. R. Rafikov and B. L. Tsetlin

(Presented by Academician V. A. Kargin, June 25, 1958)

As is well known, it is possible to distinguish between two types of linear polymer, according to the nature of the radiochemical changes which they undergo; the two types are: those polymers which are vulcanized and those polymers which are broken down. The class to which a given polymer belongs is judged from the nature of the changes in the mechanical and thermomechanical properties, the solubility, and the viscosity of the solutions, i.e., in those properties from which it is possible to estimate only the over-all change in the molecular structure of the polymer. At the same time, in the discussion of the results of experimental studies, it is often assumed that two types of reaction take place simultaneously in a linear polymer under the influence of radiation, namely the formation of cross-linkages and the rupture of bonds in the principal chains of the macromolecule, while the observed over-all process is determined by the reaction which predominates. It is only possible to judge whether those opposed reactions do in fact take place simultaneously, and to estimate their relative rates, from indirect evidence [1, 2].

The aim of the present work was to obtain experimental proof that reactions involving breakdown and structure-formation take place simultaneously in polyamides under the influence of ionizing radiation. The material chosen for study was the soluble mixed polyamide "anide G-669" which is the product of the condensation of hexamethylenediamine with adipic and azelaic acids and caprolactam [3]. It has already been established that the over-all effect of ionizing radiations on this polyamide [4], as in the case of polyhexamethylenediamide [4, 5] is that of radiation vulcanization.

The G-669 specimens were irradiated in the form of plates with a thickness of 1 mm, both in air and in vacuo. The source used consisted of an x-ray tube of the TRB-3 type [6], operating at a voltage of 80 kilowatts and current of 20 milliamps.* The strength of the radiation dose was of the order of $5 \cdot 10^{16}$ ev/cc·sec., time of irradiation 1-20 hours.

Figure 1 gives the thermomechanical-compression curves for specimens of anide G-669 for different radiation-dose strengths. The curves presented were recorded continuously using the instrument described in [7] and illustrate the general nature of the over-all process of radiation vulcanization. Analogous results were obtained from a study of the solubilities of the irradiated specimens: even after irradiation for only 3 hours, a fraction insoluble in acetic acid appears (7% by weight), while the proportion of this fraction increases with increase in the radiation dose and amounts to 25% after 5 hours and to 76% after 10 hours irradiation.

The determination of the average molecular weight M_w for the polyamide, by measuring the light scattering in ethanol solution, showed that under the influence of radiation the average molecular weight increases sharply: for the nonirradiated specimen $M_w = 14500$, while for a specimen irradiated for only 1 hour $M_w = 55000$.

Figure 2 gives curves showing the relationship between the viscosity of solutions and the concentration for anide G-669 in cresol and acetic acid. As a result of the irradiation, the value of $[\eta]$ decreases for the cresol solutions and increases for the acetic acid solutions. At the same time the slope of the concentration

*The irradiation of the specimens was carried out using the x-ray apparatus of the USSR Academy of Sciences Institute of Physical Chemistry. The authors have to express their thanks to Professor N. A. Bakh and V. I. Zatulovskii for making it possible to carry out this work.

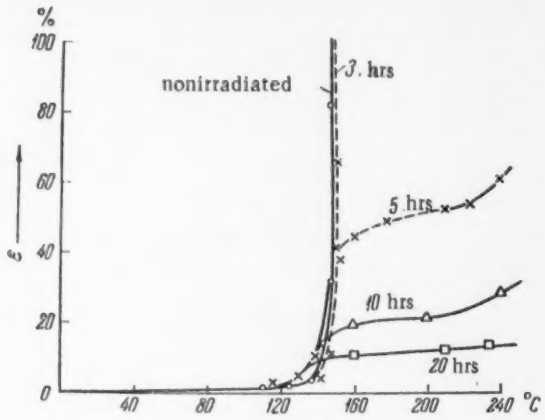

Fig. 1. The thermomechanical compression curves for anide G-669 for different radiation doses (unit load 0.8 kg/cm^2).

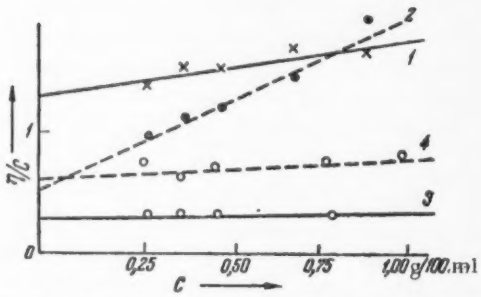

Fig. 2. The viscosity of solutions of nonirradiated specimens of anide G-669 (1,3) and of specimens of anide G-669 irradiated for 1 hour (2,4). 1,2) solvent cresol; 3,4) solvent acetic acid.

curves increases in both cases, which indicates an increase in the Huggins constant [8] in the equation:

$$\eta / C = [\eta] + k [\eta]^2 C$$

Figures 3 and 4 give the results of the turbidimetric titration of nonirradiated and irradiated specimens of anide G-669 in the form of the integral and differential solubility distribution curves. The titration data given refer to the system in which the solvent used was acetic acid and the precipitant used was water. In the case of specimens which had received relatively large radiation doses and contained an insoluble "gel-fraction," the magnitude of the latter was determined independently and taken into account in the construction of the integral distribution curves; the appropriate values were recorded on the y-axis (dotted lines in Fig. 3). It should be remembered that for the irradiated specimens, the results obtained reflect only approximately the molecular weight distribution, since the irradiation may to a certain extent alter the relationship between the solubility of the polymer and its molecular weight. These curves, however, enable us to judge fairly accurately the general nature of the change in the molecular-weight distribution. An examination of Fig. 4 shows that as a result of the irradiation the maximum on the original differential distribution curve splits into two: two maxima appear, one of which is displaced towards the region of the insoluble fractions with high molecular weights, and the other to the low molecular-weight region. As the radiation dose increases, these two maxima continue to "move apart." In the case of radiation doses in excess of the dose producing gel formation, the differential curves given in Fig. 4 correspond to the solubility distribution within the sol-fraction, as a result of which the magnitude of the "high molecular-weight maximum" decreases as the insoluble fraction increases.

The experimental data obtained show that under the influence of radiation, processes involving the formation of cross-linkages and processes involving breakdown of the principal chains in the macromolecules take place simultaneously in the polyamide. The fact that reactions involving structure formation take place is proved by the increase in the value of M_w, the displacement of the maximum on the solubility distribution curves towards less soluble fractions, and finally by the appearance, at sufficiently high radiation doses, of an insoluble three-dimensional fraction together with loss of fluidity at the melting point of the original polymer. The fact that reactions involving breakdown of the principal chains take place is indicated by the "splitting" of the differential distribution curves, i.e., by the appearance of a second maximum on the curves in the region of relatively readily soluble fractions, this maximum being shifted continuously further into the region of low molecular weights. As a result of the fact that processes of structure formation and breakdown are taking place simultaneously, the original polyamide, with its usual relatively narrow distribution, breaks down, as it were, into two independent fractions – one of low molecular weight and one of high molecular weight. This may be explained by the fact that interaction of the primary polymeric radicals leads to the formation of new molecules, whose size is either considerably greater (interaction of the radicals with neighboring macromolecular chains) or considerably less (disproportionation and isomerization of the radicals, interaction of the radicals with low molecular-weight fragments) than that of the original polymer. At the same time, in the case under

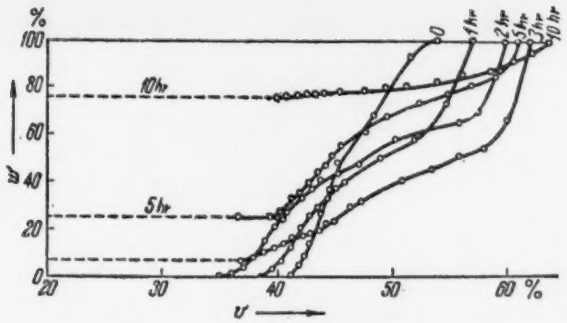

Fig. 3. Integral solubility distribution curves for specimens of anide G-669 for different radiation doses.

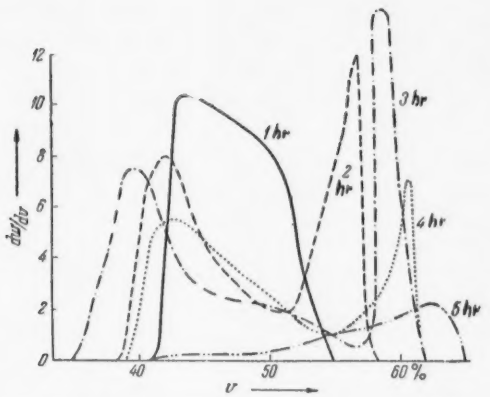

Fig. 4. Differential solubility distribution curves for specimens of anide G-669 for different radiation doses.
1) nonirradiated; 2) irradiated for 1 hour; 3) 2 hours; 4) 5 hours; 5) 10 hours.

consideration, the processes of structure formation predominate and the final result of the changes is vulcanization. The amount and "density" of the three-dimensional structures increases smoothly with increase in radiation dose, as can be seen from the data obtained from studies of the thermomechanical properties and the solubility. Even in the first stages of the process, the degree of branching of the polymeric molecules increases to a considerable extent, as is indicated by the nature of the change in the viscosity of the solutions and primarily by the increase in the Huggins constant for the solutions of irradiated specimens.

The data presented show that the complex study of the change in mechanical properties, in the properties of solutions, in the molecular weights and in the molecular-weight distribution functions makes it possible to estimate fairly completely the change in the molecular structure of polyamides during radiochemical changes.

The application of analogous methods of study will obviously make it possible to separate the parallel reactions of structure-formation and breakdown in polymers of different structure and to establish the factors which influence their relative rates.

LITERATURE CITED

[1] B. L. Tsetlin, N. G. Zaitseva and V. A. Kargin, Report of the AN SSSR Institute of Physical Chemistry, No. 676 (April, 1953); B. L. Tsetlin, N. G. Zaitseva, V. M. Korbut and V. A. Kargin, Coll. The Action of Ionizing Radiations on Inorganic and Organic Systems, Izd. AN SSSR, 1958, p. 362.*

[2] A. R. Schultz, P. J. Roth and G. B. Rathman, J. Polym. Sci. 22, No. 102, 495 (1956).

[3] V. V. Korshak and T. M. Frunze, Izv. AN SSSR, Div. Chem. Sci. 1957, 558.**

[4] B. L. Tsetlin and S. R. Rafikov, Izv. AN SSSR, Div. Chem. Sci. 1957, 1411.**

[5] A. Charlesby, Nature, 171, 167 (1953).

[6] V. I. Zatulovskii, N. I. Vitushkin, D. I. Nariadchikov and V. I. Petrovskii, Proc. of the 1st All-Union Conference on Radiation Chemistry, Izd. AN SSSR, 1958, p. 313.*

* In Russian.
** Original Russian pagination. See C. B. Translation.

[7] B. L. Tsetlin, V. I. Gavrilov, N. A. Velikovskaia and V. V. Kochkin, Factory Labs., No. 3, 352 (1956).

[8] M. Huggins, J. Am. Chem. Soc. 64, 2716 (1942).

Received June 23, 1958

THE STRUCTURE OF WATER

I. Z. Fisher and V. K. Prokhorenko

(Presented by Academician I. I. Cherniaev, June 26, 1958)

The most reliable and direct information on the structure of liquids is obtained from the study of the scattering of x-rays by liquids by using the angular scattered-radiation intensity relationships to establish the radial atomic-distribution function g(r). Until recently the study of the g(r) function was directed for the most part towards the estimation of the average coordination numbers of the atoms in the liquid and a comparison of the results of this estimation with the corresponding crystal structures. It has been shown in a work by the authors [1] that a knowledge of the g(r) function also enables us to obtain an estimate of the fluctuations in the average coordination numbers of the atoms in the liquid, and the appropriate calculations were presented for liquid argon at various temperatures. From our point of view the fluctuations in the coordination numbers are a no less important characteristic of the structure of a liquid than the coordination numbers themselves, since they may serve as a direct measure of the deviation of the local structure of a given liquid from the structure of the corresponding crystal.

The problem of the structure of water is of particular interest. We have used the equations obtained in [1] to calculate the fluctuations in the first two coordination numbers of the oxygen atoms in water, and to establish a correlation between the fluctuations in both coordination numbers. The calculations were carried out using the experimentally obtained radial distribution functions for water at various temperatures given in [2]. The results of the calculations for the first coordination number are given in Table 1.

The numbers in the first column in the Table indicate the temperature to which the corresponding g(r) functions from [2] refer, those in the second column indicate the position of the first minimum of the function $4\pi r^2 g(r)$, those in the third indicate the average value of the first coordination number, which is equal to the area under the graph of the function $(4\pi r^2/v)g(r)$ between $r = 0$ and $r = r_1$. The last two columns give the results of the calculations of the absolute and relative magnitudes of the mean-square fluctuation of the first coordination number. The error in the calculation amounts to approximately 0.1 for the data in the third and fourth columns of the Table.

Table 2 gives the results of analogous calculations for the indistinct $4\pi r^2 g(r)$ peak which is found at low temperatures in the region of $r \sim 3.6$ A, and which is produced by the atoms which are displaced and introduced into the empty spaces in the water structure [3, 4]. The coordination number $\overline{z}_2$ is defined as the area under the curve $(4\pi r^2/v)g(r)$ between $r = r_1$ and $r = r_2$, where r_2 is the position of the second minimum in the function $(4\pi r^2/v)g(r)$. The last column of the Table gives the values of the quantity

$$\delta = \overline{\Delta z_1 \cdot \Delta z_r} \Big/ \sqrt{\overline{(\Delta z_1)^2} \cdot \overline{(\Delta z_r)^2}},$$

which is a measure of the correlation between the first and second coordination numbers.

It can be seen from the Tables that the level of fluctuation in both coordination numbers is approximately the same and is very high. The large negative value of δ indicates the fine structure of the order fluctuations in water.

From the experimental $4\pi r^2 g(r)$ curves from [2] it is also possible to pick out a "normal" second coordination sphere in a region approximately between $r = 3.9$ A and $r = 5.7$ A, which corresponds closely to the

TABLE 1

t, °C	r_1, A	$\bar{z}_1$	$\sqrt{(\Delta z_1)^2}$	$\sqrt{(\Delta z_1)^2}/\bar{z}_1$
1.5	3.3	4.5	1.5	0.33
13.0	3.3	4.4	1.5	0.35
30.0	3.3	4.6	1.5	0.33
62.0	3.45	5.0	1.4	0.28
83.0	3.5	5.0	1.3	0.26

TABLE 2

t, °C	r_2, A	$\bar{z}_2$	$\sqrt{(\Delta z_2)^2}$	$\sqrt{(\Delta z_2)^2}/\bar{z}_2$	δ
1.5	3.9	3.0	1.5	0.51	−0.52
13.0	3.8	2.5	1.4	0.56	−0.56

coordination of water molecules in ice. Unfortunately the data given in [2] are not sufficient for a rigorous calculation of the fluctuations of the particles in this coordination sphere. The approximate value of $\overline{(\Delta z)^2}$ which we have obtained proves to be not less than 30% of $\bar{z}$ itself at all temperatures at which the "normal" second coordination sphere may be picked out.

The stable existence of approximately fourfold coordination in water at all temperatures has naturally led to the conclusion that the "quasicrystallinity" of water is comparatively great (over short distances). The extremely high level of the fluctuations in the coordination numbers contradicts this, however. The level of the fluctuations is of the same, or even greater order of magnitude than in liquid argon [1]. It should also be remembered that the number of peaks which can be distinguished in the g(r) function, and which determine the dimensions of the region of closest order in the liquid, is equal to 2-3 for water and is the same as the number of g(r) peaks for all known simple liquids [5]. Water is therefore no more "quasicrystalline" than other simple liquids. This is in complete accordance with the comparatively low value for the coefficient of internal viscosity of water.

The results which we have obtained are in good agreement with the ideas of O. Ia. Samoilov regarding the influence of temperature on the structure of water and of the important part played by translatory motion of the water molecules in the explanation of its structure and of its physical and physicochemical properties [3, 4]. The fluctuations in the first coordination number may serve as a direct measure of the intensity of the translatory movement of the molecules of liquid from their mean equilibrium positions to new equilibrium positions as a result of thermal motion. It can be seen from Table 1 that the fraction of molecules undergoing translatory displacement in water is very high. The anomalous relationship between $\sqrt{\overline{(\Delta z)^2}}$ and temperature (decrease in $\sqrt{\overline{(\Delta z)^2}}$ with increase in t) for water corresponds exactly to the tendency shown by its structure when the temperature is increased, to approach the structure which is common to all simple liquids [3, 4] and in which the level of the relative fluctuations is somewhat lower than in water.

The authors take this opportunity to express their thanks to O. Ia. Samoilov for fruitful discussion of the results of this work.

LITERATURE CITED

[1] V. K. Prokhorenko and I. Z. Fisher, J. Phys. Chem. 31, 2145 (1957).

[2] J. Morgan and B. E. Warren, J. Chem. Phys. 6, 666 (1938).

[3] O. Ia. Samoilov, J. Phys. Chem. 20, 1411 (1946).

[4] O. Ia. Samoilov, The Structure of Aqueous Solutions of Electrolytes and the Hydration of Ions, Izd. AN SSSR, 1957 [in Russian].

[5] N. S. Gingrich, Prog. Chem. 15, 297 (1946).

V. I. Lenin State University, Byelorussia

Received June 23, 1958

THE MOLECULAR ORBITALS OF RADICALS WITH NONALTERNATING RINGS

M. E. Diatkina, S. N. Dobriakov and E. M. Shustorovich

(Presented by Academician I. I. Cherniaev, June 26, 1958)

In [1] we have calculated molecular orbitals for certain systems containing three condensed rings, these systems being the analogs of benzonaphthenyl with five- and six-membered rings. When the number of electrons is odd, systems of this type are found to differ from the benzonaphthenyl radical in the fact that the nonbonding level of the latter passes over into a bonding level on replacing one of the six-membered rings by five-membered ring (so that the molecule readily picks up an electron to form an anion), whereas this same level becomes antibonding when a six-membered ring is replaced by a seven-membered ring (so that electron loss and conversion into a position ion is facilitated). In systems involving three five-membered rings (I) with 10 π-electrons, it was found that there are six bonding and four antibonding orbitals, whereas in systems with three seven-membered rings (II) and 16 π-electrons, there are only seven bonding levels and nine antibonding. Thus in systems I and II there is met that anomalous distribution of molecular orbitals which was first found by Bergmann and his colleagues [2] for fulvalene (III), "fulvadiene" (IV), "fulvatriene" (V), "heptafulvalene" (VI), "heptafulvadiene" (VII), and "heptafulvatriene" (VIII), and which differentiates compounds I – VIII from the alternating hydrocarbons. In each of the alternating hydrocarbons which contains an even number of π-electrons, the number of bonding levels is equal to one half of the number of electrons, so that in the ground state of the molecule the bonding levels are occupied by pairs of π-electrons and the antibonding levels are empty. In I and III – V, on the other hand, the number of bonding levels exceeds the number of pairs of π-electrons by one.

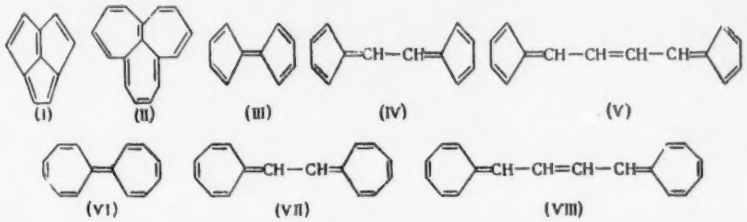

From this it can be concluded that such compounds should show a tendency to pick up an additional electron to form a singly charged anion (which will be paramagnetic, in distinction to the anions corresponding to the cyclopentadienyl radical and its analogs); or even to gain a pair of electrons to form a doubly charged diamagnetic anion. On the other hand, the number of bonding levels is one less than the number of pairs of π-electrons in II, VI, VII and VIII. Here the ready loss of an electron to produce a singly charged cation-radical, or even the loss of an electron to produce a singly charged cation-radical, or even the loss of two electrons to give rise to a doubly charged cation*, is to be expected. The difference between the systems I - VIII and the alternating hydrocarbons appears again in the lack of agreement between the number of bonding molecular orbitals and the number of

*This does not mean that the compounds under consideration cannot exist as neutral molecules, for the ease of gaining or losing an electron is determined, not merely by the presence of an excess bonding or antibonding level, but also by the energy of this level. Thus, although the last occupied level of VI is nonbonding, its exchange energy is not great (–0.20 v), and, because of the destabilization resulting from the presence of electrons in the antibonding level, VI can exist as a neutral molecule of low stability.

double bonds which can be written into the structural formulas of the compounds. In the alternating hydrocarbons, the number of bonding orbitals is always equal to the number of double bonds. On the other hand, although there are six bonding levels in the case of I, it is possible to write a structural formula with five double bonds. It is also true of the molecules of III – V that the number of bonding levels is in excess of the number of double bonds. In the compounds containing seven-membered rings, the number of bonding levels is less than the number of double bonds. Thus, there are only seven bonding ortibals in II to correspond to the eight double bonds. The systems of III – VIII have been investigated in connection with the problem of thermochromy. The presence or absence of thermochromy is determined by the ease of transition of the molecule into a triplet state. In this conneection it is interesting to note that the systems I and II which we have investigated are characterized by the fact that the highest occupied levels in the respective neutral molecules (the last bonding level in I and the first antibonding level in II) are doubly degenerate. This indicates that two levels of identical energies are available for the last two electrons, since, in addition to the single state in which both electrons occupy one degenerat level, a triplet state in which there is one electron on each level is also possible. The respective energies of the singlet and tiplet states are identical within the framework of the simplified method of molecular orbitals. If account were taken of the electronic interaction it would probably be found that there is a difference between the energies of these two states, but it can be assumed that this difference would not be large, and it can therefore be anticipated that either the triplet state will be the fundamental one for the neutral molecules in systems I and II, or that the energy of transition into the triplet state will be so small that thermochromy will arise.

TABLE 1

Molecule	Number of π-electrons	Number of levels			Predicted stable state
		Bonding	Nonbonding	Antibonding	
(IX) 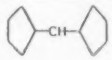	11	6	—	5	A⁻
(X) 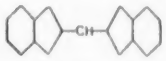	19	10	—	9	A⁻
(XI) 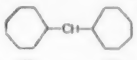	15	7	—	8	A⁺
(XII) 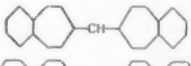	23	11	--	12	A⁺
(XIII) 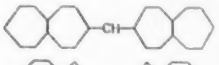	25	11	1	13	A⁺
(XIV) 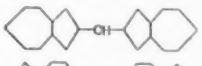	21	10	1	10	A
(XV) 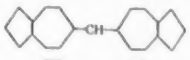	21	10	1	10	A
(XVI) 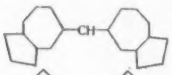	21	10	1	10	A
(XVII) 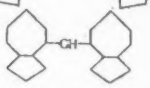	21	11	—	10	A⁻
(XVIII) 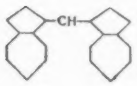	21	10	—	11	A⁺

The above-described peculiarities of systems with nonalternating rings suggests a consideration of other compounds with five- and six-membered rings, that is to say, radicals analogous to diphenylmethyl and dinaphthylmethyl containing cyclopentadienyl, cycloheptatrienyl and azulenyl groups. Calculations have been carried out by the simplified method of molecular orbitals, introducing those assumptions which are customary in such work. In Table 1 there are listed the systems which have been studied together with the number of

bonding, nonbonding, and antibonding molecular levels. In distinction of diphenylmethyl, this table shows that the first four of these systems have no nonbonding levels, and that the diphenylmethyl level of zero exchange energy goes into a bonding level in the system with five-membered rings (XI). Thus, it can be expected that IX would be stable in the form of the singly charged anion, just as is the cyclopentadienyl radical, and that XI would be stable in the form of a singly charged cation such as tropylium. Similar behavior should be met in systems containing not only a nonalternating ring but also a condensed six-membered ring (X and XII). There is a nonbinding level in the radical with heptalenyl groups (XIII) but in this case there are only 11 bonding orbitals, on which only 22 π-electrons can be distributed, so that the nonbonding level is occupied by a pair of electrons, and the unpaired electron passes over to the antibonding level. Here it is natural to expect, not only a ready transformation into a singly charged positive ion, as is the case with tropylium and XI, but also a further loss of electrons from the nonbonding level. The systems XIV – XVIII represent isomeric diazulenylmethyls which differ in regard to the position of the CH group in the azulene system. In the case of XIV – XVI, it is to be seen that we have to deal with radicals containing the same numbers of bonding and antibonding levels, plus one level of zero exchange energy. Just as in the alternating hydrocarbon radicals, the π-electrons, in pairs, occupy all of the bonding levels in these systems, and the one unpaired electron is in the nonbonding level. The formulas show that this situation will always arise when the CH group is united with a ring atom which is separated by at least two bonds from atoms which are common to the five- and six-membered rings, and that regardless of whether the CH group itself is in a five- or a six-membered ring. The situation proves to be different when the CH group is joined to a C atom which is, in turn, adjacent to a C atom that is common to the five- and six-membered rings. When the CH group is joined to a seven-membered ring, as in XVII, there will be 11 bonding and 10 antibonding levels. There are, however, only 21 π-electrons in this radical, and calculations show that it should pick up an extra electron and be converted into a negative ion. On the other hand, there are only 10 bonding and 11 antibonding levels in XVIII where the CH group is joined to a five-membered ring; there is accordingly, place for only 20 electrons in the bonding levels, so that the last electron must occupy an antibonding level and the system must be stable in the form of a positive ion. The result is confirmed by the data of F. N. Stepanov and N. A. Aldanova [3] who have obtained the diazulenylmethyl structure of XVIII in cationic form.

LITERATURE CITED

[1] M. E. Diatkina and E. M. Shustorovich, Proc. Acad. Sci. USSR, 117, 1021 (1957).*

[2] E. Bergmann and J. Hirschberg, et al., Bull. Soc. Chim. France, 18, 697 (1951).

[3] F. N. Stepanov and N. A. Aldanova, in press.

Received June 23, 1958

*Original Russian pagination. See C. B. Translation.

POLAROGRAPHY AT HIGH PRESSURES

S. G. Mairanovskii, M. G. Gonikberg and A. A. Opekunov

(Presented by Academician A. N. Frumkin, June 21, 1958)

Considerable interest attaches to the use of polarography for investigating electrode process and chemical reactions at high pressures. The present communication contains a description of an apparatus and a technique of polarography (with a dropping mercury electrode) for work at pressures up to 3000 kg/cm^2; in the apparatus described here there were obtained the first results from a study of the effect of pressure on the polarographic behavior of certain simple ions.

The construction of the apparatus is shown in Fig. 1. Pressure was generated in the steel vessel 1 by compressing oil with a pressure multiplier. Through the side wall of the lower part of this vessel there was inserted the three-lead electrical cable 4 by means of which the cell electrodes were connected to the electrical measuring circuit. The polarographic cell, 3, and the mercury reservoir, 6, were fastened on the steel frame 8 to which the steel cup 2 was attached. The cell itself was in the form of a glass cylinder into the upper part of which the capillary dropping electrode, 9, and the salt bridge of the comparison electrode, 5, were inserted through ground seals. The lower open end of the cell, which was constricted and serrated, was immersed into the mercury with which the cup 2 was filled. This mercury formed a seal which separated the test solution from the compressing medium (oil) and at the same time served as a bottom and an anode for the cell.

The capillary dropping electrode was equipped with a blade for the forced break-off of the drop [1], so that constancy of the drop period under variation of the electrode potential was assured. For the electrode which was employed, experiment showed the drop period, $\underline{t}$ to remain practically unaltered, even when the pressure was raised from atmospheric to 3000 kg/cm^2. This electrode had the characteristics; m = 1.147 mg$\cdot$ $\cdot$sec^{-1}, t = 0.19 sec. The capillary electrode was joined through a vacuum rubber tube to the glass reservoir 6, containing the mercury. The low rate of flow, $\underline{m}$, of the mercury, and the use of a reservoir 6 of rather large cross-section (about 3 cm diameter) assured that the height of the mercury column would remain practically constant in the course of an experiment (2-3 hours).

A saturated calomel electrode (s.c.e.), 5, served as the reference electrode, the end of the salt bridge (KCl solution) of this electrode being sealed by tightly rolled filter paper and an agar-agar plug. This electrode had a siphon which was filled with mercury, this siphon serving as a seal which would permit equalization of the pressures inside and outside of the electrode.

The entire vessel 1 (Fig. 1) was placed into a water bath in which constancy of temperature (25 ± 0.1°) was maintained with the aid of a sensitive thermostat.

The sequence of the experimental operations was as follows. Mercury was poured into the cup 2 and the cell put in place. The pressure reservoir 6 with the mercury was attached to the holder 8 and the dropping electrode 9 inserted in the cell, after which the oxygen of the air was removed by blowing the cell out with nitrogen. Then the cell was filled under a current of nitrogen with the test solution which had been previously aerated with nitrogen, and the comparison electrode 5 was introduced. Following this the holder with the cell was set into the lower part of the vessel 1 and the electrode leads sealed to the ends of the cable 4; then the cock under the reservoir 6 was opened, the upper part of the vessel (the cap) was screwed onto the lower part, and the entire vessel was filled with oil and immersed in the thermostated bath. After equalization of the temperatures (20-30 minutes) a check polarogram was taken at atmospheric pressure. The pressure was then

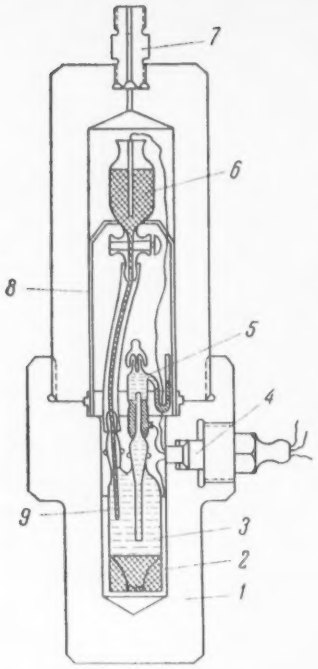

Fig. 1. A cell for polarography under pressure.

increased to 1000 or 3000 kg/cm^2 and, after again equalizing the temperatures, polarograms were obtained under pressure.

Polarographing was carried out in the usual manner, a potential difference being established between the anode (the mercury in cup 2) and the dropping electrode 9 with the aid of a potential divider, and the current flowing in the circuit being then measured on a M-95 microammeter (with a sensitivity of 5-10 μa over the entire scale). The potential of the dropping electrode was measured against the comparison electrode by a P-4 potentiometer having an extended range of measurement [2].

Experiments were carried out on two solutions: a) 1.00 mM TlCl and 0.75 mM HCl in 0.1 N KCl; b) 0.65 mM $CdSO_4$, 0.90 mM $ZnSO_4$ and 0.40 mM HCl in 0.1 N KCl. The experimental results are presented in Table 1 and in Figs. 2 and 3.

A consideration of the experimental data leads to the following conclusions:

1) The Tl^+ half-wave potential (relative to the s.c.e. at the same pressure) and the value of the limiting current remain practically unaltered on raising the pressure from atmospheric to 3000 kg/cm^2.

2) On elevating the pressure to 3000 kg/cm^2, the half-wave potentials for Cd^{2+} and Zn^{2+} are displaced in the direction of more negative values (by 35 and 41 mv, respectively), the value of the limiting current rising somewhat as the pressure is increased from atmospheric to 1000 kg/cm^2.

3) The half-wave potential for the irreversible discharge of H^+ moves in the direction of less negative values (by 24-27 mv) on raising the pressure to 3000 kg/cm^2; the value of the limiting current increases over the entire investigated range of pressures.

4) For each of the investigated ions, the wave slopes are practically independent of the pressure (see Fig. 3).

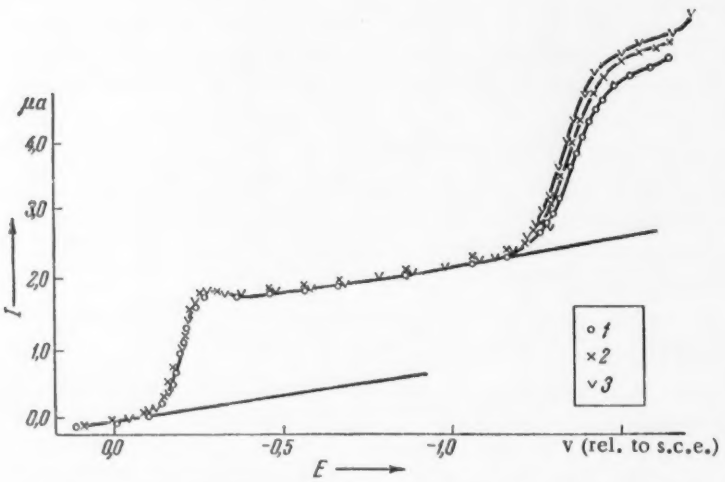

Fig. 2. Polargrams of a TlCl, HCl solution on a KCl background at the pressures:
1) 1; 2) 1000; 3) 3000 kg/cm^2.

TABLE 1

The Pressure Variation of the Polarographic Characteristics of Ions. $E_{1/2}$ is Given in Volts Relative to the s.c.e.; i_l is Given in μa

Pressure kg/cm²	Tl^+		Cd^{2+}		Zn^{2+}		H^+ (C = 0,75 mM)		H^+ (C = 0,40 mM)	
	$E_{1/2}$	i_l	$E_{1/2}$	i_l	$E_{1/2}$	i_l	$E_{1/2}$	i_l	$E_{1/2}$	i_l
Atm.	—0,459	1,53	—0,593	1,30	—0,998	1,77	—1,629	2,34	—1,633	1,21
1000	—0,459	1,54	—0,610	1,41	—1,018	1,89	—1,618	2,60	—1,625	1,34
3000	—0,459	1,53	—0,628	1,40	—1,039	1,85	—1,602	2,74	—1,609	1,42

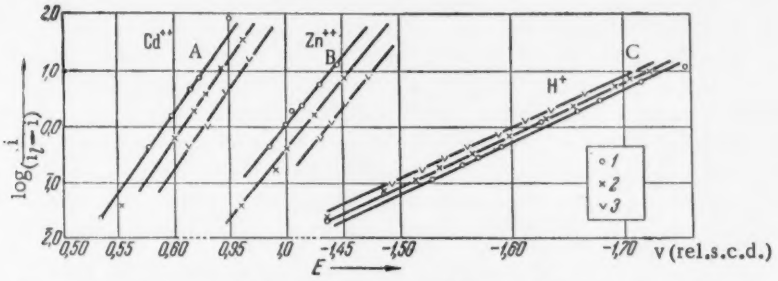

Fig. 3. Graphs of log (i/i_l) vs i for the Cd^{2+} (A), the Zn^{2+} (B) and the H^+ (C) waves at various pressures: 1) 1, 2) 1000; 3) 3000 kg/cm².

For a reversible system, the variation of the half-wave potential can be represented by the equation [3]:

$$\left(\frac{\partial E_{1/2}}{\partial P}\right)_T = -\frac{\Delta V}{nF}, \qquad (1)$$

in which ΔV is the volume alteration in the system resulting from the passage of unit quantity of electricity, n is the number of electrons transferred in the electrode reaction, and F is the value of the Faraday. Experiment shows that for the electrode reaction

$$2Tl^+ + 2Cl^- + 7Hg \rightarrow Tl_2Hg_5 + Hg_2Cl_2,^*$$

$(\partial E_{1/2}/\partial P)_T \approx 0$ and, consequently, $\Delta V \approx 0$. Setting the values of the molar volumes of the various substances into the equation for the reaction, using twice the molar volume of $TlCl_s$ for the unknown volumes of $2Tl^+ + 2Cl^-$, we find the volumes of the substances on the left side of Equations (1) to be ~ 3 cm³/ mole less than those on the right side. It has been noted above that $\Delta V \approx 0$, so that this calculated volume difference should be looked on as being the volume change resulting from the dissolving of two moles of TlCl in a 0.1 N potassium chloride solution to form $2Tl^+ + 2Cl^-$. The published data [5] on the densities of aqueous TlCl, KCl solutions are, unfortunately, lacking in precision. Thus, calculations based on these data show the dissolving of TlCl in 0.05, and in 0.2, N KCl solutions to be accompanied by a certain expansion, whereas dissolving in 0.1, and in 0.5, N KCl leads to a slight contraction.

The very careful investigations of Cohen and Piepenbrock [6] show the dissolving of TlCl in 1.0 N KOH containing KCl to result in a volume increase of 8 cm³/ mole. Thus it is likely that the dissolving of TlCl in 0.1 N KCl is also accompanied by a small increase in volume of the order of 1.5 cm³/ mole. It should be noted

*Thallium amalgam has the composition Tl_2Hg_5 [4].

that there is an increase in volume even in the formation of thallium amalgam from thallium and mercury [4].

In distinction to the Tl^+ wave, the Cd^{2+} and Zn^{2+} waves are associated with rather large negative values of the quantity $(\partial E_{1/2}/\partial P)_T$. The discharge of these ions is accompanied by an increase in volume which arises from the breakdown in the hydrate films, and this results in a positive value for ΔV in Equation (1).

The observed diminution of the hydrogen overvoltage under pressure is of considerable interest and demands further study. The difference in the $E_{1/2}$ values for the hydrogen waves in the two experiments (last columns of Table 1) is related to the well-known effect of the displacement of $E_{1/2}$ to more positive values with increasing H^+ concentration in solutions containing an indifferent electrolyte. We will now consider the effect of pressure on the value of the limiting diffusional current. This diffusional current is determined by the Il'kovich Equation:

$$i_l = 607\, m^{2/3} t^{1/6} CnD^{1/2}\,, \qquad (2)$$

in which C is the concentration of the depolarizer, D is its coefficient of diffusion, and the factor 607 contains the value of the mercury density, d raised to the 2/3 power. Combining m and d, it is possible to replace these quantities in (2) by $w^{2/3}$, w being the volume of mercury flowing from the dropping mercury electrode in unit time. If there is a high degree of dropping constraint and the period of constrained dropping is many times less than that drop period observed when the capillary is operated without a blade, an analysis of the functioning of blade-equipped electrodes shows the drop size to be independent of the surface tension of the mercury at the solution-mercury interface, and to be solely determined by the angle of inclination of the blade and its distance from the end of the capillary. As has been noted above, the drop period t, proves to be almost independent of the pressure. Thus under the experimental conditions, pressure does not appreciably affect the value of w.

It follows that the only quantities in Equation (2) which vary with the pressure are the concentration C (which increases as the pressure rises) and the coefficient of diffusion, D which diminishes with the pressure. We will now replace the product $CD^{1/2}$ in Equation (2) by $v^{-1}\eta^{-1/2}$ (v is the specific volume, and η, the viscosity of the solution) which is proportional to it. According to the data of Bridgman [7], the pressure variations of v and $\eta^{1/2}$ are mutually compensating to a considerable degree. Thus the value of $v \cdot \eta^{1/2}$ for water at 30° is altered by only 0.3% on increasing the pressure from atmospheric to 3000 kg/cm^2. For this reason only a very insignificant alteration in i_l is to be anticipated under the experimental conditions.

In actuality, the value of the limiting current for the Tl^+ ions at 25° remains practically unaltered over the pressure interval up to 3000 kg/cm^2. This situation is, however, not repeated for the other ions which have been studied, the observed alterations in i_l falling far beyond the limits of error of measurement, and further studies are needed to discover the cause of this variation.

LITERATURE CITED

[1] E. M. Skobets and N. S. Kavetskii, Zav. Lab. 15, 1299 (1949).

[2] S. G. Mairanovskii and N. N. Silin, Zav. Lab. 25 (1959).

[3] E. Cohen and K. Piepenbrock, Zs. phys. Chem. A, 170, 145 (1934).

[4] T. W. Richards and F. Daniels, J. Am. Chem. Soc. 41, 1732 (1919).

[5] J. A. V. Butler and E. S. Hiscocks, J. Chem. Soc. 1926, 2554.

[6] E. Cohen and K. Piepenbrock, Zs. phys. Chem. A, 167, 365 (1933).

[7] P. V. Bridgman, The Physics of High Pressures (in Russian), 1935.

The N. D. Zelinskii Institute of Organic Chemistry
of the Academy of Sciences of the USSR

Received June 20, 1958

THE ADSORPTION OF HYDROCARBONS AT RAISED TEMPERATURES

I. V. Smirnova and K. V. Topchieva

(Presented by Academician P. A. Rebinder, July 2, 1958)

In order to establish the mechanism of contact changes undergone by hydrocarbons it must first of all be possible to examine the elementary stage of the process taking place at the surface of the catalyst. Adsorption methods of studying individual hydrocarbons of different structure can be used to determine the orientation of the molecules on the surface of the catalyst and to find the molecular constants. Adsorption measurements carried out at raised temperatures under the conditions which precede the catalytic decomposition of hydrocarbons are therefore of importance in the study of heterogeneous catalysis processes.

The present communication gives the results of a study of the adsorption of isopropylbenzene, isopropenylbenzene, propenylbenzene, allylbenzene and cyclohexene from solutions onto aluminum oxide, which, as is well known, catalyzes many important processes, including the isomerization of hydrocarbons. In the case of several of these hydrocarbons (isopropylbenzene, allylbenzene, cyclohexene) the catalytic changes in both the vapor and the liquid phases have already been studied and a mechanism for the process suggested [1-4].

Alkylaromatic hydrocarbons with an unsaturated bond in the side chain (propenylbenzene, isopropenylbenzene) are of particular interest, since they appear as intermediate products in the suggested schemes by which the catalytic processes take place. We have compared the adsorption of these hydrocarbons with the adsorption of n-propylbenzene, which has a similar structure and the same number of carbon atoms in the molecule, and also with the adsorption of benzene.

The study of the above series of hydrocarbons is important, in our opinion, also because of the fact that it makes it possible to examine the influence shown by a conjugated double bond in the side chain of the aromatic ring (n-propylbenzene and propenylbenzene, isopropylbenzene and isopropenylbenzene) on the process of adsorption from solution. It is also possible to compare the relative ease of adsorption of hydrocarbons with the unsaturated bond in different positions (allylbenzene–propenylbenzene). The measurements of the adsorption from solution were carried out by an interferometric method [5]. The solvent used was normal heptane. The adsorbent was industrial (rod) aluminum oxide with a specific surface of 250 m^2/g [5] and a pore radius of 40 A. Measurements of the adsorption were carried out at 20, 30 and 40°. The adsorption isotherms for the individual hydrocarbons studied at 20 and 40° are given in Figs. 1 and 2. The molecular constants for the hydrocarbons studied, calculated from the adsorption measurements, are given in Table 1.

The thickness of the adsorbed layer of benzene molecules on the surface of the aluminum oxide is equal to the calculated theoretical thickness of the benzene ring, 3.7 A [7]. The benzene molecules are therefore arranged in planar fashion parallel to the surface of the catalyst.

Similar values for τ are also found for the other alkylaromatic hydrocarbons studied: isopropylbenzene, propenylbenzene, isopropenylbenzene. These molecules are evidently arranged on the surface in the same way as the benzene molecules, i.e., with the plane of the benzene ring parallel to the surface of the aluminum oxide. Thus the presence of the conjugated double bond in the side chain of the alkylaromatic molecule does not alter its plane-parallel orientation in the monolayer when adsorbed on the catalyst surface. The allylbenzene molecules are probably in a less planar arrangement. The decrease in the value of τ for n-propylbenzene is evidently related to the lower density of its monolayer compared with those of the other hydrocarbons studied. The arrangement of the molecules of the hydrocarbons studied parallel to the surface of the aluminum oxide is also retained as the temperature is increased.

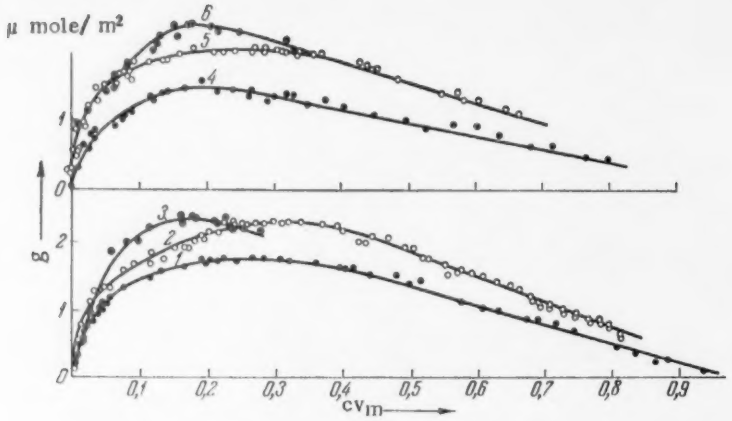

Fig. 1. Absolute adsorption isotherms for isopropylbenzene (1), benzene (2), isopropenylbenzene (3), n-propylbenzene (4), allylbenzene (5) and propenylbenzene (6) at 20°.

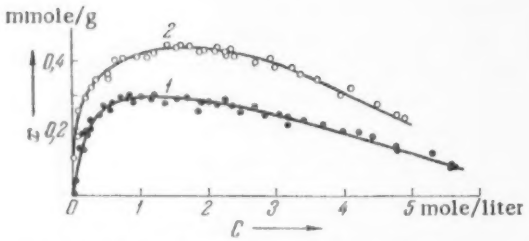

Fig. 2. Adsorption isotherms for n-propylbenzene (1) and allylbenzene (2) at 40°.

Analysis of the data given in Table 1 shows that the change from an aromatic hydrocarbon with a saturated alkyl radical to one with a radical carrying an unsaturated bond is accompanied by a considerable reduction in the molecular area ω_0, i.e., the area covered by one molecule in the compact monolayer (n-propylbenzene–propenylbenzene, isopropylbenzene–isopropenylbenzene).

The magnitude of the molecular area, covered by one molecule of benzene at 20° in the compact monolayer on aluminum oxide, ω_0 = 44 A^2, which is close to the value obtained for the adsorption of benzene from solution in n-heptane onto silica gel [8].

When the temperature is increased, the fraction of the surface taken up by each adsorbed molecule increases, while the thickness of the adsorbed layer decreases slightly. This "thinning" of the adsorbed layer is evidently related to the fact that the adsorbed molecules of the hydrocarbons under study are not fastened to the surface and acquire a greater mobility as the temperature is increased. This conclusion is of considerable interest from the point of view of catalysis.

The adsorption measurement data obtained at 20° show that propenylbenzene, isopropenylbenzene and allylbenzene, which contain a double bond in the side chain, are adsorbed to a greater extent than the aromatic molecules having a saturated alkyl radical with the same number of carbon atoms. The adsorption maxima for propenylbenzene and isopropenylbenzene correspond to lower concentration values than the adsorption maxima of allylbenzene, isopropylbenzene and n-propylbenzene.

This shift of the adsorption maxima cannot be explained by the lower molecular volumes v_m of these compounds (see Table 1) but is related to the increase in the adsorption potential [9, 10] with the appearance of a conjugated double bond in the side chain of the aromatic molecule. Evidence for this is also provided by the decrease in the molecular area ω_0 for these hydrocarbons.

The effect of the double bond in the side chain of the aromatic nucleus in increasing the adsorption accords with its high reactivity on aluminum oxide. It is known from the literature [1, 2] that the active centers on aluminum oxide bring about catalytic isomerization as a result of a shift in the position of the double bond in a side chain.

TABLE 1

Hydrocarbon	V_m cc/mole	τ, Å	ω_0, Å²	G_{max} μ mole/m²	Adsorption potential, cal/mole
I. 20°					
Benzene	88,8	3,7	44		
n-Propylbenzene	139,4	2,8	81	1,47	1550
Isopropylbenzene	139,5	3,9	60	1,75	1100
Allylbenzene	132,4	4,1	52	2,05	1190
Propenylbenzene	129,3	3,8	54	2,37	1760
Isopropenylbenzene	129,7	3,8	56	2,37	1860
II. 40°					
n-Propylbenzene	141,5	2,3	99	1,17	1970
Allylbenzene	134,4	3,6	63	1,75	1610

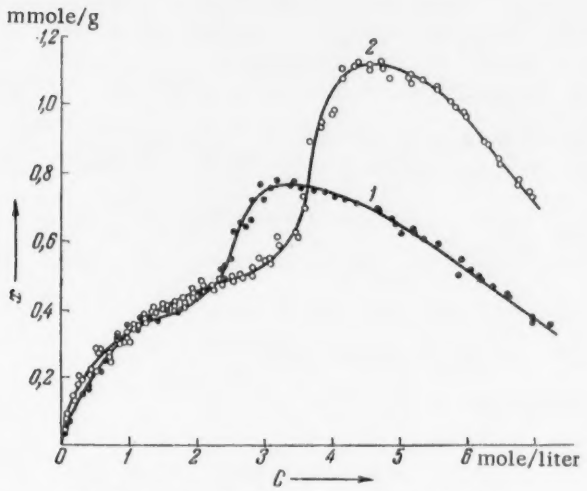

Fig. 3. Adsorption isotherms for cyclohexene: 1) at 30°; 2) at 20°.

Calculation shows that the shift of the double bond in the side chain of an aromatic molecule into the conjugated position as we go from allylbenzene to propenylbenzene also brings about a considerable increase in the adsorption potential, although the magnitude of the maximum adsorption increases only slightly. The greater ease of adsorption of propenylbenzene compared with allylbenzene provides justification for applying to the treatment of the results of the catalytic isomerization of allylbenzene into propenylbenzene a kinetic equation which assumes that the reaction products are more strongly adsorbed than the starting materials.

Analysis of the results obtained at 40° shows that for both the hydrocarbons studied, increase in temperature leads to a decrease in the adsorption. At the same time the maxima on the adsorption isotherms of allylbenzene and n-propylbenzene correspond to lower concentrations than the maxima obtained at 20°, which is related to an increase in the adsorption potential of approximately 400 cal/mole.

Examination of the adsorption from solution of the series of individual hydrocarbons studied leads to the conclusion that a conjugated double bond shows specific behavior on the aluminum oxide surface. In the general planning of this work, considerable interest was attached to a comparison of the adsorption of cyclic hydrocarbons containing different numbers of double bonds in the ring.

It is known that the chemical nature of the adsorbent has a considerable influence on the adsorption of

hydrocarbons having an unsaturated bond. Thus benzene is adsorbed on silica gel to a greater extent than cyclohexene [11, 12], but K. V. Topchieva [13] has shown that the adsorption picture is changed when aluminosilicate catalysts or aluminum oxide are considered. When cyclohexene vapor is adsorbed, an increase in the density of the cyclohexene monolayer is observed, and this is explained by orientation of the molecules with the double bond towards the catalyst surface. This assumption, together with the irreversibility of the adsorption isotherm for cyclohexene vapor, enables us to speak of chemisorption of the latter, which is of importance for catalysis. The adsorption isotherms obtained for the adsorption of cyclohexene from n-heptane solution onto industrial aluminum oxide at 20 and 30° are given in Fig. 3. In contrast to the isotherms which we have given earlier, they have a point of inflection after which the adsorption increases sharply, passes through a maximum, and falls linearly. The shape of the isotherms indicates that rearrangement of the cyclohexene molecules takes place in the range of concentrations above the point of inflection. Calculation of the absolute adsorption isotherms to a first approximation [6] shows that the area occupied by a molecule of cyclohexene in the compact monolayer is equal to approximately 27 A^2. At the point of inflection on the isotherm, the average area occupied by a molecule on the aluminum oxide surface amounts to approximately 60 A^2.

Thus the cyclohexene molecules are adsorbed on the aluminum oxide surface at first in planar fashion, as in the case of benzene molecules, but afterwards, as the concentration increases, they rearrange themselves and stand on edge, with the double bond directed towards the catalyst surface.

As the temperature is increased, the maximum on the adsorption isotherm is shifted towards the region of lower concentrations, i.e., at 30° the greater part of the adsorbed cyclohexene molecules are arranged with their edges towards the catalyst surface. Since the isomerization of cyclohexene on aluminum oxide starts at 40° under the conditions of the experiment, it is evident that this orientation precedes the catalytic change.

Thus the presence of one double bond in the molecule of a cyclic hydrocarbon undergoing adsorption on a catalyst introduces a number of peculiar features into the adsorption process.

LITERATURE CITED

[1] K. V. Topchieva, A. I. Pletiushkina and I. A. Zen'kovich, J. Gen. Chem. 34, 631 (1958).*

[2] K. V. Topchieva, A. I. Pletiushkina and V. A. Tronova, J. Gen. Chem. 34, 638 (1958).*

[3] A. P. Ballod and K. V. Topchieva, Prog. Chem. 20, 161 (1951).

[4] K. V. Topchieva, A. P. Ballod, I. V. Patsevich and N. Rtishcheva, Bull. AN SSSR, Div. Chem. Sci. 1954, 478.*

[5] I. V. Smirnova, K. V. Topchieva and L. P. Mil'kova, J. Phys. Chem. 32, 43 (1958).

[6] A. V. Kiselev, Proc. Acad. Sci. 61, 657 (1948).

[7] L. Pauling, The Nature of the Chemical Bond, 1947, p. 192.**

[8] A. V. Kiselev and Iu. A. El'tekov, Proc. Acad. Sci. 100, 107 (1955).

[9] V. K. Semenchenko, Colloid J. 9, 125 (1947).

[10] O. M. Dzhigit, A. V. Kiselev, M. G. Terekhova and K. D. Shcherbakova, J. Phys. Chem. 22, 107 (1948).

[11] G. Spengler and K. Krenkler, Erdöl u. Kohle, 3, 120 (1950).

[12] E. A. Mikhailova and B. A. Kazanskii, Studies in Chromatography, Izd. AN SSSR, 1952, p. 155.

[13] K. V. Topchieva, J. Phys. Chem. 27, 411 (1953).

Physical Chemistry Department,
M. V. Lomonosov State University, Moscow

Received June 18, 1958

*Original Russian pagination. See C. B. Translation.

**Russian translation.

THE EXTRACTION OF SULFIDE INCLUSIONS FROM MOLTEN SLAGS BY MEANS OF AN ELECTRIC FIELD

V. V. Khlynov and O. A. Esin

(Presented by Academician I. P. Bardin, June 25, 1958)

In the present work we report the results of studies which we have carried out on the use of the electrocapillary movement of liquid-metal drops [1] for the extraction of sulfide inclusions from molten slags.

The experiments were carried out at a temperature of approximately 1400° in corundum or porcelain boats filled with molten factory-waste slags with the following composition (percentages): CaO 15, Al_2O_3 10; SiO_2 43; Fe_{total} 20; MgO 10; Ni 0.1-0.2; Co 0.02 and S 0.15-0.2. The greater part of the nickel and cobalt in these slags is in the form of inclusions of matte with the composition Ni 15; Co 0.5-0.6; S 16-17 and Fe 65 and dimensions of between 10^{-4} mm and 0.2 mm (the white points in Fig. 1a). The current was supplied by means of carborundum rods, which reduced the iron oxides only in the very small slag volumes directly in contact with the rods.

In the preliminary experiments a drop of matte with large radius r = 0.9–1.3 mm was immersed in the slag and a constant electric field with intensity E = 5–7 volts/cm applied for times varying between 2 and 10 minutes. The cell was then cooled rapidly and broken up, and the distance moved by the drop measured. It was established that the inclusions move towards the cathode at rates $u = 7-10 \cdot 10^{-3}$ cm/second, corresponding to mobilities of $v = u/Er = 1.0-1.5 \cdot 10^{-2}$ cm/second · volt.

In order to find out why the direction of movement was found to be the reverse of that observed earlier [1] and the mobility considerably less, we studied the influence of slag composition. The results of experiments with Ni_3S_2 drops in slags of different composition containing no iron are given in Table 1. They show that the mobility of the drops is inversely proportional to the viscosity (η) of the slag. In agreement with this, the charge density at the drop surface (ϵ), calculated from the formula [3]

$$\epsilon = v \cdot 2\eta, \tag{1}$$

was practically the same in all cases, namely: $12-13.5 \cdot 10^{-6}$ coulombs/cm^2.

The data obtained with various concentrations of iron oxide present in the slag are given in Table 2. Increase in the FeO concentration at first reduces the mobility of the drops but from 8% FeO onwards, the direction of their movement is reversed. In other words, the charge on the sulfide, which is negative in a slag containing no iron, decreases with the addition of FeO, passes through zero, and becomes positive. As the FeO concentration increases, the transfer of iron ions from the slag to the sulfide evidently begins to play a greater part in the formation of the double layer:

$$Fe^{2+}_{(slag)} \rightarrow Fe_{(sulfide)} - 2e, \tag{2}$$

instead of the reverse transfer of nickel ions:

$$Ni_{(sulfide)} \rightarrow Ni^{2+}_{(slag)} + 2e. \tag{3}$$

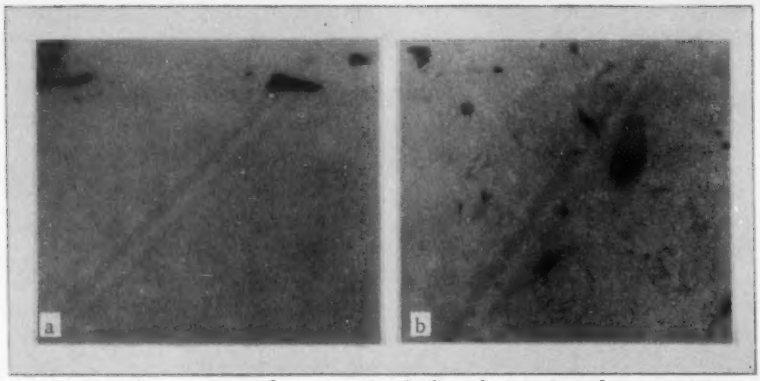

Fig. 1. Microsections of a waste slag before the passing of current (a) and after the passage of a current of 0.05 amps. for 5 minutes (b). White spots – matte inclusions, dark regions – pores. × 340.

TABLE 1

The Mobility of Ni_3S_2 Drops in Slags Containing no Iron

Slag composition, %			η, poises [8]	r, cm	E, volts/cm	u, cm/sec.	v, cm/sec · volt	Direction of movement
FeO	CaO	SiO_2						
23	43	34	1	0,1	3	$6 \cdot 10^{-3}$	$20 \cdot 10^{-3}$	Towards the cathode
23	37	40	1,5	0,09	3	$6,1 \cdot 10^{-3}$	$22 \cdot 10^{-3}$	Towards the cathode
23	35	42	2	0,1	3	$5,9 \cdot 10^{-3}$	$19,7 \cdot 10^{-3}$	Towards the cathode
23	31	46	4	0,08	3	$5,8 \cdot 10^{-3}$	$24 \cdot 10^{-3}$	Towards the cathode
23	31	46	4	0,11	3	$5,9 \cdot 10^{-3}$	$18 \cdot 10^{-3}$	Towards the cathode
23	31	46	4	0,135	3	$6 \cdot 10^{-3}$	$15 \cdot 10^{-3}$	Towards the cathode
23	31	46	4	0,135	9	$17 \cdot 10^{-3}$	$14 \cdot 10^{-3}$	Towards the cathode

TABLE 2

The Influence of the FeO Content of the Slag on the Movement of the Drops

Slag composition, %			η, poises [2]	r, cm	E, volts/cm	u, cm/sec	v, sec/cm · volt	Direction of movement
CaO	SiO_2	Al_2O_3						
48	42	10	6	0,11	2,55	2,8	10	Towards the anode
41	47	12	18	0,12	2,55	0,95	3,1	Towards the anode
36	51	13	30	0,10	2,55	0,5	1,95	Towards the anode
30	56	14	75	0,11	2,55	0,25	0,9	Towards the anode

As the FeO content reaches 8%, process (2) starts to predominate. Further increase in the FeO concentration, however, does not lead to an increase in the mobility of the drops but to a decrease in their mobility, in spite of the increase in their positive charge and the decrease in the viscosity of the slag. In this connection the most simple formula (1) proves to be inapplicable.

In fact, the high value of the exchange current [4] at the boundary between the metal and a slag containing appreciable concentrations of FeO, together with the high limiting diffusion currents (i_{lim}) [5], provide evidence that theories dealing with an ideally polarizable drop cannot be applied to the case under consideration. The equation defining the mobility of a partly polarizable drop [6]:

$$v = \frac{\epsilon r}{2\eta(1 + r/2\kappa w)} \qquad (4)$$

TABLE 3

The Mobility of Sulfide Drops in Slags Containing 23% FeO

Slag composition %				r, cm	E, volts/cm	u, cm/sec.	v, cm/sec · · volt	Direction of movement
CaO	Al_2O_3	SiO_2	FeO					
52	41	7	—	0,1	2,2	4,5	20	Towards the anode
50,5	40	7	2,2	0,1	2,2	4,5	20	Towards the anode
49,5	39,1	7,15	4,25	0,09	2,2	2,7	13,5	Towards the anode
47,2	37,3	7,3	8,2	0,1	2,2	$1,3 \cdot 10^{-2}$	$6 \cdot 10^{-2}$	Towards the cathode
39,5	31,2	7,7	21,4	0,11	2,2	$3,6 \cdot 10^{-3}$	$15 \cdot 10^{-3}$	Towards the cathode

contains a depolarization coefficient k (the expression in brackets), in which κ is the electrical conductivity of the electrolyte, and

$$w = \frac{RT}{nFi_{lim}}, \tag{5}$$

where n is the number of charges on the ion, F is the Faraday. For the particular case, assuming that the polarization is a concentration polarization [4, 5, 7] and taking $i_{lim} = 0.5$ (% FeO) amps/cm^2, and $\kappa = 0.3$ $ohm^{-1} \cdot cm^{-1}$, we have, for a drop with r = 0.1 cm in a slag containing 20% FeO, the fairly high depolarization coefficient k = 25. The decrease in the polarizability of the drop is probably also the main reason for the decrease in its mobility in slags containing iron oxides.

Further confirmation of this is provided by the results of experiments with slags containing a constant concentration of FeO (23%) and variable CaO and SiO_2 concentration (Table 3). It was found that in this case the mobility of the drops was almost independent of the viscosity of the slag, in spite of the fourfold increase in the latter. It is evident that the retarding influence of the increase in viscosity is here compensated by an increase in the force moving the drop. This can hardly be put down to an increase in the charge on the drop, since this is not observed when CaO is replaced by SiO_2 in slags containing no iron. The most probable explanation is that the compensation is related to a reduction in the limiting diffusion current and the consequent reduction in the depolarization coefficient.

It is interesting to note that the direction of movement of the nickel sulfide drops coincides with that observed for the matte in a waste slag, while the mobilities of sulfide drops and matte differ little from one another. It is possible that this is caused by a similarity in the compositions of the surface layers of both types of drop, resulting from the reaction:

$$Ni_{(sulfide)} + Fe^{2+}_{(slag)} = Fe_{(sulfide)} + Ni^{2+}_{(slag)}. \tag{6}$$

In order to extract the drops of matte from molten (1400°) waste slags, a current of 0.05-0.1 amp. was passed through the slags with a voltage drop of 7-15 volts/cm. The cell was then rapidly cooled and sections taken at different places along the length of the boat. When these sections were examined under the microscope it was found that the number of beads in the slag surface layer to a depth of 0.1 mm had not changed appreciably. Probably the presence in this layer of a very viscous film, rich in Fe_2O_3, paralyzed the movement of the inclusions. On the other hand the number of drops in the bulk of the slag had fallen sharply (see Fig. 1a and 1b) while the number in the region of the cathode had increased.

The experiments carried out have thus confirmed that it is possible to extract valuable sulfide inclusions from molten waste slags using electrocapillary movement.

Two interesting features were observed in these experiments. A considerable number of drops observed in the cathode region had dimensions (up to 1-1.5 mm) which were much larger than those of the original drops.

At the same time the actual mobility of fine drops proved to be many times greater than that calculated according to Equation (4). For example, after a current of 0.05 amp (E = 12 volts/cm) had been passed for 10 minutes, a central region of the cell 5 cm long contained no inclusions with dimensions less than $3 \cdot 10^{-5}$ cm. In other words, beads of this size have moved a distance of at least 3 cm. Their mobility ($vr = 4 \cdot 10^{-4}$ cm/second per volt/second) is thus more than 100 times greater than that calculated using Equation (4) ($vr = 3.3 \cdot 10^{-6}$ cm/second per volt/second). These features are evidently the result of the mutual entrainment of the drops as they move. It is known that layers of electrolyte adhering to a drop in an electrical field undergo a tangential movement which terminates behind the drop [3]. This movement, which is more powerful around large drops, may entrain finer drops situated close to the large drops and lead to coalescence. Actual observation of mercury drops in a solution of KCl in glycerol confirms this. The fine drops of Hg situated around large drops (2 mm) rapidly coalesce with the large drop when a current is switched on.

This coalescence increases the rate of removal of inclusions from the slag. As a particular example, the observed mobility ($4 \cdot 10^{-4}$) of drops of matte, according to Equation (4), corresponds to a radius of 10^{-3} cm. The number of beads of this size in the slag is fairly high. Their rate of movement evidently also determines the rate of extraction of the finer matte particles.

LITERATURE CITED

[1] V. V. Khlynov and O. A. Esin, Proc. Acad. Sci. 120, No. 1, 134 (1958).*

[2] J. S. Machin and Tin BooYee, J. Am. Ceram. Soc. 31, No. 7, 200 (1948).

[3] A. N. Frumkin, Bull. AN SSSR, Div. Chem. Sci. 1945, 223.

[4] Iu. P. Nikitin and O. A. Esin, Proc. Acad. Sci. 116, No. 1, 63 (1957).*

[5] O. A. Esin and V. A. Chechulin, J. Phys. Chem. 19, 573 (1945).

[6] O. A. Esin and G. A. Toporishchev, J. Phys. Chem. 31, 474 (1957).

[7] P. P. Kozakevich, S. P. Leiba and E. P. Komar', J. Phys. Chem. 13, 248 (1939).

S. M. Kirov Ural Polytechnical Institute

Received June 24, 1958

*Original Russian pagination. See C. B. Translation.

THE PART PLAYED BY THE EMULSIFIER IN THE OXIDATION-REDUCTION INITIATION OF EMULSION POLYMERIZATION

A. I. Iurzhenko, N. Ia. Ivanova and V. D. Enal'ev

(Presented by Academician P. A. Rebinder, July 3, 1958)

It has been established by a number of authors [1, 2] that one of the important factors influencing the kinetics of polymerization in emulsions is the nature of the emulsifying agent. The nature of the emulsifier used not only influences the rate of the polymerization process but also has a determining effect on the properties of the polymers formed [3].

This influence shown by the emulsifier on the kinetics of the polymerization process in emulsions must be related first of all to the purely colloid-chemical properties of the soaps used, namely: the critical concentration of micelle formation, the magnitude and shape of the micelles and the ability of the micelles of emulsifier to bring the monomer and the initiator into colloidal solution, since the micelles of the surface-active emulsifier, as has been shown earlier, form the sites where the polymerization process takes place in emulsions.

In our studies of emulsion polymerization in the presence of various emulsifiers we have observed a number of peculiar features in the polymerization process which takes place when the emulsifier used is cetylpyridinium bromide (CPB). The experiments have shown that in this case the part played by the emulsifier cannot be ascribed solely to a purely colloid-chemical factor.

The study was carried out by a dilatometric method using a dilatometer which made it possible to avoid contact between the polymerization system and the atmosphere [4]. The system was stirred by means of a magnetic stirrer. All the experiments were carried out with a hydrocarbon to aqueous-phase ratio of 1:9. The initiator used was isopropylbenzene hydroperoxide (IHP), the monomer – styrene.

Studies were made of the polymerization kinetics at various temperatures. In one series of experiments sodium carbonate was added to the aqueous phase in amounts corresponding to a concentration of 0.1 g-equivs. per liter of aqueous phase. The results of these experiments are given in Fig. 1. It can be seen from the data presented that the rate of the polymerization reaction is considerably greater than when other types of emulsifier are used (sulfonic acid soaps, salts of fatty acids), other conditions being the same; CPB brings about a satisfactory rate of polymerization at low temperatures (4 and 18°) which is not the case when the other emulsifiers are used. The most important difference observed in polymerization in the presence of CPB is that, when sodium carbonate is present in the aqueous phase, the rate of polymerization passes through a maximum as the temperature is increased.

It is interesting to note that in the experiments carried out at 40 and 60°, the polymerization develops at a certain speed in the initial stages, after which it rapidly slows down and soon stops altogether; this is naturally related to the exhaustion of the initiator. When the temperature is reduced the polymerization proceeds at a satisfactory rate and the yield of polymer is simultaneously increased.

In the experiments carried out in the absence of sodium carbonate, a regular increase in the rate of the polymerization process is observed as the temperature is increased, while the linear relationship $S = f(t)$ is preserved up to a considerable degree of polymerization (Fig. 2).

It may be concluded from a comparison of the kinetic data obtained in experiments with and without the

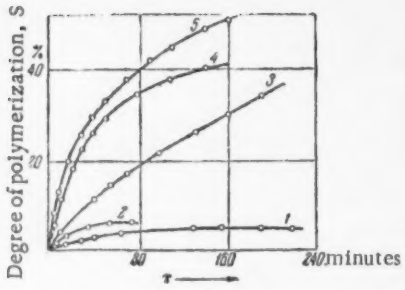

Fig. 1. Kinetics of the polymerization of styrene in the presence of sodium carbonate.
Concentration: Na_2CO_3 0.1 N, CPB 0.01 M (in the aqueous phase), IHP 0.01 M (in the hydrocarbon phase). 1) 60°; 2) 40°; 3) 4°; 4) 30°; 5) 18°.

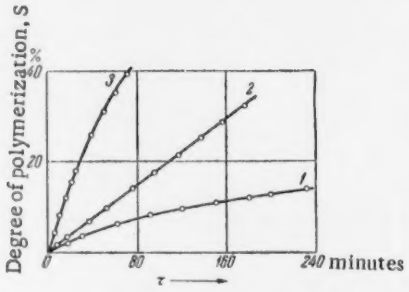

Fig. 2. Kinetics of styrene polymerization.
Concentration: CPB 0.01 M (in the aqueous phase), IHP 0.01 M (in the hydrocarbon phase). 1) 20°; 2) 40°; 3) 60°.

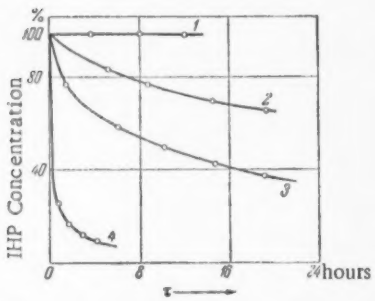

Fig. 3. Kinetics of IHP decomposition.
Concentrations: IHP, CPB 0.01 M, Na_2CO_3 0.1 N (in aqueous solution), 1) IHP, t = 100°; 2) IHP + CPB, t = 100°; 3) IHP + CPB + Na_2CO_3, t = 20°; 4) IHP + CPB + Na_2CO_3, t = 50°.

addition of sodium carbonate that the addition of sodium carbonate and increase in the temperature bring about the same effect – an increase in the rate of polymerization.

The rate of the polymerization process is dependent on the rate of initiation, which in turn is dependent on the process of initiator decompositon, which forms a source of primary free radicals. When the concentration of free radicals increases sharply as a result of rapid initiator decomposition, however, a considerable fraction of the radicals are used up unproductively by recombining with one another. At the same time the increased rate of decomposition of the initiator leads to its exhaustion in the very early stages of the polymerization. As experiment shows, accelerated initiator decomposition of this kind is brought about by CPB.

The decomposition of IHP used as initiator in aqueous solution is accelerated considerably by the addition of CPB even in the absence of Na_2CO_3. An even greater acceleration of the decomposition of IHP is observed when CPB and sodium carbonate are present together. Data on the kinetics of IHP decomposition under various conditions are given in Fig. 3.

The considerable increase in the rate of decomposition of IHP under the influence of CPB, which is not observed when other emulsifiers are used, is explained, in our opinion, by an oxidation-reduction reaction taking place between the IHP and the CPB; the reaction, moreover, proceeds more rapidly in the presence of sodium carbonate. This point of view is confirmed by the fact that the polymerization of styrene in the presence of an oxidation-reduction initiator system consisting of IHP and a pyrophosphate complex of ferrous iron shows analogous relationships (Fig. 4).

Increase in the temperature brings about an increase in the initial rate of polymerization with a reduction in the final yield of polymer, i.e., the initiator system is exhausted in the earlier stages of the polymerization process. The same effect is brought about by the addition of sodium carbonate.

It was established by separate experiments that the oxidation-reduction reaction in the IHP–Fe^{++} system takes place more rapidly when the temperature is increased and when sodium carbonate is added.

It appears probable that in emulsion polymerization using the emulsifying and initiating agents mentioned above, the activation is the result of hydrolytic opening of the pyridinium ring in alkaline medium [5, 6]:

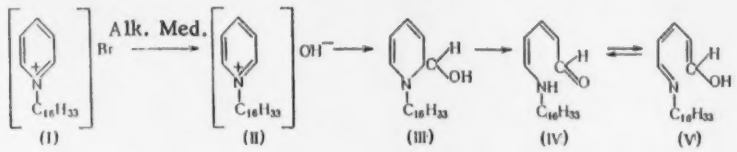

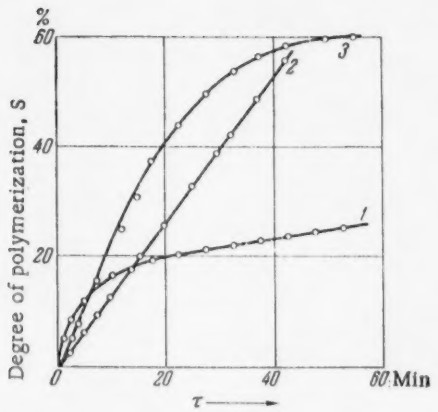

Fig. 4. Kinetics of styrene polymerization in the presence of an oxidation-reduction system consisting of IHP and a pyrophosphate complex of ferrous iron. Concentration of Nekal in the aqueous phase 2%, concentration of IHP 0.03 M (in the hydrocarbon phase).
1) Temperature 5° in the presence of Na_2CO_3; 2) 5° without sodium carbonate; 3) 15° without sodium carbonate.

The role of activators may be taken both by the aldehyde group and also by the >NH group [7], which are formed when the ring opens. Further evidence for this scheme is provided by the fact that the final products of the decomposition are shown by experiment to have a yellow–orange color, which should be the case for compounds IV and V, which are derivatives of glutaconic aldehyde.

A comparison of the data presented leads to the conclusion that a surface-active emulsifier (in this case cetylpyridinium bromide) may play a double role in emulsion polymerization.

In the first place it may act as an ordinary emulsifier, stabilizing the original monomer emulsion and forming a latex, and also facilitating the course of the polymerization process in the aqueous phase by dissolving monomer and initiator together.

In the second place, the emulsifier may act as polymerization activator by causing induced decomposition of hydroperoxide, which leads to a sharp increase in the rate of the polymerization process even at low temperatures, at which polymerization does not take place under ordinary conditions.

By activating the decomposition of IHP as a result of an oxidation-reduction reaction, CPB increases the rate of formation of the primary free radicals, the rate of the initiation reaction, and consequently the rate of the polymerization process as a whole.

LITERATURE CITED

[1] A. I. Iurzhenko, Proc. of the 3rd Conference on High-Molecular Weight Compounds, Izd. AN SSSR, 1948, p. 54 [in Russian].

[2] I. M. Kolthoff and W. J. Dale, J. Am. Chem. Soc. 69, 441 (1947).

[3] N. S. Tsvetkov and A. I. Iurzhenko, Colloid J. 15, 308 (1953).*

[4] T. I. Iurzhenko and V. A. Puchin, Zavodskaia Lab. 21, 205 (1955).

[5] Th. Zincke, Lieb. Ann. 330, 368 (1904); 330, 328 (1904).

[6] Heterocyclic Compounds, 1, IL, 1953, p. 330 [in Russian Translation].

[7] G. S. Withby, N. Wellman, O. W. Floutz and H. L. Spehens, Ind. and Eng. Chem. 42, 445 (1950).

Ivan Franko State University, Lvov

Received May 16, 1958

*Original Russian pagination. See C. B. Translation.

THE DISTRIBUTION OF IMPURITY IN A MONOCRYSTAL OF METALLIC ZINC POSSESSING A HONEYCOMB-LIKE SUBSTRUCTURE

M. Valoukh and I. B. Borovskii

(Presented by Academician I. P. Bardin, July 10, 1958)

A number of studies have shown [1] that many metal monocrystals, prepared by crystallization from a melt, have different characteristic types of substructure. One of the most frequently encountered types of substructure in metal monocrystals formed at intermediate growth rates and temperature gradients is the prismatic type. The cross-section of the prismatic filaments of the substructure, which passes through the monocrystal in the direction of its growth, appears like a honeycomb.

A qualitative theoretical explanation of the substructure obtained has been given in a paper [2], in which the formation of the substructure is related to the presence of impurities in the metals. In the nonequilibrium crystallization process, the impurities bring about the formation of zones of concentration supercooling in the layer of the melt adjoining the boundary between the two phases (liquid–solid). In this zone it is easy for spontaneous crystallization of the metal to take place with the production of microscopic nuclei showing statistical distribution and no preferred orientation on the plane of separation. The concentration gradient close to the microscopic nuclei causes diffusion of the impurity atoms, which results in nonequilibrium distribution of these impurity atoms in the substructure which is formed. From a general consideration of the diagram of state for the main metal–impurity metal system, it follows directly that when the impurity increases the melting point of the metal, the concentration of the impurity should increase in the center of the substructure filament. In the case where the impurity brings about a reduction in the melting point the concentration of the impurity should increase at the edges of the substructure filament. The dimensions of the "cells" of the substructure are determined by the "sphere of influence" of the initial microscopic nuclei formed. The latter in turn depends on the rate of growth of the monocrystal, the temperature gradient, the relative rate of diffusion and the solution volume.

Increase in the concentration of impurity atoms at the edges of the substructure filaments was first established using a radiographic method in a study of the substructure of a monocrystal of lead containing antimony as impurity (by means of the radioactive isotope Sb^{124}). The decrease in the concentration of impurities at the edges of substructure filaments, predicted from general theoretical considerations, has not been observed experimentally. The aim of the present work was to study the distribution of an impurity (copper) within the substructural units of a zinc monocrystal.

The Chokral'skii method was used to prepare a monocrystal of zinc containing 0.7% of copper.* The rate of removal of the monocrystal from the melt was 10 mm/minute, temperature gradient approximately 20°/cm. The concentration of other elements present was less than 0.01%. A section was cut from the monocrystal obtained in a direction perpendicular to the axis. The fibrous honeycomb-like structure was revealed after chemical polishing (Fig. 1). The distribution of the copper within the substructural units of the zinc monocrystal was examined by the x-ray spectral method for studying the chemical composition of alloy microvolumes [3], using a RSASh-2 apparatus [4].

*The monocrystal was prepared in the Karlov Institute of Physics, Prague University.

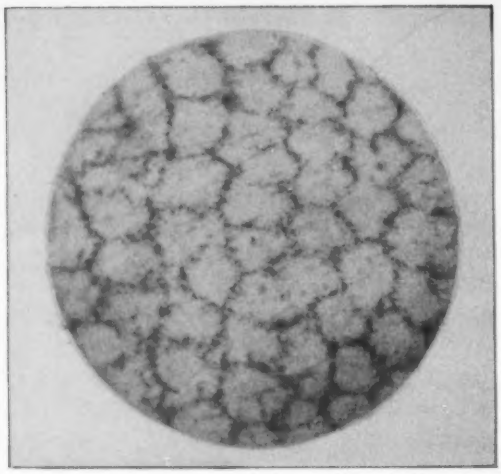

Fig. 1. Microstructure of a monocrystal of zinc + 0.5% copper, after etching.

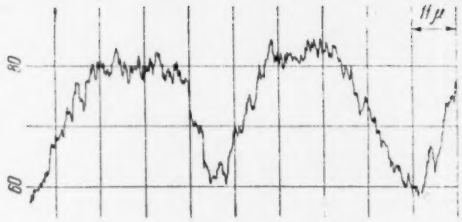

Fig. 2. Copper distribution within the section of a monocrystal of zinc + 0.5% copper.

Figure 2 gives concentration curves showing the distribution of copper within the substructural units. The figure shows clearly the sharp increase in the copper concentration from the edge to the center of the filament. (or cell). Quantitative analysis showed that the copper concentration in the center was equal to 0.7%, while that at the edge was equal to 0.4%.

The results obtained provide convincing proof of the general theory that an impurity which increases the melting point of a metal is concentrated in the center of the substructural units, and also show that the x-ray spectral method of studying the chemical composition of a substance in a microvolume can be applied to the examination of this interesting phenomenon.

In conclusion the authors have to express their thanks to L. E. Loseva, who studied the distribution of copper using the RSASh-2 apparatus, and to M. Bochak and P. Krakhotvil, who prepared the zinc monocrystal.

LITERATURE CITED

[1] M. J. Buerger, Zs. Krist. 89, 242 (1934); B. Chalmers, Proc. Roy. Soc. A, 175, 100 (1940); R. B. Ponds and S. W. Kessler, J. Metals, 3, 1156 (1951).

[2] J. W. Rutter and B. Chalmers, Canad. J. Phys. 31, 15 (1953).

[3] I. B. Borovskii, Coll. Problems in Metallurgy, to Academician I. P. Bardin on his 70th Birthday, Izd. AN SSSR, 1953, p. 135 [in Russian].

[4] I. B. Borovskii and N. P. Il'in, Zavodskaia Lab. No. 10 (1957).

Metal Physics Department, Prague University
A. A. Baikov Institute of Metallurgy,
USSR Academy of Sciences

Received July 7, 1958

THE BEHAVIOR OF THE ANTIMONIDES OF ALUMINUM, GALLIUM AND INDIUM IN THE LIQUID STATE

V. M. Glazov and A. A. Vertman

(Presented by Academician G. V. Kurdiumov, July 12, 1958)

The aim of the present work was to study the relationship between temperature and the magnetic susceptibility of the antimonides of aluminum, gallium and indium, and to compare the data obtained with certain of their thermodynamic and kinetic properties. The study of these compounds in the fused state is of practical importance, since the basic processes involved in the technology of their production for use as semiconductors (purification by crystallization methods and the preparation of monocrystals) are related to the liquid state. The study of the properties of melts formed by these compounds is also of interest in connection with the theory of the liquid state, since at the present time there remains to be solved the problem of the structure exhibited by melts containing intermetallic compounds, and also the question of which factor determines the distribution of the atoms in the liquid state: the structure of the pure components or the structure of the solid alloy [1].

It is possible to reach definite conclusions regarding the structure of a liquid on the basis of a comparison of various physicochemical properties, which are related to one another in as much as they are all, in the end, dependent on one fundamental factor – the state of the electrons in the melt. In this connection it is appropriate to establish the relationship between the various properties of the liquid.

The magnetic susceptibility is an extremely sensitive characteristic, which reacts to extremely small changes in the state of the electrons (or even to changes in the state of part of the total number of electrons) in the melt, so that this property is of particular importance in this connection.

The study of the relationship between the magnetic susceptibility and composition in the liquid state in systems containing intermetallic compounds [2] has established the fact that chemical interaction takes place between the components in the liquid state (the ordinate for the chemical compound is indicated by a clearly defined minimum).

Studies have already been made of the relationship between temperature and the electrical conductivity, density and viscosity of the compounds considered in the present work [3, 4]. It has also been shown [4] that the liquidus lines in the aluminum–antimony, gallium–antimony and indium–antimony systems have a single maximum, which indicates the stability of these compounds on fusion. The curves showing the variation of the electrical conductivity and density with temperature in the liquid state are smooth [3]. The study of the variation of viscosity with temperature has revealed a deviation from the regular shape of the curves with a definite superheating, which was related to the onset of appreciable dissociation of the compounds in the liquid state. In addition, the study of the free energy of activation for viscous flow in melts of the antimonides of aluminum, gallium and indium [5] has shown that the shape of the energy curve differs from that of typical metals in the period preceding crystallization, and this has been related to definite changes in the structure of the short-range order in these melts.

All the above [4, 5] changes are evidently related to corresponding fundamental changes in the state of the electrons in the melts of the antimonides of aluminum, gallium and indium. It was therefore decided to make a detailed study of the variation in the magnetic susceptibility of these compounds in the liquid state with change in temperature.

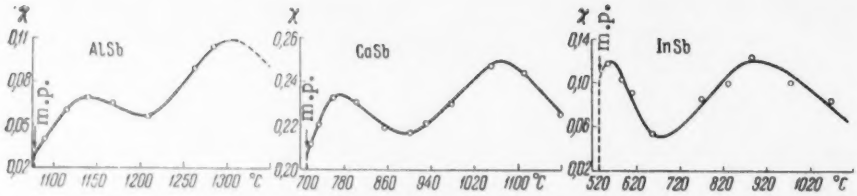

Fig. 1. Variation of the magnetic susceptibility (in arbitrary units) with change in temperature for the compounds AlSb, GaSb, InSb.

The starting materials used were specimens of the compounds AlSb, GaSb and InSb synthesized earlier and purified by the methods of zone refining. The specimens of gallium and indium antimonides were placed in evacuated quartz ampoules. The compound AlSb was placed in a corundum crucible which in turn was placed in an evacuated quartz container. The determination of the magnetic susceptibility was carried out by Faraday's method using the apparatus described in detail in [6]. The magnetic susceptibility values taken were the average values from three measurements. The average error in weighing amounted to ±0.2 mg. The results of the measurements are given in Fig. 1.

It can be seen from the graphs that the curves showing the relationship between magnetic susceptibility and temperature for the compounds AlSb, GaSb and InSb in the liquid state are similar in shape. This indicates that when all three compounds are heated, the processes which take place within them are of identical or very closely related character.

The curves showing the relationship between the magnetic susceptibility and the temperature can be divided into four regions. At first, as the melts are heated above the melting point, the magnetic susceptibility increases, reaches a maximum, and then decreases. As the heating is continued the magnetic susceptibility again increases, again reaches a maximum, and again decreases.

When the data obtained are compared with the results of the studies on the relationship between temperature and the viscosity [4] or the free energy of activation for viscous flow [5] for the antimonides of aluminum, gallium and indium, attention is drawn to the following points:

1) The first maximum (starting from the m. p.) on the curves showing the relationship between the magnetic susceptibility and the temperature for these substances coincides fairly accurately with the minimum on the curve showing the relationship between the free energy of activation for viscous flow, while the presence of this minimum has been related to the rebuilding of the structure of short-range order, which is accompanied by a corresponding change in the number of atoms in the first coordination sphere [5].

2) The minimum shown on the magnetic-susceptibility curve when the molten compounds are heated further corresponds approximately to the temperatures at which the deviation from the regular shape of the curves showing the relationship between the viscosity and temperature are observed. These deviations are evidently related to the onset of appreciable dissociation of the chemical compounds AlSb, GaSb and InSb in the liquid state [4].

On the basis of the results obtained, together with the results of previous work, it is thus possible to imagine the following probable picture of the behavior of the compounds under study in the liquid state [4].

At the melting point the molten compounds have approximately the same short-range ordered structure as in the solid state. As the temperature increases, the coordination number increases (with a corresponding increase in the magnetic susceptibility of the fused compounds) and at a certain temperature approaches that of close-packing. An analogous conclusion regarding the changes in the liquid state for elements exhibiting a friable structure in the solid state was reached in the paper [7], on the basis of electron-diffraction studies of liquid films of tin and bismuth. The temperature at which relatively close-packing is attained in the liquid corresponds to the first maximum on the curves showing the relationship between magnetic susceptibility and temperature and to the minimum on the curves showing the relationship between the free energy of activation of viscous flow and temperature [5].

When the heating is continued to a certain limit in melts of the compounds AlSb, GaSb and InSb, no changes take place apart from those which take place in any liquid when it is heated (weakening of the forces of molecular interaction, increase in the intermolecular distances, increase in the number of vacant sites, etc.). In this temperature range in the liquid state the chemical compound is relatively stable. Further evidence for this is provided by the presence of single turning points (the minimum electrical conductivity and the maximum viscosity) on the composition–property isotherms corresponding to this temperature interval. In this region the properties change in regular fashion; the magnetic susceptibility and the viscosity decrease smoothly, while the free energy of activation of viscous flow increases linearly. When a certain temperature is reached, determined by the individual properties of the compound, the latter begins to undergo intensive dissociation (this temperature is indicated by the minimum on the curves showing the relationship between the magnetic susceptibility and temperature and by the deviation from regular shape of the curves showing the relationship between viscosity and temperature for these compounds [4]).

When heating is continued, the degree of dissociation increases and in consequence the magnetic susceptibility increases. When certain definite appreciable degrees of dissociation are reached, the temperature factor starts to predominate and the magnetic susceptibility again starts to decrease.

It is thus possible, on the basis of a study and comparison of various physicochemical properties of melts of the antimonides of aluminum, gallium and indium, to set up a picture of their behavior in the liquid state. The information obtained on the behavior of these compounds in the molten state should also be taken into account in their synthesis and purification by crystallization methods, and also in the preparation of monocrystals with a more perfect structure.

LITERATURE CITED

[1] V. I. Danilov, The Structure and Crystallization of Liquids, Kiev, 1956, p. 225.

[2] K. Honda and H. Endo, J. Inst. Metals, 37, 37 (1927).

[3] N. P. Mokrovskii and A. R. Regel', J. Tech. Phys. 22, No. 8, 1281 (1952).

[4] V. M. Glazov and D. A. Petrov, Bull. AN SSSR, Div. Tech. Sci. No. 4 (1958).

[5] D. A. Petrov and V. M. Glazov, Proc. Acad. Sci. 120, No. 2 (1958).*

[6] A. A. Vertman and A. M. Samarin, Zavodskaia Lab. No. 3 (1958).

[7] A. N. Bublik and A. G. Buntar', Crystallography, 3, No. 1 (1958).

A. A. Baikov Institute of Metallurgy,
USSR Academy of Sciences

Received June 28, 1958

*Original Russian pagination. See C. B. Translation.

THEORY OF THE FLUCTUATIONS IN CRYSTAL SENSITIVITY IN NUCLEAR PHOTOGRAPHIC EMULSIONS

G. I. Zel'tser and A. L. Kartuzhanskii

(Presented by Academician A. F. Ioffe, June 25, 1958)

The formation of the latent image in the crystals of a photographic emulsion is necessarily of a statistical character. This is particularly true in the case where the latent image formation is the result of the passage of an ionizing particle through the emulsion. In this case both the ionizing action of the particles and the properties of the crystals of the emulsion may undergo fluctuations. An attempt made by K. S. Bogomolov [1, 2] to construct a theory of the ionization fluctuations in emulsions consisting of identical crystals (or consisting of several groups, within each of which all the crystals are identical) proved unsuccessful, since it led to results which are contradicted by experiment [3]. Moreover, the failure of this theory shows that the ionization fluctuations, even for relativistic particles, plays in general a small role, and that the experimentally observed flucutations in the average density of the particle tracks should rather be related to fluctuations in the sensitivity of individual crystals. This variation of the theory is presented below.

Let us express the sensitivity of the crystals by the number $\underline{n}$ of Ag atoms which must be formed in the crystals in order to make it developable. Any sensitization of the emulsion towards particular ionizing particles reduces $\underline{n}$, while fluctuations in the sensitivity appear as simultaneous fluctuations in $\underline{n}$. Let us assume that before sensitization of the emulsion the particle track had a grain density ν_n (≥ 0) per unit length of track, and a grain density after sensitization of ν_s ($> \nu_n$). From this it is possible to find [4, 5] the reduction (Δn) in the number $\underline{n}$ of electrons formed by the particle in an individual crystal and the total for all the crystals touched by the particle within a certain region of the track; the number ν_0 of crystals lying in unit length of the track, a quantity required for the calculation, is given by the Zhdanov formula. Thus in order to make the crystals developable after sensitization, it has been necessary to form $\nu_0 \Delta n$ fewer electrons per unit length of track. If we neglect the loss of electrons, i.e., if we assume that every electron formed led finally to the formation of a Ag atom, then we can say that the formation of $\nu_0 \Delta n$ fewer Ag atoms has been required.

The action of the sensitizer may thus be regarded as equivalent to the formation of $\nu_0 \Delta n$ Ag atoms without exposure (in the case of reducing sensitizers, triethanolamine for example, these atoms are actually formed). Neglecting the fraction ν_n / ν_0 of crystals which would have been developable even before sensitization, we have now to examine the distribution of these $\nu_0 (1 = \nu_n / \nu_0) \Delta n$ Ag atoms among $\nu_0 - \nu_n$ crystals. If they were distributed regularly, then either all $\nu_0 - \nu_n$ crystals, or else none of them, would become developable; as a result of fluctuations, however, only those $\nu_s - \nu_n$ crystals in which a sufficient number of Ag atoms had been formed would become developable. In order to determine, by comparison with experimental results, the number of Ag atoms (assuming them to be concentrated in one center) necessary for developability, we must solve the following problem: for an arbitrary distribution $\underline{r}$ of indistinguishable spheres (Ag atoms) in $\underline{s}$ boxes (crystals), what fraction on the average of the total number of boxes contain a given number of spheres ?

Let us denote the fraction of boxes containing not less than $\underline{i}$ spheres by α_i. It can be shown that the value of α_i is given by the formula

$$\alpha_i = \frac{\binom{s+r-i-1}{r-i}}{\binom{s+r-1}{r}}, \qquad (1a)$$

where the symbol $\binom{a}{b}$ denotes the binominal coefficient C_b^a. Since r and s in the data used in our problem relate to unit track length, which is arbitrarily chosen, the values of α_i should be replaced by their asymptotic values when $r, s \to \infty$, $r/s = \lambda = \text{const}$. It is readily seen that then

$$\alpha_i = \left(\frac{\lambda}{1+\lambda}\right)^i. \tag{1b}$$

From the formulae (1) we can calculate the fraction of boxes containing exactly i spheres:

$$\Delta\alpha_i = \alpha_i - \alpha_{i+1} = \frac{\binom{s+r-i-2}{r-i}}{\binom{s+r-1}{r}}, \tag{2a}$$

and also its asymptotic value

$$\Delta\alpha_i = \frac{\lambda^i}{(1+\lambda)^{i+1}} = \frac{\alpha_{i+1}}{\lambda}. \tag{2b}$$

The formulae (2) give the sensitivity distribution of the crystals, since, as a result of the fact that the spheres are indistinguishable, it is a geometric (see, for example, [6]) and not a Poisson distribution.

If each crystal has N sensitivity centers, in each of which a group of Ag atoms may be formed, then when the atoms are distributed among the separate centers it is necessary to take into account the fact that the presence of a group of Ag atoms in one of the centers is ineffective if another center in the same crystal already contains such a group. It is therefore necessary to examine the distribution of r spheres among s groups of boxes (each group containing N boxes) such that at least one of the boxes in each group contains not less than i spheres. The fraction of box groups satisfying this condition is given by the following formula (only the asymptotic value is given), which becomes formula (1b) when N = 1:

$$\alpha_i(N) = \left(\frac{\lambda}{1+\lambda}\right)^{N(i-1)+1} + \frac{1}{\lambda}\sum_{l=i}^{N(i-1)}\left(\frac{\lambda}{1+\lambda}\right)^{l+1} W_{li}, \tag{3}$$

where

$$W_{li} = \sum_{k=1}^{N}(-1)^{k-1}\frac{\binom{N}{k}\binom{N+l-ik-1}{l-ik}}{\binom{N+l-1}{l}}.$$

Here the first term in the sum accounts for those crystals in which the number of atoms is sufficiently high for at least one center to have not less than i Ag atoms, while the second term in the sum accounts for those crystals in which a group of i or more atoms in one center is possible, but not obligatory; W_{li} represents the probability of formation of such a group.

Before we give the results of a comparison of the formulae obtained with the experimental data, we would point out that these formulae contain no arbitrary parameters. The extent of the agreement with experiment which is reached, as will be shown in a moment, is therefore by itself more important for the confirmation, in principle, of the accuracy of our model, than the improvement of this agreement by the introduction of various semiempirical coefficients.

The formulae (1) may be applied to the particularly fine-grained emulsion of Perfilov [7]. The crystals of this emulsion have only one sensitivity center each (if they have any at all), while the electron loss in them

is negligibly small, since the diameter of the crystals ($\sim 0.08\mu$) does not exceed the length of the free path of electrons in the crystals. In the aging process this emulsion is brought to a relativistic sensitivity (track density $\nu_n \approx 25$-30 grains per $100\,\mu$ of track), and afterwards sensitized further with triethanolamine to give a track density ν_s of up to 60 grains per $100\,\mu$. It is readily shown by calculation (taking ν_0 as 870 grains per $100\,\mu$ [7]) that the second sensitization leads to a reduction in the number of electrons (and hence in the number of Ag atoms, since the electron loss is negligible) by a total of $\Delta n = 0.16$. In the absence of fluctuations this result would be physically absurd, bur for an arbitrary distribution of $\nu_0(1 - \nu_n/\nu_0)\Delta n \approx 140$ atoms of Ag among $\nu_0 - \nu_n \approx 840$ crystals ($\lambda = 1/6$) we have $\alpha_1 = 14\%$ of the crystals with at least one Ag atom and $\alpha_2 = 2\%$ of the crystals with not less than 2 atoms. The latter is fairly close to the increase in track density obtained by experiment ($\sim 3\%$ of ν_0) and shows that the action of the triethanolamine produces a group with at least two atoms, i.e., a subcenter, as also follows from other data [3, 8].

The formulae (1) are also applicable to the increase in fog with secondary sensitization of the same emulsion. This amounts to approximately 2-4 grains per 1000 μ^3, i.e., approximately 10^{-6} times the total number of crystals. For $\lambda = 1/6$, this fraction is the same as the fraction of crystals for which $i = 7$, i.e., which have 7 or more Ag atoms; since they have been developed without exposure, then the minimum developable center for this emulsion is one containing 7 atoms, which is in good agreement with data obtained for other relativistic emulsions [9].

In the case of the more coarsely grained emulsion R-NIKFI ($\bar{d} = 0.28\,\mu$), Formula (3) should be used, since it has been established by electron microscopy [10] that the crystals of this emulsion have normally 2-3 sensitivity centers. Further sensitization with triethanolamine increases the density of relativistic tracks in this emulsion from 30-35 to 60-80, and in some cases to 100 grains per $100\,\mu$ (the last figure is achieved with a considerable simultaneous increase in fog) [11]. Taking ν_0 equal to ~ 300 grains per $100\,\mu$ [1, 2], $\nu_n = 30$, $\nu_s = 60$-80, we have $r = 500$-800, $s = 270$, $\lambda = 2$-3. The increase in density observed experimentally, which is ~ 10-20% of ν_0, then corresponds to $i \approx 4$-5, which is at least double the value for $\bar{i}$ for Perfilov's emulsion. This, however, becomes readily understood, if we take into account the fact that in coarser crystals the electron loss is high and amounts to at least 50%. The number of Ag atoms in a center is then no longer $\bar{i}$ and amounts to ~ 2, i.e., in this case also subcenters are formed. The increase in fog amounts to 1-2 grains per 1000 μ^3 (approximately 10^{-4} times the total number of crystals) for $\nu_s = 60$-80, $\lambda = 2$-3 and increases rapidly to 5-6 and more grains per 1000 μ^3 ($\sim 10^{-3}$ times the total number of crystals) with further increase in the track density, for example up to $\nu_s = 100$ (for which $r = 1100$, $\lambda = 4$). These data are in accordance with Formula (3) for $i \approx 8$-12, which again does not contradict the available experimental data [9].

LITERATURE CITED

[1] K. S. Bogomolov, J. of Sci. and Appl. Photography and Cinematography, 1, 401 (1956).

[2] K. S. Bogomolov, J. of Sci. and Appl. Photography and Cinematography 2, 161 (1957).

[3] A. P. Zhdanov, A. L. Kartuzhanskii and L. I. Shur, J. of Sci. and Appl. Photography and Cinematography 3, 139 (1958).

[4] A. P. Zhdanov and L. I. Shur, Apparatus and Tech. Exp. No. 4, 29 (1957).

[5] A. L. Kartuzhanskii, Proc. Acad. Sci. 114, 1199 (1957).*

[6] W. Feller, Introduction to Probability Theory and Its Applications, IL, 1952, p. 67 [Russian trans.].

[7] N. A. Perfilov, N. R. Novikova and E. I. Prokof'eva, Report to the Conference in the Joint Institute for Nuclear Studies, Dubna, February 1957; see also Atomic Energy 4, 45 (1958).

[8] A. P. Zhdanov, A. L. Kartuzhanskii, I. V. Ryzhkova and L. I. Shur, J. of Sci. and Appl. Photography and Cinematography 3, No. 4 (1958).

[9] A. L. Kartuzhanskii, J. of Sci. and Appl. Photography and Cinematography 3, 81 (1958).

[10] A. L. Kartuzhanskii, J. of Sci. and Appl. Photography and Cinematography 3, 16 (1958).

[11] A. P. Zhdanov, A. L. Kartuzhanskii, I. V. Ryzhkova and L. I. Shur, J. of Sci. and Appl. Photography and Cinematography 3, 53 (1958).

Received June 21, 1958

*Original Russian pagination. See C. B. Translation.

THE RELATIONSHIP BETWEEN THE CHEMISORPTIVE PROPERTIES OF METALS AND THE STRUCTURE OF THE SPECIMENS

N. N. Kavtaradze

(Presented by Academician V. I. Spitsyn, July 7, 1958)

The increasing number of facts indicating the close relationship between the catalytic activity of metals and their chemisorptive capacity, together with the recognition [8] that solids with the same chemical composition have an approximately constant specific catalytic activity, has made it necessary to show experimentally that the specific chemisorptive capacity (i.e., the magnitude of the adsorption on unit surface) is constant for substances with the same composition. From the point of view of contemporary ideas of the nature of catalysis and taking into account the Law of Mass Action, the specific catalytic activity of solids may be shown to be constant if their specific chemisorptive capacity is constant.

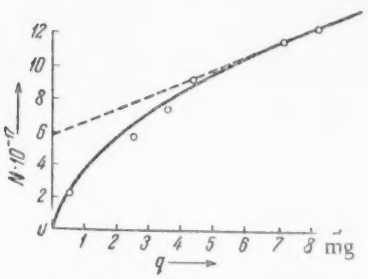

Fig. 1. Relationship between the surface area of nickel layers condensed at −78°, and the quantity of metal in the layer.

From the available experimental data [1-4] it may be stated that in a number of cases the specific chemisorptive capacity of solids, particularly metals, is constant and independent of their geometric structure.

It is known that the structure of metal layers changes as condensation of their vapors takes place [5, 6]: at first there is formed a certain number of nuclei particles – little islands of apparent or latent crystalline granules separated by free spaces. The particles of Ag, Au, and Cu are spherical in shape, while those of Zn and Cd have a regular crystalline form and are of larger dimensions (up to 200 A). Increase in the quantity of metal in the layer leads to development of the layer as a result of the growth and combination of the particles initially formed (no new centers of crystallization are formed), accompanied by a gradual decrease in the porosity and the formation of a compact layer. Further condensation of the metal leads to an increase in the thickness of the layer and to changes in its relief.

The results of measurements of the adsorption of hydrogen on layers of nickel at different stages of the layer development, given in Table 1 and Fig. 1, show that during the structural changes described above and with increase in the quantity of metal in the layer, its chemisorptive capacity increases, with a proportionate increase in the stable adsorption, i.e., the atomic chemisorption, and in the weak, reversible adsorption, i.e., the molecular chemisorption. It can be seen from Table 1 that the ratio between the molecular and atomic adsorption remains practically constant, i.e., change in the structure has no influence on the qualitative side of the phenomenon.

Table 2 gives data characterizing the effect of heating the nickel layer, i.e., recrystallization, on the hydrogen adsorption. It can be seen that in this case also, change in the layer structure has practically no influence on the qualitative side of the phenomenon.

We have still to find what determines the increase in the chemisorptive capacity of the layers relative to hydrogen as the layer grows and its structure changes. This question may be answered by data on the measurement of the surface area of the nickel layers by adsorption of krypton at −195° and by the results of a

TABLE 1

The Adsorption of H_2 at −195° on Layers of Ni Condensed at −78°

Specimen No.	q	h, Å	$N_a \cdot 10^{14}$	$N_m \cdot 10^{14}$	$N_\Sigma \cdot 10^{14}$	N_m, % of N_Σ
1	0.595	32	23,4	0,87	24,3	3,5
2	2,62	141	56,8	2,33	59,1	3,9
3	3,70	198	71,8	2,7	74,5	3,6
4	4,41	236	94,1	4,56	98,7	4,6
5	7,2	386	115,8	4,62	120,4	3,8
6	8,28	440	124,1	4,62	128,7	3,5

Note: q) weight of layer in mg; h) average thickness; N_a) number of H_2 molecules irreversibly chemisorbed on the Ni, and N_m) number of H_2 molecules reversibly chemisorbed, at $P = 2 \cdot 10^{-2}$ mm; N_Σ) total hydrogen adsorption ($N_\Sigma = N_a + N_m$).

TABLE 2

The Effect of Heating the Nickel Layer for 30 Minutes on the Magnitude of the Adsorption and on the Ratio Between the Irreversible (N_a molecules) and Reversible (N_m molecules) Adsorption of Hydrogen in Percentages of the Total Adsorption N_Σ

Specimen No.	T_K, °C	T_p, °C	h, Å	$N_a \cdot 10^{14}$	$N_m \cdot 10^{14}$	N_m, % of N_Σ
1	—78	—78	440	124	4,62	3,6
2	—78	—78	386	116	4,65	3,8
3	0	200	1350	14,8	0,3—0,4	2—3
4	0	0	1457	37,2	0,6—0,7	2

Note: T_K) condensation temperature; T_p temperature at which heating for 30 minutes took place.

comparison of the values obtained with the quantity of hydrogen adsorbed on the same layers at the same temperature. From the data in Table 3 it may be stated that the hydrogen chemisorbed at −195° almost completely (97-98%) covers the surface in an atomic layer, i.e., that the quantity of chemisorbed hydrogen defines the magnitude of the surface of the nickel layer. From this it follows that the increase in the chemisorptive capacity of a metal layer as its growth proceeds and its structure changes is related to the increase in the total surface which accompanied these processes. This conclusion is also confirmed by the data of Porter and Tompkins [7] obtained by the study of iron layers. The value of the chemisorption of H_2, related to unit surface, i.e., the specific chemisorptive capacity, remains constant.

Examination of the data presented leads to the conclusion that change in the structure of layers of nickel and similar metals during condensation or as a result of heating (recrystallization) has practically no qualitative or quantitative influence on their specific chemisorptive capacity. The fact that the specific chemisorptive capacity for a number of metals, and, possibly, other substances, is constant when their chemical composition is constant explains the fact that the specific catalytic activity is approximately constant [8].

TABLE 3

The Adsorption of H_2 and Kr on the Same Nickel Layer at −195°

Specimen No.	τ	h, Å	$N_{H_2} \cdot 10^{15}$	$N_{Kr} \cdot 10^{15}$	S_{Kr}	$\sigma_{H_2} \cdot 10^{-16}$, $см^2$	$\sigma_H \cdot 10^{-16}$, $см^2$
1	30	1500	11,6	9,71	180	15,5	7,7
2	15	1838	14,2	11,6	215	15,1	7,5
3	30	2535	14,5	11,8	219	15,0	7,5

Note: τ − time of heating layer, in minutes; h − average thickness of layer; NH_2 − number of molecules of adsorbed hydrogen; N_{Kr} − number of krypton atoms covering the nickel surface (calculated according to BET and the Langmuir equation); S_{Kr} − area of layer in cm^2, calculated from the krypton adsorption (σ_{Kr} taken as equal to 18.5 A^2); σ_{H_2} and σ_H − units of surface corresponding to a molecule or an atom of hydrogen according to the calculated area.

LITERATURE CITED

[1] N. N. Kavtaradze, Proc. of the All-Union Conference on Heterogeneous Catalysis, 1953, M, 1955, p. 150.*

[2] N. N. Kavtaradze, Electronic Phenomena in Catalysis and Adsorption, Izd. AN SSSR, 1955, p. 235.*

[3] N. N. Kavtaradze, Coll. Works of the Conference on Adsorption, dedicated to the 200th Anniversary of the M. V. Lomonosov State University, Moscow, 1957, p. 73.*

[4] N. N. Kavtaradze, Proc. Acad. Sci. 114, No. 4, 822 (1957).* *

[5] R. S. Sennett and G. D. Scott, J. Opt. Soc. Am. 40, No. 5, 203 (1950).

[6] R. S. Sennett, T. A. McLauchlan and G. D. Scott, Canad. J. Phys. 30, No. 5, 370 (1952).

[7] A. S. Porter and F. C. Tompkins, Proc. Roy. Soc. A, 217, 529 (1953).

[8] G. K. Boreskov, Proc. of the All-Union Conference on Heterogeneous Catalysis, 1953, M. 1955, p. 5.*

Institute of Physical Chemistry,
USSR Academy of Sciences

Received July 4, 1958

* In Russian.

** Original Russian pagination. See C. B. Translation.

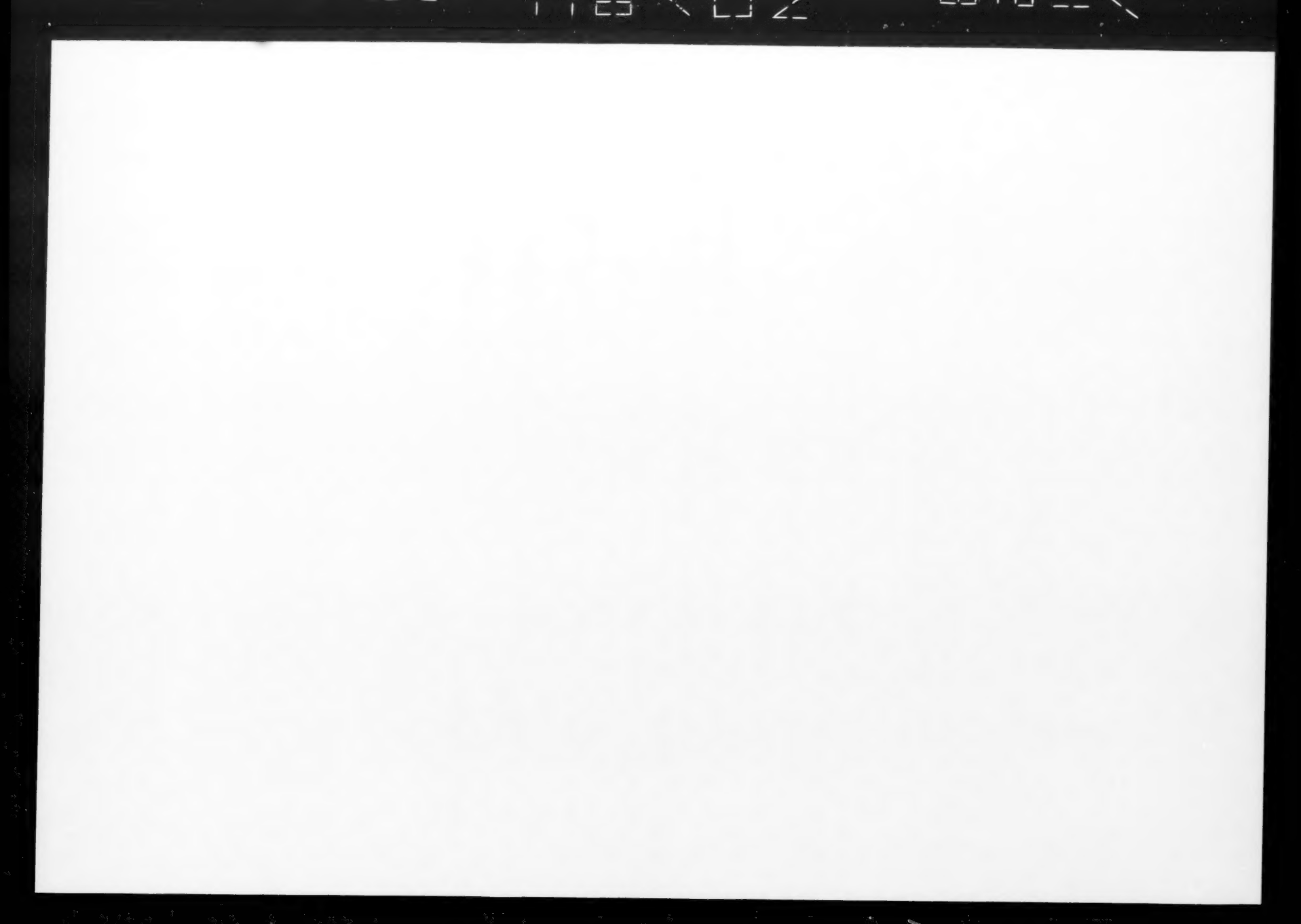

THE ROLE OF CHAIN BRANCHING AND RUPTURE IN THERMAL CHAIN FLAME PROPAGATION

L. A. Lovachev

(Presented by Academician V. N. Kondrat'ev, July 7, 1958)

A chain reaction mechanism for the decomposition of A, which involves two active centers successively reacting with A and regenerating one another, can be represented by a simplified scheme involving active centers of the one type P:

$A \rightarrow 2P$ (generation)	$Q_R = h_R R(T')$;
$P + A \rightarrow 2C + P$ (propagation)	$Qn = hFn = hK(T')n_A n$;
$P \rightarrow 3P$ (branching)	$Q_V n = h_V V n = h_V K_V(T')n_A n$;
($P \rightarrow$ linear rupture)	
$P + P \rightarrow A$ (rupture)	$Q_W n^2 = h_W W(T')n^2$.

On the right, expressions have been written for the rate of evolution of heat. Here, h_i is the heat of reaction; K_i is the reaction-rate constant; W is the rate constant for second-power chain rupture; n_A is the dimensionless weight concentration of A, and $\underline{n}$ is the dimensionless weight concentration of P. The rate of linear branching or chain rupture can be written as $K_V n_A n = iKn_A n$, from which it follows that $i = V/F = K_V/K$, $\underline{i}$ being the coefficient of chain branching ($i < 0$ corresponds to linear chain rupture).

With $\lambda = c\rho D_A$, the following system of equations is obtained for the stationary propagation of a laminar unidimensional flame:

$$\lambda pp' - Bcp + Q_\Sigma n + Q_W(n^2 - n_f^2) - Q_R = 0, \tag{1}$$

$$Dp^2 n'' - p(B - Dp')n' + R + Vn - W(n^2 - n_f^2) = 0, \tag{2}$$

where $B = u\rho$; $D = \rho D_p$; $Q_\Sigma = Q + Q_V$; $T' = T + T_0'$; $D_0 = D_m q$; $D_p \sim (T')^a$; $q = \frac{\mu_0}{\mu_m}\left(\frac{T'_0}{T'_m}\right)^{a-1}$; $p = \frac{dT}{dx}$; $p' = \frac{dp}{dT}$; $n' = \frac{dn}{dT}$; $n'' = \frac{d^2n}{dT^2}$; $\underline{x}$ is a coordinate; $\underline{u}$ is the flow rate; ρ is the density; T' is the temperature (°K); D_A is the diffusion coefficient of A; D_p is the diffusion coefficient of P; λ is the thermal conductivity of the mixture; $\underline{c}$ is the heat capacity of n_t is the equilibrium flow concentration of P.

The index zero will be used to designate quantities in the initial state ($T' = T_0'$); the index $\underline{f}$ will apply to the final state ($T' = T_f'$), and the index $\underline{m}$, to the state in which the temperature gradient has its maximum value $p = p_m$ ($T' = T_m'$). The extremal values of the reaction rate functions are zero, and the boundary conditions for (1) and (2) are those which were adopted in [1].

The concentration n_m corresponding to $T = T_m$ will be written [1] as:

$$n_m = t + [R_{pm} + V_m n_m - W_m n_m^2 - Blp_m]N, \tag{3}$$

where

$$l = \frac{n_f - n_0}{T_f}; \quad t = n_0 + lT_m; \quad r = T_m(T_f - T_m); \quad R_p = R + Wn_f^2; \quad N = \frac{r}{2D_m p_m^2}; \quad T_m = 0{,}5T_f:$$

Determining n_m from (3), substituting in (1) with $p = p_m$ and $p'_m = 0$, and setting $B = \eta_{p_*}$ [1], with $\eta = 4D_0/\kappa T_m$ and $\kappa = cD_0/\lambda_0$:

$$p_*^6\eta_l A_1 - p_*^4(\eta^2 A_2 + \eta_l A_3 + A_5) - p_*^2(\eta_l A_4 - A_6 - \eta A_7 + A_8) + A_9 = 0, \tag{4}$$

where

$$A_1 = 4cD_{mf}^2 f;\ A_2 = (c + lh_W)^2 gr^2;\ A_3 = 2D_m r(c + 2cV_{mf} - lh_W - 2tlQ_{Wmf} - 2ctfW_m);\ A_4 = r^2(lQ_{\Sigma m} - cV_m + lV_m h_W - cV_{mf}^2);\ A_5 = 4D_m^2(t^2 fQ_{Wm} + th_W - fQ_{pm});\ A_6 = 2D_m tr(Q_{\Sigma m} + V_m h_W);\ A_7 = 2r^2(lfQ_{Wm}R_{pm} + cfW_m R_{pm} - cgQ_{pm} - lfW_m Q_{pm});\ A_8 = 2D_m r(Q_{pm} + 2tR_{pm}Q_{Wmf} - 2tfW_m Q_{pm} + 2fV_m Q_{pm} + h_W R_{pm});\ A_9 = r^2(Q_{\Sigma m}R_{pm} + V_m Q_{pm} + V_m h_W R_{pm} + fV_m^2 Q_{pm} + 2fW_m R_{pm}Q_{pm} - fQ_{Wm}R_{pm}^2 - gQ_{pm}^2);\ Q_{pm} = Q_{Rm} + Q_{Wm}n_t^2;\ f = h_W/Q_{\Sigma m}\ \text{and}\ g = W_m/Q_{\Sigma m}.$$

Solving (4) for p_*, we find for the rate of flame propagation

$$u_0 = \frac{B}{\rho_0} = \frac{1}{\rho_0}\eta_l p_*. \tag{5}$$

If, as before [1], the initiation, of rate R, is neglected, i.e., if it is supposed that $A_7 = A_8 = A_9 = 0$ (and if it is also assumed that $W_m n_t^2 = 0$), the expression then obtained for the determination of p_* is

$$p_*^4\eta A_1 - p_*^2(\eta^2 A_2 + \eta_l A_3 + A_5) - (\eta A_4 - A_6) = 0, \tag{6}$$

from which it follows that

$$p_*^2 = \frac{(\eta^2 A_2 + \eta A_3 + A_5) - [(\eta^2 A_2 + \eta A_3 + A_5)^2 + 4\eta A_1(\eta A_4 - A_6)]^{1/2}}{2\eta A_1}. \tag{7}$$

Decomposing the radical of (7) into a series, and supposing that $A_4 \cong A_4' = r^2(lQ_{\Sigma m} - cV_m)$; $A_3 \cong A_3' = 2D_m r(c + 2cV_m f)$, $A_5 \cong A_5' = 0$, (5) gives

$$u_0 = \varphi\psi\frac{1}{\rho_0}\left(\frac{n_f Q_{\Sigma m}D_m}{2cT_f}\right)^{1/2} = \varphi\psi\frac{1}{2\rho_0}\left[n_f\left(K + \frac{h_V}{h}K_V\right)_m(\rho D_p)_m\right]^{1/2}, \tag{8}$$

where

$$\varphi = 2\left[\frac{2q}{\varkappa}\left(1 - \frac{2q}{\varkappa}\right)\right]^{1/2}, \tag{9}$$

$$\psi = \left(\frac{1 + \frac{K_{Vm}}{K_m}\left[\frac{h_V}{h} + \frac{\varkappa}{(\varkappa - 2q)}\frac{h_W}{h} + \frac{2qn_{Am}}{t(\varkappa - 2q)}\right]}{1 + \frac{K_{Vm}}{K_m}\left[\frac{h_V}{h} + 2\frac{h_W}{h}\right] + \frac{2q}{\varkappa}\frac{W_m}{K_m}}\right)^{1/2} \tag{10}$$

or

$$\psi \simeq \left(\frac{1 + i\frac{2qn_{Am}}{t(\varkappa - 2q)}}{1 + \frac{2q}{\varkappa}\frac{W_m}{K_m}}\right)^{1/2}. \tag{11}$$

The coefficient φ expresses the relation existing between u_0 and the ratio of the coefficient of diffusion of P, multiplied by the heat capacity and the density, to the thermal conductivity (the quantity κ). On the other hand, κ also enters into the relation (10) for ψ. The effect of the second-power chain rupture depends on the ratio of the constants W_m and K_m. It is thus clear that, under strictly analogous conditions, the effect of second-power chain rupture will be the more pronounced, the higher the combustion temperature T_f', since with decreasing T_f', K_m diminishes and W_m rises. A decrease in κ will increase the relative effect of W on u_0. In the case of linear chain branching, the effect of W will be the less pronounced, the larger the branching velocity constant, K_{Vm}. The effect of linear chain branching on u_0 will be the less marked, the smaller $t = n_f/2$ (because of the diminution in the diffusional current of active centers, decreasing n_f increases the relative importance of initiation and chain branching), and the smaller the value of κ (since there is in this case a decrease in the relative number of active centers which are supplied to the reaction zone by diffusion).

TABLE 1

The Effect of Chain Branching and Rupture on the Rate of Flame Propagation, u_0 (cm/sec) in the Case of the Decomposition Flame of Hydrazine

	Linear Branching												
	0	0	$5\cdot10^{-3}$	10^{-2}	$5\cdot10^{-2}$	10^{-1}	0	0	$5\cdot10^{-3}$	10^{-4}	$5\cdot10^{-4}$	10^{-3}	$5\cdot10^{-3}$
	$W = 0$	$W \neq 0$					$W = 0$	$W \neq 0$					
	$T_0' = 300°K$, $T_f' = 1950°K$						$T_0' = 300°K$, $T_f' = 1280°K$						
From (5) & (6)	146	140	144	148	173	202	8,58	5,10	5,45	5,79	8,05	10,2	20,3
From (8), (9) & (10)	146	135	139	142	164	181	8,58	5,11	5,47	5,82	8,08	10,2	20,3
From (8), (9) & (11)	146	137	143	148	186	224	8,58	5,11	5,47	5,82	8,08	10,2	20,4

Under strictly analogous conditions, the effect of linear chain rupture ($K_V < 0$ or $i < 0$) is the more pronounced, the smaller n_f (because of the fall-off in the diffusional current, diminishing n_f results in an increase in the relative importance of chain branching and rupture). Fundamentally, this effect appears as a result of changes in the second member in the numerator of (10), or (11). Thus, decreasing κ also increases the effect of linear chain rupture on u_0. The constant W_{Vm} still enters into relation (8) and diminishes u_0, if $h_V \neq 0$.

To illustrate the preceding, numerical calculations were carried out on the decomposition flame of hydrazine, which had been investigated earlier in [1]. All of the starting data from [1, 2] were taken over without alteration. As additional starting data in these calculations, it was assumed that: $h_V = 0$; $Q_V = 0$; $Q_\Sigma = Q$; $h_W = 3\cdot10^3$ cal/g; and $h_R = 2\cdot10^3$ cal/g. The coefficients of Equation (4) were evaluated, and it was established that the value of p_* determined according to (4) was practically identical with that obtained from (6). Proof was thereby had of the justification of the assumption which had been made earlier [1] and accepted in the derivation of (6), to the effect that it was possible to neglect the initiation of the active centers in comparison with the much greater supply of these centers through diffusion.

From a comparison of the data for $i = 0$ and $W = 0$ with that for $i = 0$ and $W \neq 0$, it follows that the second-power chain rupture exerts a very minute influence of u_0 at high T_f' and a more considerable influence at lower T_f'. Calculation through the approximate relations (8) and (9), by application of (10) or (11), gives results which are close to those obtained through (5) and (6). In [1] an evaluation was made of the value of $i > 0$ which would be required for compensating the effect of a second-power chain rupture. The data of Table 1 confirm the correctness of this evaluation.

If n_f is expressed through the equilibrium constant, it is seen from (8) that a diminution of the pressure P_Σ will increase n_f and that this will lead to an increase in u_0. In the case of combustible mixtures with low

heating value, T_f' is left practically unaltered by an increase in P_Σ so that in a relation of the type $u_0 \sim P_\Sigma^k$ the value of the exponent $\underline{k}$, must be approximately $k = -0.25$ when calculated from Equation (8). Depending on the initial composition, it can be that $k < -0.25$ for lean hydrocarbon mixtures. In combustible mixtures having moderate, or high, heating capacities, the fall in T_f' which results from a decrease in P_Σ can partially, or completely, compensate for the effect of an increase in n_f so that $k > -0.25$ or $k=0$ (u_0 is independent of P_Σ). It is even possible that u_0 decreases with falling pressure ($k > 0$).

Let us consider the roles of the coefficients φ and ψ. In mixtures with high T_f', $\underline{q}$ will increase with a diminution in P_Σ when $\kappa > 1$ to give an increase in φ (9), and there is, accordingly, a decrease in $\underline{k}$. With a decrease in P_Σ, there will be a decrease in the second member of the numerator of (11) since $W \sim \rho^3$ and $K \sim \rho^2$. This results in a decrease in $\underline{k}$. A diminution of P_Σ will thus lead to a more marked increase in u_0 (as compared with the increase at $k = -0.25$) in mixtures with low T_f' (see Table 1). With a decrease in P_Σ there is an increase in $t = n_f/2$. As a result, the effect of linear chain rupture diminishes (if $K_V < 0$ or $i < 0$), and this leads to an increase in ψ (a diminution in $\underline{k}$). Because of the more rapid rise in n_f, the effect of a diminution in P_Σ will be more pronounced in mixture with low T_f'. A decrease in P_Σ thus leads to a diminution in the effect of linear chain branching (if $i > 0$) and, accordingly, to a decrease in ψ (to an increase in $\underline{k}$).

The dependence of u_0 on D_P and λ is expressed principally through the radical of (8) and the coefficient φ of (9). It is to be seen from (9) that the influence of κ on u_0 can vary, depending on the ratio $2q/\kappa$. With a decrease in κ, the second-power chain rupture will prove to exert a more pronounced effect on u_0, since ψ will thereby diminish. Linear chain rupture will act in this same direction (if $i < 0$). A diminution in κ will lead to an increase in the importance of the role of the linear chain branching (11). All of this is related to the fact that with a diminution in κ, the relative number of active centers which are delivered into the reaction zone by diffusion decreases, and the importance of chain initiation, branching, and rupture thus increases.

LITERATURE CITED

[1] L. A. Lovachev, Proc. Acad. Sci. USSR, 120, No. 6, 1287 (1958). •

[2] D. B. Spalding, Phil. Trans. Roy. Soc. London, A, 249, No. 957, 1 (1956).

The Institute of Chemical Physics of the
Academy of Sciences of the USSR

Received July 4, 1958

• Original Russian pagination. See C. B. Translation.

CONCERNING CERTAIN SOLUBILIZATION RULES FOR ALBUMINOUS SYSTEMS

V. A. Pchelin, V. N. Izmailova and K. T. Ochurova

(Presented by Academician P. A. Rebinder, July 7, 1958)

Solubilization* in aqueous solution of soaps, and other active substances, has been systematically studied in [1-7], and elsewhere, so that the basic principles of this phenomenon are well established at the present time.

Although albuminous substances are high-molecular compounds having chemical properties which are radically different from those of the usual soaps, they show surface activity, just as the soaps do, and as a result, they have the ability to solubilize;a fact which was first pointed out by D. L. Talmud [8]. Since [8], only isolated works have appeared in this field [9]. At the same time, solubilization in albuminous systems is of much interest both for the theory of the structure of albumin, and for the study of the biologically important processes of transfer and exchange of matter in living organisms, and the phenomenon thus stands in need of systematic investigation.

The present work aims at establishing relations between the state (form) of albuminous macromolecules in solution and their ability to solubilize substances which are poorly soluble in water, specifically the hydrocarbons.

Gelatine was chosen as the albuminous component. Gelatine is a typical polyampholyte which is readily soluble in water and possesses clearly expressed surface activity. In addition, gelatine, under certain conditions, can pass from the fibril into the globular form [10, 17].

The gelatine was subjected to a preliminary purification by high-voltage, multiple-chamber electrolysis, following the technique which has been developed by V. A. Kargin and T. A. Matveeva [11]. Purification of the 1% gelatine solution continued for 30-40 hours, on the average, with potential differences of 1500 v and 400 v in the middle chamber, and in the auxiliary chambers, respectively. The purity of the resulting product was controlled by the current strength in the apparatus. At the end of the purification, the current strength corresponded to the electrical conductivity of doubly distilled water and amounted to approximately 8-10 ma. In addition, the purity of the product was also checked through a determination of the ash content. After purification, the ash content, as determined with four decimal place accuracy, was equal to zero. A semiquantitative spectral analysis showed only traces of sodium after the purification.

Benzene was the substance selected for dissolving, and it was carefully purified by well-known methods [12]. Doubly distilled water was invariably used for the preparation of the albuminous solutions.

Quantitative measurements on the solubilization effect were carried out by the refractometric method which has been proposed and developed by A. I. Iurzhenko [13]. This technique is based on the fact that the index of refraction increases steadily as a hydrocarbon is added to a solution of a surface-active substance, becoming constant once saturation is reached. In addition, it has been shown by S. S. Voiutskii [7] that the liquid solubilities can be determined from the rule of additivity of the specific refractivities. The experimental results are unaffected by the presence of excess hydrocarbon in the form of emulsified droplets. Abbe and Pulfrich refractometers were employed for determining the indices of refraction.

*The term "solubilization" is usually used to designate the spontaneous increase in the solubility of a substance which is poorly soluble, or practically insoluble, in a given solvent, which results from the addition of surface-active materials.

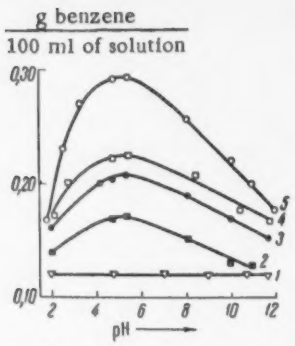

Fig. 1. The relation between the solubilization of benzene in gelatine solutions of various concentration C, and the pH of the medium:
1) C = 0; 2) C = 0.11%; 3) C = 0.21%; 4) C = 0.43 %; 5) C = 0.86 %. t = 20°.

The state of albumin molecules in solution depends primarily on the pH, and it was for this reason that that factor was first studied. The pH of the medium was altered over the interval from pH 2 to pH 11 by the addition of HCl or NaOH. The isoelectric point of the dialyzed gelatine was determined from the maximum turbidity and minimum viscosity at 20°. The data show the isoelectric point of the dialyzed gelatine to lie at pH 5.2, which is in agreement with the result obtained by G. Weber [14].

The determination of the solubilization of benzene was carried out in the following manner. Refractive indices were first measured for gelatine solutions of various concentrations and various pH's. Benzene was then added in excess, and the refractive index of the aqueous layer measured once more after equilibrium had been established (~ 48 hours). Through calculations, the solubility of the benzene was obtained in grams per 100 ml of gelatine solution. The results of such measurements at 20° are presented in Fig. 1. From these data it is to be seen that the greatest solubilization of benzene at each investigated concentrations was that which was observed at the isoelectric point. In the acidic and basic regions, the solubility is considerably less than at the isoelectric point, but is,all the same, greater than in pure water. The discovery of the maximum in the solubilizing action at the isoelectric point presents a new effect characterizing the isoelectric state of albumin. The appearance of this maximum can be explained in terms of a coiling of the branched gelatine chains at the isoelectric point, this coiling leading to the formation of globules which contain hydrophobic nuclei to give rise to solubilization just as in the case of the globular albumins and the soap micells. In strongly acidic and basic solutions, the mutual repulsions of the uniformly charged functional groups results in a straightening of the chain, and the solubilization diminishes. The fact that the solubilization does not entirely disappear is probably to be explained by the sorption of the benzene molecular or the nonpolar segments (side chains) of the micromolecules of the gelatine.

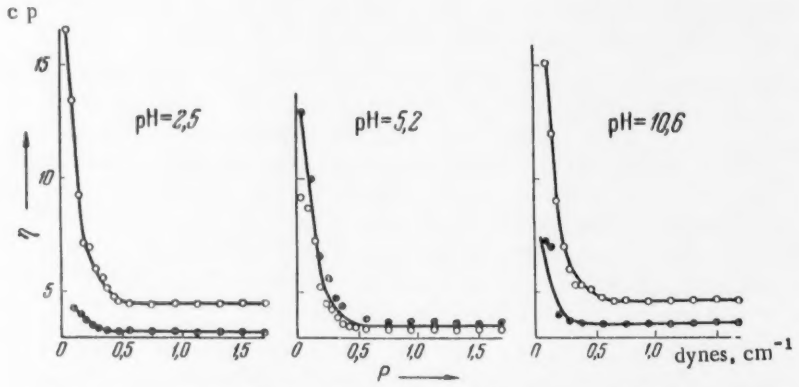

Fig. 2. The relation between the structural viscosity η, and the sheer stress, P, for a 0.43% gelatine solution at various values of the pH:
1) Prior to solubilization; 2) after solubilization of benzene.

It was of interest in this connection to study the change in the viscosity of gelatine solutions arising from the dissolving of benzene. These viscosities were determined in an elastoviscosimeter of the rotational type such as has been developed by S. P. Alekhin and one of us [15].

In Fig. 2 data is presented on the viscosity of a 0.43% gelatine solution at 20°.

It is to be seen from Fig. 2 that the structural viscosity shows a slight increase after solubilization at the isoelectric point of pH 5.2. This is clearly related to the fact that gelatine globules at the isoelectric point

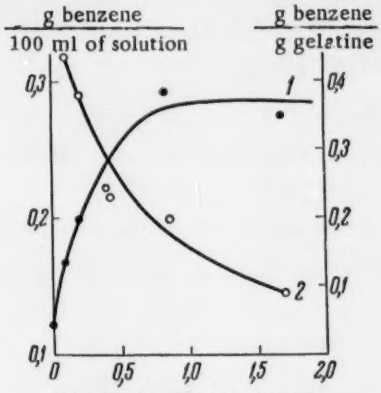

Fig. 3. The relation between the concentrations of gelatine solutions and the solubilization (1), and the reduced solubilization (2), of benzene.

have a rather open structure so that benzene penetrating within these globules changes their dimensions only insignificantly.

In the acidic and basic regions on either side of the isoelectric point (see Fig. 2, pH 2.5 and 10.6) a marked decrease in the structural viscosity is observed after the dissolving of the benzene. It can be supposed that "fixing" of the hydrophobic particles will result from sorption of the benzene and that there will be a partial coiling of the molecules as a consequence of the mutual van der Waals attractions of the nonpolar portions of the chain [16].

The graph of Fig. 3 shows the relation between the solubilization of benzene and the concentration of gelatine in solution. From Fig. 3, 1, it is to be seen that there is a linear increase in the solubilization up to a gelatine concentration of 0.5%, after which the value of the solubilization becomes constant. Curve 2 shows the amount of benzene which is bound to 1 g of gelatine to diminish with an increase in the gelatine concentration. It is noteworthy that there is a correspondence between the observed limit of solubilization at a concentration of 0.5% and the beginning of structuralization in the system (with the formation of a gel) [10]. On the other hand, the increase in the reduced amount of bound benzene with increasing concentration is a result of the separation of the macromolecules of gelatine, one from another, to facilitate the process of globulization.

Investigation was also made of the solubility of benzene in gelatine solutions at 30°, and the dependence of this solubility on the pH of the medium. Here there was no longer a characteristic maximum in the solubilization at the isoelectric point, but the solubility of benzene in the gelatine solutions was still somewhat greater than in water. The disappearance of the maximum and the decrease in the magnitude of the solubilization are to be explained by the absence of globules in gelatine solutions at higher temperatures, a fact which has been already noted in the literature [10].

LITERATURE CITED

[1] A. S. C. Lawrence, Trans. Farad. Soc. 33, 325, 815 (1937); 34, 660 (1938).

[2] McBain, Solubilization and Related Phenomena, N. Y., 1955.

[3] R. S. Stearns, H. Oppenheimer, E. Simon and W. D. Harkins, J. Chem. Phys. 15, 496 (1947).

[4] H. B. Klevens, Chem. Rev. 47, 1 (1950).

[5] K. A. Pospelova and P. A. Rebinder, Acta Physicochim. USSR, 16, 71 (1942); P. A. Rebinder, Colloid J. 8, 157 (1946); K. A. Pospelova and Z. N. Markina, Proc. Second All-Union Conference on Colloid Chem. Kiev, 1952; P. A. Rebinder and K. A. Pospelova, Introductory article in the book of V. Clayton, Emulsions (in Russian), Foreign Lit. Press, 1950; Z. N. Markina, K. A. Pospelova and P. A. Rebinder, Proc. Acad. Sci. USSR, 99, 121 (1954); Colloid J. 16, 366 (1954); Proc. Third All-Union Conference on Colloid Chem. 1956, p. 410;** Z. N. Markina and P. A. Rebinder, Proc. Acad. Sci. USSR, 109, 1156 (1956).

[6] A. I. Iurzhenko, J. Gen. Chem. 16, 1171 (1946).

[7] L. E. Peregudova and S. S. Voiutskii, Colloid J. 10, 309 (1948).

[8] D. L. Talmud, J. Phys. Chem. 15, 532 (1941).

[9] S. E. Bresler and D. L. Talmud, Proc. Acad. Sci. USSR, 43, 326, 367 (1944); S. E. Bresler, Biochemistry, 14, 180 (1949); G. A. Deborin, Proc. Acad. Sci. USSR 67, 889 (1949); G. A. Deborin and L. B. Gorbachev, Proc. Acad. Sci. USSR 82, 943 (1952); D. L. Talmud, Conference on Albumin, 1948, p. 18;** B. A. Talmud, Proc. Acad. Sci. USSR 79, 643 (1951); D. L. Talmud, Colloid J. 8, 252 (1946).

*Original Russian pagination. See C. B. Translation.

**In Russian.

[10] P. I. Zubov, Z. N. Zhurkina and V. A. Kargin, Proc. Acad. Sci. USSR 67, 659 (1955).

[11] V. A. Kargin and T. A. Matveeva, Proc. Acad. Sci. USSR 105, 294 (1955).

[12] K. Weigand, Experimental Methods in Organic Chemistry (in Russian), Part 1, 1951, p. 48.

[13] A. I. Iurzhenko, Reports of the Third Conference on High Polymer Compounds, Acad. Sci. USSR, Press, 1945 [in Russian].

[14] V. Pauli and E. Val'ko, The Colloidal Chemistry of Albuminous Substances (in Russian), 1936, p. 70.

[15] V. A. Pchelin and N. Ia. Solomchenko, Fourth All-Union Conference on Colloid Chem. Tiflis, 1958, p. 262 [in Russian].

[16] Z. N. Markina and P. A. Rebinder, Proc. Acad. Sci. USSR 109, 1156 (1956).

[17] P. V. Afanas'ev, B. A. Talmud and D. L. Talmud, Proc. Acad. Sci. USSR 55, 615 (1947).

The Department of Colloidal Chemistry of the
M. V. Lomonosov State University, Moscow

Received July 1, 1958

DETAILS OF THE KINETICS OF SUPERSATURATION IN AQUEOUS CALCIUM OXIDE SUSPENSIONS

E. E. Segalova, S. I. Kontorovich and Academician P. A. Rebinder

Study of the setting of various mineral binders has shown [1-3] the kinetics of structure formation to be largely determined by the kinetics of the supersaturation which results from putting the raw binder into suspension. Measurements of the supersaturation in various suspensions of mineral binders have been reported in the literature [4], but only for the hemihydrate of gypsum [5], and for the tricalcium [2, 6], and monocalcium [7], aluminates have maximum stable supersaturations been established which could be considered as the apparent solubilities of the respective compounds.

The present work is an investigation of the kinetics of supersaturation in aqueous calcium oxide suspensions, in which the aim was to clear up the nature of the supersaturation in these suspensions and to elucidate the characteristics of hydrational setting.

The reference literature contains no data on the solubility of CaO. It is known, however [8, 9] that calcium oxide dissolves to give solutions which are supersaturated with respect to $Ca(OH)_2$, and that the degree of this supersaturation is variable.

Here the kinetics of supersaturation in aqueous calcium oxide suspensions were developed conductimetrically in a special cell which was equipped with platinum-blacked electrodes, a stirrer and a thermometer. Measurements were carried out at 21.6 ± 0.05° in an atmosphere of nitrogen.

Figure 1 shows the variation in the electrical conductivity (concentration) of aqueous CaO suspensions and the dependence of the conductivity on the rate of agitation. An analysis of the curves of Fig. 1 proved that the rate of agitation fixed, not only the rate at which maximum conductivity was attained, but the absolute value of this maximum, as well. This is to be explained by the fact that increasing the rate of agitation increased the number of ions which succeeded in entering unit volume before the supersaturation in this volume was reduced by crystallization. The kinetics of the electrical conduction became independent of the rate of agitation only above 1600 rev/min, after the limiting effect of diffusion had been eliminated. Even at such a rate of agitation, it was not possible to detect a stable supersaturation which was independent of the charge of CaO, a fact that is to be explained by the high rate of growth of nuclei, some of which form even at relatively low supersaturations [9].

The natural procedure for detecting a stable supersaturation level was to introduce into the aqueous CaO suspensions such quantities of surface-active substances [3] as would leave the solubility practically unaltered and yet stablize the nascent nuclei, retarding their growth [10, 11] and thereby delaying the fall-off of supersaturation in the liquid phase.

This end was achieved by addition of an alcoholic sulfite waste (ASW), or glucose. Preliminary experiment had shown that these additives only insignificantly decreased the solubility of $Ca(OH)_2$. It was also shown that the addition of CaO gave rise to an adsorption of ASW out of solution and that this adsorption proceeded so rapidly and went so nearly to completion that any increase in the electrical conductivity arising from the residual ASW could be neglected (Table 1).

Figure 2 makes it clear that the introduction of the surface active additives to aqueous CaO suspensions led to a sharp increase in electrical conductivities, the introduction of sufficiently large amounts of these

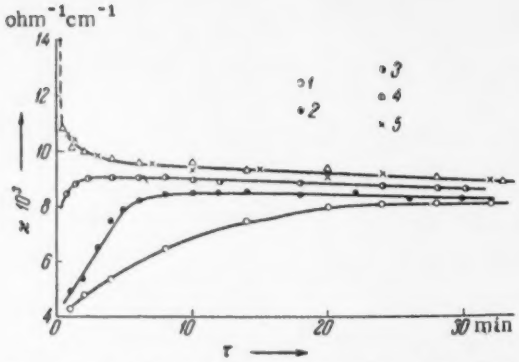

Fig. 1. The effect of the agitation rate on the kinetics of electroconductivity in aqueous CaO suspensions: S/L = 34%.
1) 120 rev/ min; 2) 400 rev/ min; 3) 800 rev/min; 4) 1600 rev/ min; 5) 2000 rev/ min.

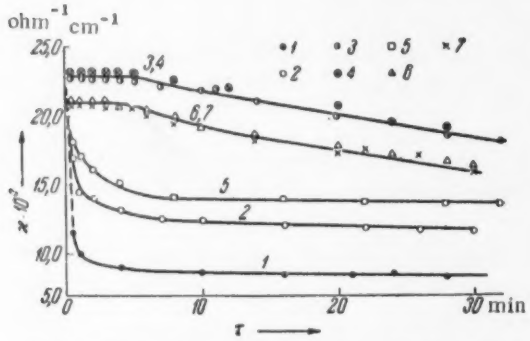

Fig. 2. The kinetics of the electrical conductivity of aqueous suspension of CaO with various additions of surface-active substances; S/L = 1.2%.
1) without addition; 2-4) glucose solutions: 2) 0.016%; 3) 0.08%; 4) 0.12%; 5-7) ASW solutions: 5) 0.15%; 6) 0.3%; 7) 0.6%.

additives resulting in a stable supersaturation level, which remained constant for 3-5 minutes, and then gradually diminished. The fact that this level stayed constant for several minutes indicated the existence of a temporary equilibrium between the dissolved CaO and the nascent $Ca(OH)_2$ nuclei. The dissolving proceeded so rapidly at the optimal agitation rate (1600 rev/ min), that maximum supersaturation was reached almost instaneously.

Thus the addition of surface-active substances prevented the growth of nuclei and set up the conditions required for a high, stable, superaturation, and this despite the fact that there was an actual increase in the rate of formation of nuclei of calcium hydroxide [12].

It was also necessary to investigate the dependence of the maximum supersaturation on the size of the charge of CaO.

In order to clear up this problem, identical charges of calcium oxide (0.5 g of CaO per 250 ml of solution) were successively introduced into a solution of a surface-active substance. With this method of introducing the calcium oxide there was avoided that strong heating of the suspension which took place when a large charge of CaO was introduced directly, and conductometric measurements could be carried out under essentially isothermal conditions. The greatest temperature rise (0.5°) was observed on introducing the first charge of CaO. The temperature rise diminished with each subsequent addition, and became practically zero after the third and fourth charges had been introduced.

In Fig. 3 the point of introduction of each charge of CaO is indicated by an arrow. From this figure it is to be seen that the introduction of CaO into a solution of a surface-active substance led to sharp increase in the electrical conductivity to a value which remained constant over several minutes. The increase in the conductivity, just like the rise in temperature, became less and less with each successive introduction of CaO, and the conductivity finally ceased to depend on the amount of CaO in the solid phase.

The fact that the maximum electrical conductivity was independent of the charge of CaO indicated the existence of a steady level of supersaturation, which could be considered as the apparent solubility of the calcium oxide. The dissolving of the CaO continued to the establishment of that maximum supersaturation which fixed the apparent equilibrium concentration of ions in the solution in the presence of the solid calcium oxide. Further dissolving took place only in proportion to the crystallization of the hydrated oxide nuclei out of solution, the growth of these nuclei being retarded by the surface-active additive. This temporary equilibrium was maintained as long as the suspension retained solid calcium oxide which could pass into solution and the amount of surface-active substance was adequate for the stabilization of the nascent nuclei.

Once it had been established that the stable level of the electrical conductivity was independent of the charge of CaO, experiments were then undertaken to measure the apparent solubility of calcium oxide corresponding to this level through the direct analytical determination of the hydroxyl ions in solution. These experiments proved, however, that the customary method of filtering a sample of the suspension through a filter

TABLE 1

Concentration of initial ASW solution, %	Electrical conductivity of initial ASW solution κ, 10^3 ohm^{-1} · cm^{-1}	Concentration of ASW in solution 2 minutes after the addition of CaO, %	Electrical conductivity of the ASW solution 2 minutes after the introduction of CaO, κ, 10^3 ohm^{-1} · cm^{-1}
0.08	0.17	0.0125	0.05
1.6	2.3	0.175	0.17
3.2	3.7	0.23	0.45

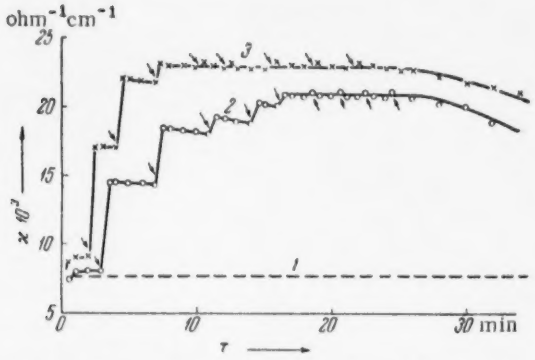

Fig. 3. The relation between the size of the charge of CaO and the electrical conductivity of a suspension of CaO containing a surface active substance: 1) electrical conductivity of a saturated $Ca(OH)_2$ solution; 2) 0.8% ASW solution; 3) 0.08% glucose solution.

of 2 μ pore diameter, did not give reproducible results, even under constancy of the electrical conductivity, i.e., at fixed solution concentration, colloidal nuclei of $Ca(OH)_2$ which had been stabilized by the surface-active substance passing into the filtrate.

The concentration of the solutions containing the colloidal particles could be potentiometrically determined with the hydrogen electrode after it had been proven that this electrode was not poisoned by the surface-active substances, ASW and glucose.

The measured values of the p_aH were 12.98 for suspensions of CaO in ASW solution and 13.01 for suspensions in glucose solutions. The smaller value of p_aH in the first case is clearly to be explained by the diminished solubility of the CaO in the presence of the calcium ions of the calcium lignosulfites. A conversion of the p_aH values to concentrations, without taking activity coefficients into account, gave a maximum supersaturation (apparent solubility of CaO) of the order of 2.70 g/l in the ASW solutions and 2.85 g/l in the glucose solutions. The actual solubility of the CaO was larger, since the activity coefficient is considerably less than unity in such concentrated solutions.

LITERATURE CITED

[1] E. E. Segalova, V. N. Izmailova and P. A. Rebinder, Proc. Acad. Sci. USSR 110, No. 5 (1956); E. E. Segalova, E. S. Solov'eva and P. A. Rebinder, Proc. Acad. Sci. USSR, 114, No. 1 (1957);* E. E. Segalova and P. A. Rebinder, Outlines of Reports, Fourth All-Union Conference on Colloid Chemistry, 1958, p. 130.

[2] E. S. Solov'eva and E. E. Segalova, Outlines of Reports, Fourth All-Union Conference on Colloidal Chemistry, 1958, p. 136.

[3] E. E. Segalova, E. S. Solov'eva and P. A. Rebinder, Proc. Acad. Sci. USSR, 113, No. 1 (1957).*

[4] R. H. Boque, The Chemistry of Portland Cement, N. Y., 1947.

[5] P. P. Budnikov, Gypsum, Its Study and Applications (in Russian), 1943; P. F. Konovalov and E. I. Morozov, Cement, 5 (1956); Ia. L. Zabezhinskii, V. B. Ratinov and T. I. Rozenberg, Proc. Acad. Sci. USSR, 108, No. 6 (1956); V. B. Ratinov, Ia. L. Zabezhinskii and T. I. Rozenberg, Proc. Acad. Sci. USSR, 109, No. 5 (1956).

[6] E. E. Segalova, E. S. Solov'eva and P. A. Rebinder, Proc. Acad. Sci. USSR, 117, No. 5 (1957).*

[7] E. E. Segalova, Z. D. Tulovskaia and E. A. Amelina, Outlines of Reports, Fourth All-Union Conference on Colloidal Chemistry, 1958, p. 140.

*Original Russian pagination. See C. B. Translation.

[8] P. Mecke, Zement, 48 (1935).

[9] R. Hedin, Chemical Processes in the Hardening of Portland Cement, 1945.

[10] A. M. Smirnova and V. P. Sukhova, Outlines of Reports, Fourth All-Union Conference on Colloid Chemistry, 1958, p. 144.

[11] R. Mark and G. Young, Physical Chemistry and Its Applications to Problems of Mineralogy, Petrography and Geology (in Russian), 1933; M. Tovbin and S. Krasnova, J. Phys. Chem. 23, vol. 7 (1949).

[12] D. S. Kamenetskaia, Crystal Growth (in Russian), 1957.

The Department of Colloidal Chemistry of the
M. V. Lomonosov State University, Moscow
The Dispersed Systems Section of the Institute
of Physical Chemistry of the Academy of
Sciences of the USSR

Received July 18, 1968

AN EXPERIMENTAL INVESTIGATION OF THE STRESS DISTRIBUTION DURING RUPTURE OF POLYMERS

V. E. Gul' and I. M. Chernin

(Presented by Academician V. A. Kargin, July 14, 1958)

In the present investigation, a technique of high-speed cinematography under polarized light was developed for obtaining data on the distribution, and alteration, of the stresses which are set up during the expansion of a rupture field. Polyethylene, polymethylmethacrylate and vulcanized rubber were selected as experimental materials. As is well known, the use of polarized light for the study of the stresses in deformed specimens of transparent materials is based on the fact that these substances are doubly refracting. Thus it is not the stress in the specimen which is itself measured, but rather an optical effect is observed which arises as the result of double refraction, and it is from this that conclusions can be drawn as to the stresses at various points within the specimen. A 3000 watt projector, or an electric arc operating at constant current, was used as a source of light. This light source was so arranged that it was possible to illuminate the test specimen with parallel rays from a mirror, or from a lens system. The specimens were deformed to rupture on a RMM-60 tensile-strength machine which had been so modified as to make it applicable to these investigations. The polarizer was a herapathite polaroid set in a holder which permitted its rotation to any desired angle. A similar herapathite polaroid also served as the analyzer. In the case which is under consideration, it was possible to deduce the normal stresses in the cross-section of the specimen from lines joining similarly colored points, the difference between the principal stresses being equal to the normal stress in this section.

Investigation showed essential differences to exist between the mechanisms of rupture in polyethylene, methylmethacrylate, and vulcanized rubber. In Fig. 1 there are given the final frames in a high-speed cinematograph of the rupture of polyethylene, taken under polarized light. These frames represent the final steps in the rupture of a polyethylene which had been stretched at a rate of 500 mm/min at 20°. The specimens of polyethylene, 50 × 60 mm in dimensions, were notched, 2 mm on each side, in order to fix the direction of expansion of the rupture field. The rate of filming was 1000 frames/sec. Study of Fig. 1 shows the concluding stages of the rupture process to occur over a minute fraction of a second at comparatively high velocity, and to be characterized by the absence of overstrain at the position of expansion of the rupture field. The period which had preceded this was one conforming to the usual description of rupture processes in polyethylene: at the position of expansion of the rupture field characteristic spots were observed which indicated the existence of overstrain. In Fig. 2 there are shown frames from the high-speed cinematography which were taken just prior to the initiation of the rapid expansion of the rupture field, and at the instant of high-velocity propagation of the rupture field. There is a marked nonuniformity in the stress distribution in the specimen at the beginning of deformation. Overstrain peaks occur at the notch positions.

Further elongation is, however, accompanied by a smoothing out of these overstrain peaks. At the same time, there arises a characteristic "checking", and as this latter increases, the region of uniform stress also increases, until a rapid propagation of the rupture field finally sets in. In contradiction to the results obtained on the other polymers, no overstrain peaks are to be observed at this stage.

The rupture of linear polymers in the vitrified condition is of an entirely different character. In Fig. 3 there are shown certain frames from a high-speed cinematograph of polymethylmethacrylate, taken under polarized light. This polarization picture conforms to the current ideas as to the rupture mechanism in vitrified

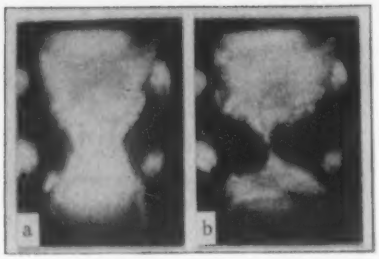

Fig. 1. Final frames in a high-speed cinematograph of the rupture of a specimen of polyethylene, taken under polarized light.

polymers. As soon as deformation begins, overstrain arises at the notch position, and this overstrain increases as the specimen is elongated. This increase in the overstrain is indicated by an increase in the intensity of darkening at the notch positions in the specimen. It is a very curious and, as it seems to us, a very important, point, that the regions of intense darkening (in the image of the specimen, photographed in polarized light) increases, though nonuniformly, as elongation proceeds in the specimen of polymethylmethacrylate. This darkening is preferentially propagated in a direction perpendicular to the elongation. As the deformation proceeds, there is a subsequent propagation of the region of overstrain, from one defect to another, in a direction perpendicular to the elongation. Judging from the intensity of darkening, the overstrain is smaller, the further a given point in the darkened region is from the edge of the defect (the notch in this case) in the specimen. There finally comes a time when the regions of darkening merge and there is an equalization in the intensity of darkening. In the plane perpendicular to the axis of elongation, overstrains arise which are at first different at different points in the section of maximum strain (depending on the distance from the edge of the defect), and finally become (Fig. 3c) equal. A field of variable overstrain exists in an unruptured specimen of polymethylmethacrylate. In the case which is under consideration, the points of equal overstrain fall on a plane which is perpendicular to the axis of elongation. It is on this plane that the specimen separates into two parts.

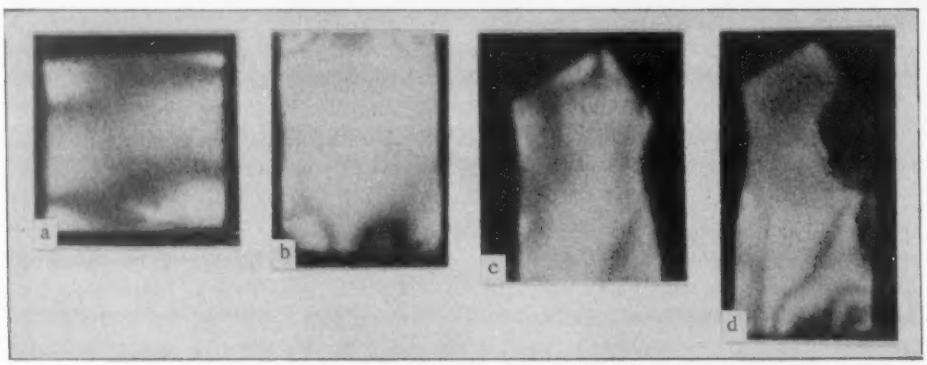

Fig. 2. Frames from a high-speed cinematograph of the rupture of polyethylene, taken under polarized light:
a) Beginning of deformation; b) beginning of "necking"; c) beginning of the expansion of the rupture field; d) at the point of high-speed propagation of the rupture field.

Sheets of vulcanized rubber from natural latex were used as an example of a polymer with a well-developed space structure. In comparison with other vulcanizates, these films were characterized by relative high strength. Specimens notched as indicated above, were stretched by 900-1000% prior to rupture. Overstrain at the notches, such as was noted above, was not observed. However, surfaces of overstrain appeared, these being oriented in parallel with the axis of elongation, rather than perpendicular to it. In the working specimens, two surfaces of overstrain appeared which were tangent to the notch boundaries. In a certain stage of the rupture process, the specimen separated into two parts along these overstrain surfaces. On further elongation, the remaining portion became steadily more nonuniform (in the sense of the distribution of stress) and the specimen broke in the holder. In view of the fact that the notches did not here fulfill their customary function of fixing the position of rupture, and the specimen, after laminating along surfaces tangent to the boundaries of the notches, deformed as if it were unnotched to rupture at an accidently determined position, it was impossible to fix the distribution of stress at the point of rapid expansion of the rupture field.

However, a consideration of Fig. 4 gives reason to believe that rupture occurred in a material which was homogeneous in terms of the stress distribution. Thus, by investigating rupture processes through the method of

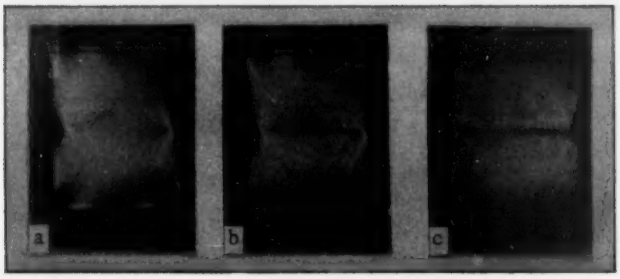

Fig. 3. Frames from a high-speed cinematograph of the rupture of polymethylmethacrylate, taken under polarized light.

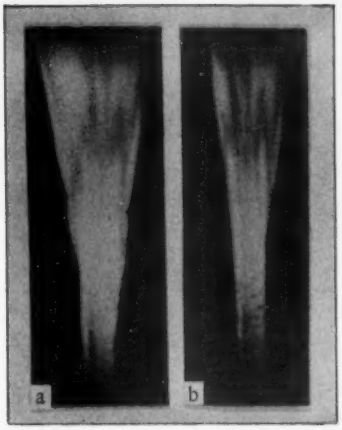

Fig. 4. Frames from a high-speed cinematograph of the rupture of vulcanized rubber film, taken under polarized light.

high-speed cinematography under polarized light, fundamental differences have been established in the stress distribution in elongated polymer specimens. Linear crystallizing polymers, such as polyethylene, are characterized by a rapid extension of the rupture surface through a zone of uniform stress. Linear vitrified polymers, such as polymethylmethacrylate, rupture along a surface perpendicular to the axis of deformation, this surface appearing initially as the locus of points of equal overstrain. Polymers with a well-developed spatial structure, such as vulcanizates from films of natural latex, are characterized by a distribution of the stresses in planes parallel to the axis of elongation. Specimen rupture occurs along these surfaces when the overstrain reaches a sufficiently high value.

In conclusion, the authors wish to express their indebtedness to Academician V. A. Kargin for a number of very valuable suggestions and for the aid which he rendered while this work was in progress, and to thank B. M. Kovarskaia for having supplied the specimens for study.

Received June 26, 1958

THE DEHYDRATION AND REHYDRATION OF QUARTZ SURFACES

S. P. Zhdanov

(Presented by Academician M. M. Dubinin, July 11, 1958)

Quartz powders which have been prepared under the usual conditions are made up of particles whose surfaces resemble those of silicagel, in that they are hydrated and carry hydroxyl groups which are joined by valence bonds to the silicon atoms [1, 2]. As a result of this hydration, tetrahedral silicate groups appear on the surface, the free vertices of these groups projecting out of the surface to be occupied by single univalent OH groups, and this, in turn, leads to valence saturation and normal coordination of the surface atoms of Si and O. The hydration of the SiO_2 surface is already known to be an exothermic process. According to the data of Brunauer and others [3], the total surface energy of amorphous SiO_2 diminishes by approximately 130 ergs/cm^2 in passing from maximal dehydration to maximal hydration. Thus, it could be expected that a newly formed quartz surface which had been brought into contact with water (either in the course of treatment with aqueous acid solutions for the removal of contaminants from the quartz powders, or in the sedimentation of these powders in water for the purpose of separating them into fractions) would be in a state of maximal hydration, with the number of hydroxyls per unit of surface corresponding to the number of Si−O−Si bonds which had been ruptured in its formation, and that the identity in the crystal structures of quartz specimens would lead to this state being the same for each of them.

On the basis of crystallochemical data, it can be shown that the possible variation in the concentration of hydroxyl per unit quartz surface in the state of maximum hydration depends on the choice of cleavage planes and is limited to the range 9.9-16.0 $\mu M/m^2$ [2]. When account is taken of that anisotropy which Englehardt has noted [4] as appearing on cleavage, the upper limit for the surface hydroxyl concentration must be lowered to 12.6 $\mu M/m^2$. Determination of the hydroxyl concentration on unit quartz surface from thermal dehydration data leads, however, to varying values which are usually much larger than the above. It is not possible to understand these experimental results if the surface hydroxyls are supposed to be the only source of the water which is evolved on calcining quartz.

In the present work investigation has been made of the vacuum-dehydration of powders of an opaque quartz ($s = 5.4\ m^2/g$), and of a rock crystal ($s = 0.58\ m^2/g$); the rehydration of the rock crystal surface after calcination at 1150° was also studied, and a comparison was made of the adsorption of water vapor on original (maximally hydrated), on maximally dehydrated, and on rehydrated rock crystal surfaces. Calcination of the quartz powders was carried out in quartz ampules which had been sealed in a vacuum system. Over each temperature interval, the water which was evolved on calcination was condensed in a trap cooled with liquid nitrogen and its amount determined by weighing, by adsorption by magnesium perchlorate, or by a volumetric method. The quantitative determination of the water evolved in the calcination of the quartz could be carried out in the apparatus which was used for studying the dehydration [1].

In Fig. 1 there are presented curves for the vacuum dehydration of various quartz specimens with maximally hydrated surfaces. Curves 2 and 5 were obtained in the present work; curves 1, 3 and 4 were taken out of the paper of Stöber [1]. Even when calculated per unit surface, the water evolved during calcination of the various quartz specimens varied over very wide limits (from 5 to 50 $\mu M/m^2$). In distinction to this, there is only an insignificant variation in the amount of structural water per unit surface of calcined silica gels whose specific areas have been accurately determined [5].

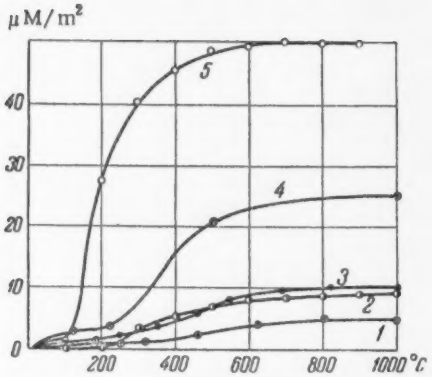

Fig. 1. Curves for the vacuum dehydration of various quartz specimens.

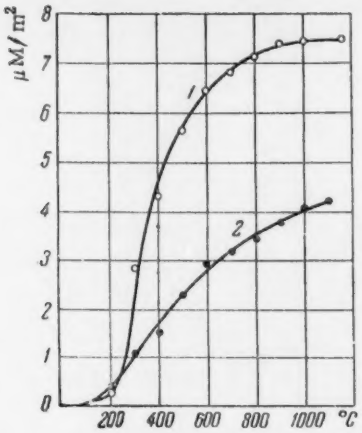

Fig. 2. A comparison of dehydration curves obtain with the initial, and with the rehydrated, quartz: 1) initial, noncalcined quartz; 2) quartz calcined at 1150° and rehydrated.

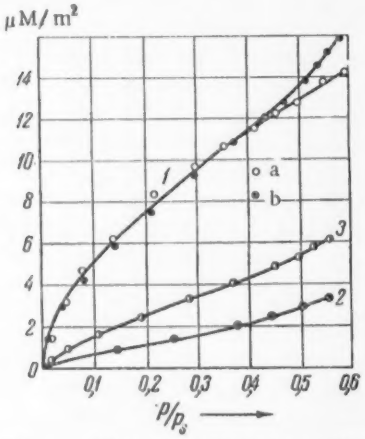

Fig. 3. Initial segments of adsorption isotherms for water on a certain quartz powder which had been variously treated:
1a) initial, maximally hydrated specimen; 1b) calcined at 1150° and then held in water for 1 month; 2) calcined in vacuum at 1150°; 3) calcined at 1150° and then held in water vapor (at $p/p_s = 1$) for 48 hours.

It is clear that the divergences among the curves of Fig. 1 cannot be explained as arising from differences in the degree of hydration of the quartz surfaces, since all of these curves were obtained with specimens whose surfaces should have been in that state of maximal hydration which corresponds to the working conditions. Such explanation becomes even more unlikely in view of the fact that the maximal possible amount of hydroxyl per unit quartz surface due to peculiarities in the crystal-lattice structure and the mechanical anisotropy of the crystals has been shown to amount to only 12.6 μ M/m². Stöber [1] ascribes the divergence of the dehydration curves which he obtained to the presence in the quartz of silaceous mineral contaminants which could serve as sources for the evolution of water during calcination. The possibility is not to be excluded, however, that these crystals contain free (molecular) water which is not removed by evacuating the unheated powders. This water could be adsorbed in the very fine fissures, or it could exist in the adsorbed state, or as a solid solution, in the crystal lattice itself. It is known that water is frequently detected spectrometrically in quartz crystals.

The precipitate rise in Curve 5 of Fig. 1 over the interval 100-200° can be ascribed to the evolution of water which was irreversibly adsorbed in fine fissures of molecular dimensions. The presence of such fissures in the crystals of our quartz specimens is confirmed by the fact that there was a considerable increase in the adsorption of water after heating to 200°, whereas the surface, measured in terms of nitrogen, remained practically unaltered [6]. The specific surface of the quartz powders as determined from nitrogen will be less than the actual when fissures are present whose hydrated surfaces are only partially available to nitrogen molecules, and the amount of structural water calculated on a 1 m² basis can then prove to be much too high. It is possible that this is another one of causes of the lack of concordance between the amounts of structural water determined from the dehydration curves of the various quartz specimens (Fig. 1). The determination of the amount of structural water on rehydrated quartz surfaces, and the investigation of the adsorption of water on such surfaces indi-

cates that a considerable part of the water which is evolved on calcining certain quartz specimens is not formed at the expense of the surface hydroxyls.

In Fig. 2 there are given dehydration curves for the rock crystal III (s = 0.58 m^2/g). Curve 1 refers to the original, not previously calcined, powder, whereas Curve 2 was obtained on this same specimen after its surface was maximally dehydrated by calcining to 1150° and then rehydrated by being held in water at room temperature for 1 month. A comparison of the curves of Fig. 2 shows a considerable number of hydroxyls to have been regenerated on the quartz surface as the result of rehydration. On the other hand, the amount of water which is evolved from a rehydrated quartz surface by calcining at any temperatures above 200° proves to be considerably less than that evolved from the initial quartz powder with maximally hydrated surface.

If these differences are related to variation in the hydroxyl concentration on unit surfaces of the initial, and the rehydrated, specimens, then these differences in degree of surface hydration should be reflected in the water adsorption isotherms, since this adsorption is very sensitive to the degree of hydration in silicates [2, 5, 7, 8]. However, it is to be seen from Fig. 3 that the adsorption isotherms for water, referred to unit surface of the initial (1a), and the rehydrated (1b), quartz practically coincide in the region of build-up of the monolayer. This could only be possible if the chemical structures and the degrees of surface hydration were approximately the same in the two cases. From these data it follows that the first calcination of the powders of rock crystal evolves not only water which is formed at the expense of the surface OH groups, but also, and irreversibly, a considerable quantity of water which was obviously located, not on the surface, but in the mass of the quartz crystals.

The concentration of hydroxyl per unit surface of rehydrated quartz as determined from the dehydration Curve 2 of Fig. 2 is 9.44 $\mu M/m^2$, allowance being made for the 0.48 $\mu M/m^2$ of H_2 which is evolved in calcination over the interval 500-1100°.

This value is only a little less than the lower limit of the hydroxyl concentration per unit quartz surface in a state of maximal hydration (9.9 $\mu M/m^2$). After calcining to 1150°, rehydration of a quartz surface can also be made to take place by maintaining the specimen in water vapors at $p/p_s = 1$. It is to be seen from isotherms 2 and 3 of Fig. 3 that the adsorption of water is considerably increased by holding the specimen in these vapors, a fact which points to the partial regeneration of the hydroxyls on the surface. The rehydration process is not completed by this exposure to the vapors, however; for its completion a longer time is required and other conditions must, perhaps, be fulfilled as well.

From the results which have been presented in the present work it follows that it is necessary to react very cautiously to an evaluation of the number of hydroxyls on a quartz surface from thermal dehydration data. The evolution of hydrogen which is observed on the calcination of quartz is of interest in various respects and deserves special study.

The author wishes to express his indebtedness to M. M. Dubinin and to A. V. Kiselev for their interest in this work and to E. V. Koromal'd for his participation in the measurements.

LITERATURE CITED

[1] W. Stöber, Koll. Zs. 145, 17 (1956).

[2] S. P. Zhdanov and A. V. Kiselev, Proc. Acad. Sci. USSR, 31, 2213 (1957).*

[3] S. Brunauer, D. Z. Kantro and C. H. Weise, Canad. J. Chem. 34, 1483 (1956).

[4] W. Engelhardt, Nachr. Akad. Wiss. Göttingen, Math.-Phys. Kl. 3, 43 (1944).

[5] L. D. Beliakova, O. M. Dzhigit and A. V. Kiselev, J. Phys. Chem. 31, 1577 (1957).

[6] S. P. Zhdanov, Proc. Acad. Sci. USSR, 120, 103 (1958).*

[7] M. M. Egorov, T. S. Egorova, V. F. Kiselev and K. G. Krasil'nikov, Proc. Acad. Sci. USSR, 114, 579 (1957).*

[8] S. P. Zhdanov, Proc. Acad. Sci. USSR, 68, 99 (1949).

The Institute of Silicate Chemistry of the
Academy of Sciences of the USSR

Received July 10, 1958

*Original Russian pagination. See C. B. Translation.

THE RELATION BETWEEN THE SURFACE STRUCTURES AND THE PHASE COMPOSITIONS OF ELECTROLYTIC DEPOSITS OF ALLOYS

Iu. M. Polukarov and V. V. Bondar'

(Presented by Academician A. N. Frumkin, July 14, 1958)

There exists at the present time a mass of accumulated material on the electrodeposition of alloys. It should be noted, however, that in the earlier studies the principal interest was directed to the search for the various conditions of electrolysis which would lead to the co-deposition of metals. Little attention was given to the structural factors, or to the nature of the component interaction during formation of the alloy, although these, to a considerable degree, determine the physicochemical properties of the deposit.

Meyer and Phillips [1] have studied the effect of various metals on the structure of the deposit which is formed in their coprecipitation with copper from cyanide solution, account being taken of the nature of the interaction of the components by going back to the data of the phase diagrams. At the same time, a number of investigations have shown [2] that the phase compositions of the deposits which are formed in electrocrystallization frequently differ from those which would be anticipated on the basis of the phase diagrams for the systems in question. In particular, it has been established that there is a possibility of forming strongly supersaturated solid solutions in the case of alloys of the eutectic type. The results of the present investigation indicate that the formation of a nonequilibrium, supersaturated solid-solution phase involves a marked alteration in the surface structure of a deposit.

In order to reduce to a minimum the influence of those extraneous factors which might affect the surface structures of alloys, the metals selected for study were those whose co-deposition could be carried out without the addition of surface-active, or complex-forming, substances. The copper – bismuth system proved to be one of the most suitable for this purpose.

According to the data of Raub [3], Cu and Bi crystallize separately in coprecipitating from perchlorate electrolytes, this being in conformity with the predictions of the phase diagram. At the same time, the ideas which have been developed in our laboratories [4] indicate that the formation of supersaturated solid solutions of bismuth in copper can also be anticipated in this system under certain conditions. By utilizing a $Cu(ClO_4)_2$ 0.6 N, $Bi(ClO_4)_3$ 0.4 N, pH 0.6 solution (solution I) there was actually obtained an alloy containing a supersaturated solid solution phase of bismuth in copper, in which there was an increase in the lattice parameter of the copper to a value of the order 3.635-3.645 A. The proportion of bismuth in this solid solution increased with increasing current density and reached 12% by weight, according to the data from x-ray measurements. With a further rise in the current density, increasing supersaturation led to so pronounced a distortion of the lattice that the lines in the x-ray diagram completely disappeared. According to the data from chemical analysis, there was always more bismuth in the alloy than would have corresponded to the increase in the lattice parameter of the copper, however, no lines, except those of copper, were to be found on the x-ray diagrams. Raub [5] has pointed to a similar situation in the silver–zinc system.

From Fig. 1 in which electron-microscopic photographs of the surfaces of deposits of alloys containing various amounts of bismuth are presented, it is to be seen that with increasing degree of supersaturation of the solid solution, the surface became smoother and smoother, acquiring luster at very high supersaturation.

The deposits which arose from a solution in which the bismuth to copper ratio was considerably greater than that of solution I, namely, $Cu(ClO_4)_2$ 0.2 N, $Bi(ClO_4)_3$ 0.8 N, pH 0.6 (solution II), were mixtures of the

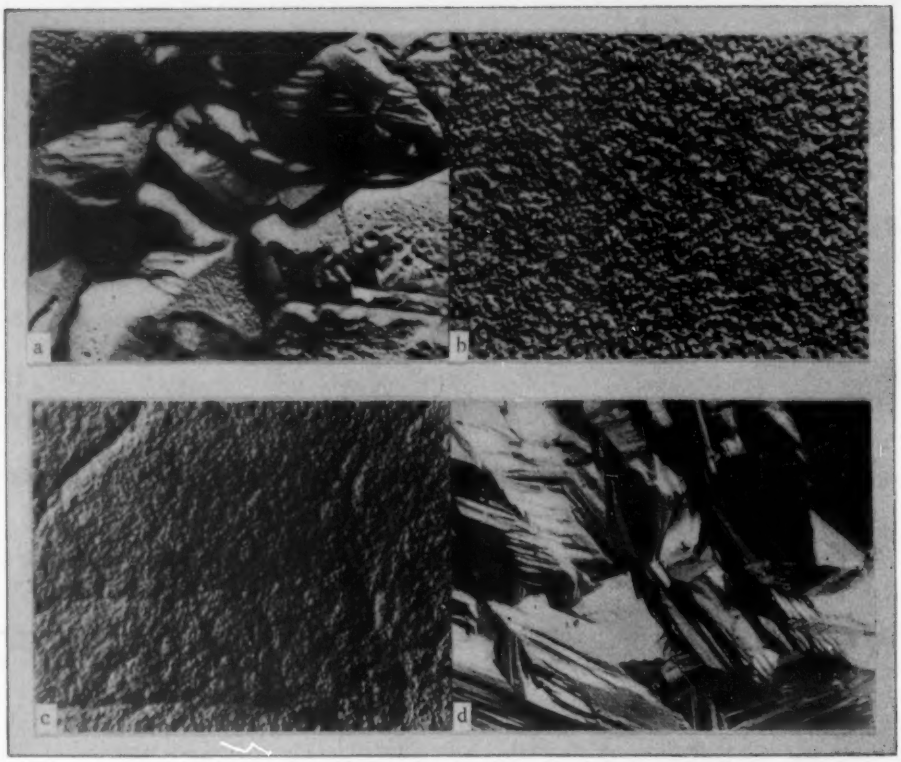

Fig. 1. The surface structures of electrolytic deposits of copper, of a copper – bismuth alloy obtained from a $Cu(ClO_4)_2$ 0.6 N, $Bi(ClO_4)_3$ 0.4 N solution and of a deposit of bismuth from a perchlorate solution.
A) Pure copper, copper parameter, a_{Cu} = 3.608 A; B) copper – bismuth alloy, 70% copper, a_{Cu} = 3.619 A; C) copper – bismuth alloy, 50% copper, a_{Cu} = 3.635 A; D) pure bismuth.

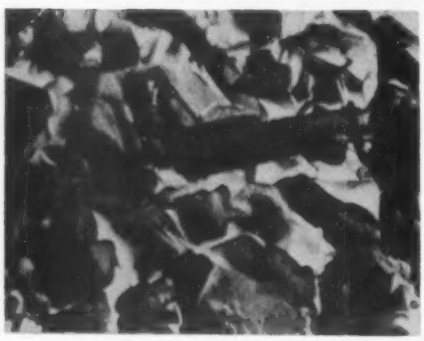

Fig. 2. The surface structure of the deposit of a copper – bismuth alloy obtained from a $Cu(ClO_4)_2$ 0.2 N, $Bi(ClO_4)_3$ 0.8 N solution. Alloy composition: copper 70%, bismuth 30%.

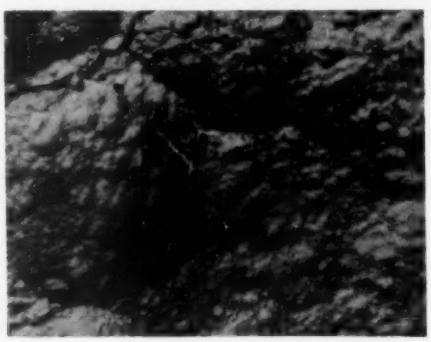

Fig. 3. The surface structure of a deposit of a copper – tin alloy obtained from a sulfate electrolyte, a_{Cu} = 3.700A.

crystals of pure copper and bismuth. In Fig. 2 there is shown a photograph of the surface of a deposit which was as obtained from solution II and had the same composition as the deposit of Fig. 1B.

The existence of a relation between the phase composition and the structure of the deposit of an alloy was confirmed by data which were obtained in investigations on copper – tin and tin – lead alloys.

The possibility of the formation of supersaturated solid solutions of tin in copper (up to 14-16%) in preparing alloys from cyanide solutions has been pointed out by Lainer [6] and by Raub [7], the latter claiming that such solid solutions could only arise under those conditions in which the discharge potentials of the ions were made to approximate one another with the aid of complex-formers and surface-active substances. The lack of justification for this point of view has been shown in the earlier papers from our laboratory [4, 8]. In the electrolysis of a solution containing 25 g/l $CuSO_4 \cdot 5H_2O$, 75 g/l $SnSO_4$, and 100 g/l H_2SO_4, the simultaneous discharge of the ions actually set in after the limiting current with respect to copper had been established. Here there appeared a solid solution which was strongly supersaturated when judged on the basis of the phase diagram. The lattice parameter for copper reached 3.745 A, a value which would correspond to a solid solution of about 22% tin by weight (according to the phase diagram, the solubility of tin in copper does not exceed 1% at room temperature [9]).

In Fig. 3 there is presented a photograph of the surface of a deposit of a copper – tin alloy. This deposit was dense and finely crystalline despite the fact that the co-deposition of the copper and tin took place under such conditions that there was a discharge of the copper ions at limiting diffusional current.

According to x-ray studies, the formation of supersaturated solid solutions is not to be observed in the preparation of tin – lead alloys from a $Sn(ClO_4)_2$ 0.8 N, $Pb(ClO_4)_2$ 0.2 N, $HClO_4$ 1 N solution, this being in agreement with the data from earlier investigations [10]. Here the deposit had a coarsely crystalline structure.

On the basis of these investigations it can be concluded that the formation of a supersaturated solid solution is of fundamental significance for the structure of an electro-deposited alloy, the production of a finely crystalline deposit being thereby promoted. Thus, the formation of finely crystalline, shiny, deposits of alloys can be expected when the electrochemical conditions favor the production of supersaturated solid solutions and there is no dimensional, or orientational, conformity between the lattices of the codepositing metals to retard the formation of nuclei of the more negative metal [11].

LITERATURE CITED

[1] W. R. Meyer and A. Phillips, Trans. Electrochem. Soc. 73, 377 (1938).

[2] E. Raub, Metalloberfläche, 7, 2, 17A (1953); T. Banarjee, Symposium on Electroplating and Metalfinishing, 1952, p. 29.

[3] E. Raub, Zs. Erzbergbau u. Metallhüttenwesen, 5, 4, 153 (1952).

[4] Iu. M. Polukarov and K. M. Gorbunova, J. Phys. Chem. 32, 762 (1958).

[5] E. Raub and B. Wullhorst, Metallforschung, 38, 41 (1947).

[6] D. I. Lainer, Monograph, The Working of Light Metals and Alloys, vol. 12, 70 (1950).*

[7] E. Raub and F. Sautter, Metalloberfläche, 11, 8, 249 (1957).

[8] Iu. M. Polukarov and K. M. Gorbunova, J. Phys. Chem. 31, 871 (1956).

[9] S. T. Konobeevskii and V. P. Tarasova, J. Phys. Chem. 9, 681 (1937).

[10] D. I. Lainer, Dissertation, Moscow, 1943. *

[11] P. D. Dankov, Proc. Second Conference on the Corrosion of Metals, Part II, Acad. Sci. USSR, Press, 1943, p. 121; P. D. Dankov, J. Phys. Chem. 20, 853 (1946).

The Institute of Physical Chemistry of the
Academy of Sciences of the USSR

Received June 21, 1958

* In Russian.

THE EFFECT OF THE RADIOACTIVITY OF BARIUM SULFATE ON ITS SORPTIONAL PROPERTIES

Academician Vikt. I. Spitsyn and V. V. Gromov

Radioactive irradiation of solid bodies can bring about various changes, the principal results being one type or another of crystal-lattice distortion [1] and the appearance of electrical charges on the crystal surface [2]. In turn, this must especially affect such physicochemical properties of these solid bodies as the reaction rates for isotopic exchange in heterogeneous systems [3], the catalytic activity [4], the sorption processes, and other phenomena as well [5].

The authors of the present communication have studied the effect of radioactivity on the sorption properties of solid bodies. Barium sulfate, a substance which has been well-studied earlier, [6-8], was chosen as a sorbent. Study was made of the adsorption of one acidic orange dye, (orange At2B) ($C_{16}H_{11}O_4N_2S$) Na, and two basic dyes, methylene blue, ($C_{16}H_{18}N_3S$) Cl, and brilliant green, ($C_{27}H_{35}N_2$)Cl, from aqueous solution. S^{35} was introduced into the barium sulfate during its precipitation and served as the source of radioactive radiation. S^{35} emits only low-energy β-particles (E_{max} = 0.169 mev) and has a comparatively long half-life period ($T_{1/2}$ = = 87.1 days). As an emitter, it possessed a number of advantages: work with preparations of high specific activity could be carried on with the minimum of shielding, and the radiation was almost completely absorbed within the $BaSO_4$ precipitate. In addition, the action of the radiation on the liquid phase was insignificant, since the solubility of $BaSO_4$ is low and the amount of radioactive sulfur which passed into solution was small.

The specimens of $BaSO_4$ were prepared by the method of Kolthoff [7] and Rutgers [8]. Hot 0.1 N solutions of $BaCl_2$ and Na_2SO_4, the latter containing a definite amount of S^{35}, were poured together at constant rate (200 ml of each solution in 30 minutes) with agitation. Agitation was then continued for 1 hour under heating to 70-80°. Following this, the precipitate was allowed to stand in contact with the mother liquid for 16 hours. The precipitates were then washed free of Na^+, Cl^- and Ba^{2+} ions, the barium salt having been added in excess in order that the smallest possible number of the radioactive anions SO_4^{2-} remain in solution. Finally, the precipitates were twice washed with ethyl alcohol, and dried to constant weight at 80-100°. The characteristics of the resulting preparations are given in Table 1.

The specific surface areas of the $BaSO_4$ precipitates were determined microscopically (1350 × magnification). The results were in good agreement with the data obtained by Rutgers [8] from the same method, and also with data from the electron-microscopic method and from a study of the sorption of various dyes by the precipitated $BaSO_4$ [7, 8].

Our experimental procedure was the following: 3 g of the precipitate was shaken for 4 hours at 25 ± 0.5° with 15 ml of dye solution of fixed concentration. Following this, the concentration of the dye in the liquid phase was determined spectrophotometrically using instruments of the types of SF-4 and SF-2M (with the latter it was possible to work at maximum optical absorption). The experimental error of measurement was within the limits 3-4%. By preliminary experiments it was established that the time required for equilibrating the liquid and solid phases was usually not in excess of 1 hour. Study was made at dye concentrations ranging from 10 to 200-250 mg/l. The solutions were characterized by the following pH values: acid orange, 5.5-5.8; methylene blue 6.2-6.9; brilliant green 3.9-4.6.

The experimental results are presented in Figs. 1, 2, and 3. Each set represents results obtained from three series of experiments carried out in parallel. The deviation from the mean did not exceed 5%. It was

TABLE 1

Characteristics of the Experimental $BaSO_4$ Precipitates

Specimen No.	Specific surface, m^2/g	Specific activity, mC/g
1	0.74	0
2	0.68	0.01
3	0.68	0.1
4	0.78	1
5	0.76	4
6	0.78	10

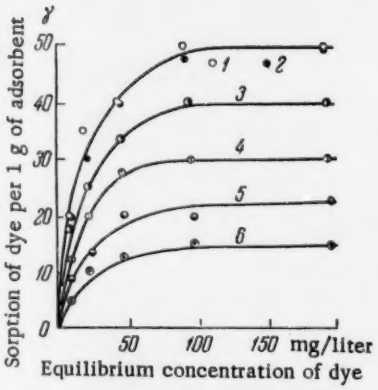

Fig. 1. The sorption of methylene blue by $BaSO_4$ precipitates of various specific activities:
1) inactive precipitate; 2) 0.01 mC/g; 3) 0.1 mC/g; 4) 1 mC/g; 5) 4 mC/g; 6) 10 mC/g.

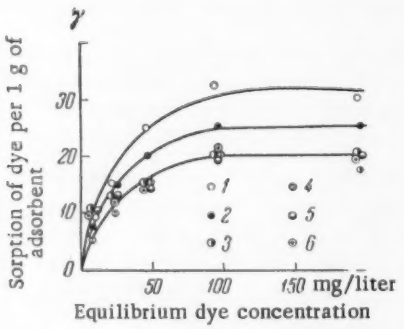

Fig. 2. The sorption of brilliant green by $BaSO_4$ precipitates of various specific activities. See Fig. 1 for explanation of the numbers.

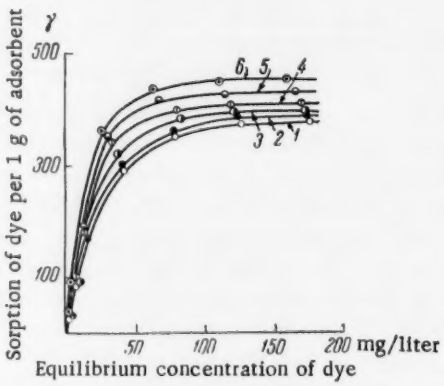

Fig. 3. The sorption of acid orange by $BaSO_4$ precipitates of various specific activities. See Fig. 1 for explanation of the numbers.

established that the acid orange dye was most strongly taken up by the precipitated $BaSO_4$, its sorption being one order higher than that of the other dyes. The methylene blue was somewhat more strongly sorbed than the brilliant green.

It is to be noted that the sorption of the two basic dyes fell with an increase in the specific activity of the barium sulfate. A preparation with an activity of 10 mC/g was characterized by a sorptive capacity of 15 γ/g for methylene blue (inactive 50 γ/g) and 20 γ/g for brilliant green (inactive, 30 γ/g). On the other hand, the sorption of acid orange increased with an increase in the radioactivity of the $BaSO_4$ preparation. Here, at an activity of 10 mC/g, the sorptive capacity of the precipitate amounted to 455 γ/g (inactive, 380 γ/g). Figure 4 shows the relation between the magnitude of the dye sorption and the specific activity of the $BaSO_4$. In the case of methylene blue, and for activities in the limits 0.01-10 mC/g, the sorptive capacity increased linearly with the logarithm of the specific activity of the $BaSO_4$. For brilliant green, a marked decrease in the

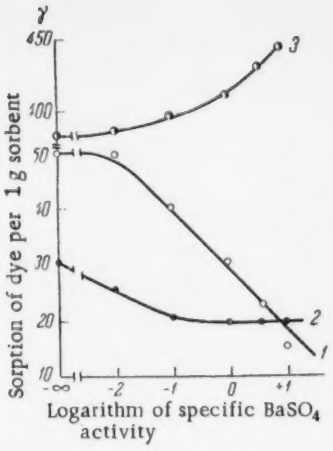

Fig. 4. The effect of the activity of $BaSO_4$ on the sorption of dyes: 1) methylene blue; 2) brilliant green; 3) acid orange.

magnitude of sorption was observed in the activity range 0.01-0.1 mC /g, but increase in the specific activity of the precipitate to 10 mC /g brought about no further appreciable fall in the sorptive capacity.

The question arose as to whether the decrease in the adsorption of the investigated basic dyes with increasing radioactivity of the sorbent was not illusory; whether it did not come about from the decolorization of the dyes under the action of the radiation. Special experiments were set up to test this supposition. To a dye solution there was added tagged sodium sulfate whose activity in terms of S^{35} exceeded by 10-, 100- or 500-fold the concentration of S^{35} in the liquid phase above a $BaSO_4$ precipitate with a specific activity of 10 mC/g. At definite intervals of time the dye concentration was checked spectrophotometrically. These experiments proved that the dyes in question were stable to the action of the β-radiation from S^{35} for 40-50 hours, even at concentrations of S^{35} as high as 8 mC/g. Such concentrations of S^{35} were far in excess of the concentrations in the investigated equilibrated solutions.

In addition, equilibrated solutions of dye were agitated in contact with barium sulfate precipitates having a specific activity of 10 mC/g for 16, and for 32 hours, instead of the customary 4 hours. Even in this case, there was no further concentration change in the dye. Thus in these experiments, it was impossible to ascribe the variation in the dye sorption by $BaSO_4$ precipitates of various specific activities to a breakdown of the dye under the action of the radiation from the S^{35}.

It is clear that there were no perceivable chemical or radiochemical changes in the liquid phase which could have affected the stability of the dyes or the magnitude of their sorption. This belief is confirmed by the fact that the pH values of the equilibrated solutions were, to within the limits of experimental error, the same as those of the initial dye solutions.

It is to be presumed that the observed variation in the dye sorption was related to the positive charge which arose on the precipitated radioactive barium sulfate as a result of the continual bombardment by β-particles. It is clear that the magnitude of such charge would increase with increasing specific activity of the precipitate. In such a case, a basic dye possessing a colored cation should adsorb more poorly on an active sorbent which is a β-radiator, and an acid dye with a colored anion, adsorb better than would be the case with an inactive sorbent. This is the situation as it has been observed in the experiments which have been described above.

LITERATURE CITED

[1] G. J. Dienes and G. H. Vineyard, Radiation Effects in Solids, N. Y. – London, 1957.

[2] P. Curie and M. Curie, Compt. rend., 130, 647 (1900).

[3] Vikt. I. Spitsyn and I. E. Mikhailenko, Proc. Acad. Sci. USSR, 121, 319 (1958).*

[4] A. A. Balandin, Vikt. I. Spitsyn, N. P. Dobrosel'skaia and I. E. Mikhailenko, Proc. Acad. Sci. USSR, 121, 495 (1958).*

[5] Vikt. I. Spitsyn, Bull. Acad. Sci. USSR, Div. Chem. Sci. 1958, 1294.*

[6] L. de Brouckère, Ann. Chim. Belg. 10, 92 (1933).

[7] M. Kolthoff and W. M. McNevin, J. Am. Chem. Soc. 59, 1639 (1937).

[8] A. M. Rutgers and W. van. den Heuvel, Experientia, 11, Fasc. 12, 481 (1955).

The Institute of Physical Chemistry of the Academy of Sciences of the USSR

Received July 25, 1958

*Original Russian pagination. See C. B. Translation.

THE SOLUBILITY OF FINELY PULVERIZED QUARTZ IN WATER

G. S. Khodakov and E. R. Plutsis

(Presented by Academician P. A. Rebinder, July 25, 1958)

The investigation of the physicochemical properties, and especially the room temperature solubility of finely pulverized quartz sand is of interest for the development of the mechanism of setting of lime-sand binders [1, 2], and for understanding the role of finely ground sand fillers in increasing the strength of cements [3]. Investigations of this kind might also be useful in studying the mechanics of grinding and could lead to an understanding of those processes which are completed with the pulverization of materials in a mill. Aside, however, from the detailed study of Dempster and Ritchie [4], there has been almost no work on effect of pulverization on the physicochemical properties of quartz, especially quartz in the highly dispersed state. This is to be explained by the fact that finely pulverized quartz sand has only recently found practical application in industry and that the dispersional analysis of particles whose dimensions are a tenth of a micron or less is a matter of difficulty.

In the present work investigation has been made of the solubility of quartz powders in distilled water. The powders in question were obtained from quartz sand from the Liuberetskii quarry by dry pulverization in a vibromill. The duration of pulverization was fixed at 2, 4, 8 or 16 minutes. The degree of dispersion of each of these powders was estimated from the value of the specific surface as determined through low-temperature nitrogen adsorption [5, 6]; with surface areas of 7-9 m^2/g for each of the investigated specimens, the corresponding mean particle dimensions were approximately 0.3 μ.

The quantity of quartz in solution was measured photocolorometrically, following a method [7] which involved the interaction of acidic solutions of silicic acid with ammonium molybdate to form a yellow silicomolybdenum complex corresponding to the composition $H_4[Si(Mo_3O_{10})_4] \cdot xH_2O$. This yellow complex was subsequently reduced to form the silicomolybdenum blue. The sensitivity of this method is as high as 1 mg/l.

Ten g of the pulverized powder was placed in a glass cylinder which was filled with 300 ml of distilled water; this cylinder was then placed on a mechanical agitator and shaken for several hours. After this the specimen was held quiescient. Control experiments showed that periodic agitation during long periods of standing did not essentially influence the rate of dissolution. A 20 cm^3 specimen pipetted from the upper portion of the vessel, was carefully centrifuged. The absence of appreciable numbers of suspended particles was indicated by the fact that elevating the temperature of the centrifuged solution to 100° did not increase its content of silicic acid.

By experiments using corundum powders in place of quartz, account was taken of the influence of the quartz from the glass of the vessel and from the steel (the latter entering into the solution through frictional wear in the mill and the balls) on the measured values of the silicic acid content of the solutions. The pulverization of, and the measurements on, the corundum were carried out under the same conditions as in the case of the quartz, the amount of ground-off steel in the corundum powder proving to be considerably greater than that in the quartz powders. These experiments showed that the amount of quartz which passed into solution from the glass of the vessel and from the steel did not exceed 4 mg/l. Measurements carried out on the unpulverized quartz sand showed an infinitesimally low solubility, which was just within the limits of sensitivity of the method. It should be noted that with the method which was used for the determination of the quartz in solution, measurement could be made of the true solubility in water [8].

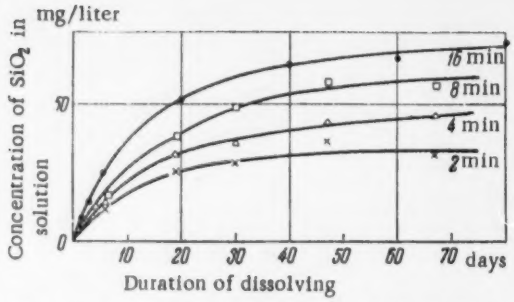

Fig. 1. The kinetics of the dissolving of quartz sand in water at 20° for various times of grinding.

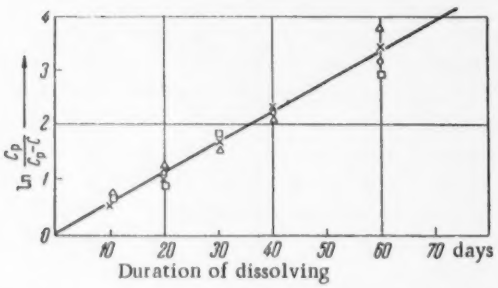

Fig. 2. The kinetics of the dissolving of quartz sand, in the coordinates, τ vs $\ln C_p/(C_p - C)$.

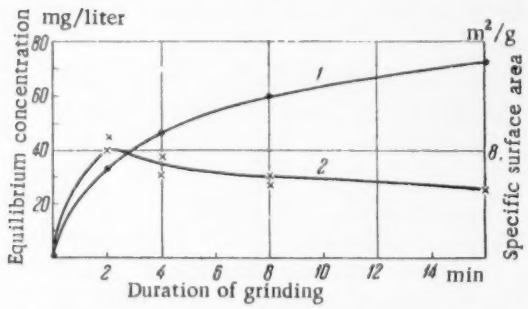

Fig. 3. The relation between the duration of grinding of the quartz sand and the equilibrium concentration of silicic acid in solution: 1) equilibrium concentration; 2) specific surface area.

In Fig. 1 there are presented the kinetic curves for the dissolving of finely pulverized quartz sand in water. The course of these curves confirms the formation of true, rather than colloidal solutions. A gradual decrease in the solubility measured after the completion of agitation would be anticipated in the contrary case. The curves of Fig. 1 are well described by the kinetic equation

$$C = C_p (1 - e^{-k\tau}), \qquad (1)$$

in which C is the concentration of the SiO_2 which has passed into solution in the time τ, C_p is the solubility, and k is the rate constant for the dissolving. The values of C_p can be determined from the data of Fig. 1; from this figure it is to be seen that saturation is reached under the experimental conditions after approximately 60-80 hours of dissolving.

It is useful to write Equation (1) in the form

$$\ln \frac{C_p}{C_p - C} = k\tau,$$

which, plotted in semilogarithmic coordinates, gives a straight line whose slope is equal to the value of k. The experimental data which are presented in Fig. 2 confirm the validity of Equation (1) for the case which is under consideration and permit an evaluation of the constant k, which the figure shows to be independent of the time of grinding and equal to 0.056 $days^{-1}$ under the experimental conditions. Figure 3, on the other hand, shows an increase in the duration of the dry grinding of the quartz to lead to an increase in the solubility C_p.

The data which have been obtained are consistent with the supposition that the experimental powders of finely pulverized quartz possessed practically identical surface areas, since this is the factor which determines the rate of dissolving under fixed conditions. On the other hand, the value of the solubility C_p, at fixed temperature is clearly determined by the physicochemical properties of the powder, and these undergo alteration in the grinding process. This point receives further confirmation from the fact that the dissolving of the finely pulverized quartz in water is fully reversible, as is to be seen from Table 1: with an elevation of the temperature the solubility of the quartz powder markedly increases, whereas lowering the temperature to room value brings about a gradual diminution in the concentration of the silicic acid.

According to our data, the room temperature solubility of finely pulverized quartz in water goes on occasion as high as 120 mg/l, a figure which is at least 20 times as great as the solubility of coarsely crystalline quartz [9].

Using the measured values of the specific surface areas, calculations based on the Kelvin equation showed the solubilities which had been observed for the finely pulverized quartz powders to be at least 16 times greater

than the theoretical. The difference would have been still larger if account had been taken of the electrical charges which are inevitably present on particle surfaces [10]. The increase in the solubility which results from grinding cannot be ascribed to the very finely dispersed fraction of the particles in the experimental powders. If the solubility were determined by such particles, it could be anticipated that there would be a diminution of concentration of silicic acid in solution as the result of a recrystallization of the small particles into larger ones [10, 11]. Comparatively high solubilities should give assurance that this latter process would take place at considerable velocity. In these experiments, however, no diminution was observed in the concentration, even when the observations were of long duration (more than a year). In addition, the experimental data show that there was no measurable alteration in the specific surfaces of powders which had stood in water for long periods of time. On the other hand, the equilibrium concentration is definitely dependent on the time of grinding of the powder, although the specific surface of the latter is not increased in the grinding process.*

TABLE 1

The Effect of Temperature on the Solubility of Finely Pulverized Quartz in Water (mg/l)

C_p	Holding time at 100°, hours		Holding time at 20°, days	
	1	3	11	25
33	60	109	–	–
60	82	169	–	–
	176	222	109	87
89	160	210	128	115

The anomalously high solubility of the finely pulverized quartz in water and the marked increase in this solubility with increasing time of grinding can be explained by taking account of the fact that grinding not only pulverizes the quartz particles but also breaks down their crystalline structures [4].

After sufficiently extensive grinding, dispersing, as such, ceases and disorganization of the crystal lattice continues up to the complete conversion of the quartz into its amorphous modification. It is thus natural to relate the observed increase in the solubility of the powders, not to their degree of dispersion, but to the disorganization of the quartz lattice and to the formation of amorphous layers (similar to Beilby layers) of enhanced free energy on the particle surfaces.

From data which have been presented above, it is possible to deduce the mechanism of the formation of the hydrosilicates of calcium and magnesium from the interaction of their hydrated oxides with finely pulverized sand in an aqueous medium at room temperature. It has been shown that up to 7-8% of quartz powder is hereby brought into combination with the lime [1], an amount which is too large to be completely accounted for by reaction on the grain surfaces [2]. It is known that the solubilities of $Ca(OH)_2$ and $Mg(OH)_2$ at 20° are 1300 and 30 mg/l, respectively; the solubility of quartz reaches 120 mg/l as we have shown. With such solubilities of the individual substances, there is possible a reaction in the liquid phase with the formation of the poorly soluble hydrosilicates of calcium and magnesium. Thus in aqueous media, those conditions are established which guarantee a very high supersaturation for the newly formed product and this, in turn, assures the recrystallization, further growth, and coalesence of extremely fine nuclei of a new phase. The result is the formation of the rocklike lime-sand crystallization structure whose strength reaches 240 kg/cm^2.

Thus the mechanism of the setting of lime-sand binders can be looked upon as being analogous to that of the solution-crystallization hardening of such mineral binders as gypsum [13, 14]. Here the strength of the solidifying lime-sand object is increased as a result of coalesence of the crystallites of the new formation in solutions which are already supersaturated with these same materials [15, 16].

In a similar fashion, it is possible to explain the role of vibromilled sand fillers in increasing the strength of low-cement concretes. Free calcium hydroxide separates out on slaking the cement with water, and this reacts in solution with the quartz to form calcium hydrosilicates whose crystallization leads to an increase in the strength of the cement product.

In conclusion the authors wish to express their sincere thanks to Academician P. A. Rebinder and to D. S. Sominskii, V. B. Ratinov and L. A. Feigin for discussion of the results and for valuable comments and to N. I. Gludina for aid in the experimental work.

*This is due to the very high intensity of energy in the mill which was employed, the limit of pulverization characteristic of the quartz sand [12] being reached after only 2 minutes of grinding.

LITERATURE CITED

[1] D. S. Sominskii, G. G. Kornienko, V. V. Komonova and G. S. Khodakov, Scientific Report, VNIITISM,* No. 28 (1957).

[2] V. F. Abrosenkova, G. I. Logginov and P. A. Rebinder, Proc. Acad. Sci. USSR, 115, No. 3, 509 (1957).**

[3] P. A. Rebinder and N. V. Mikhailov, Report at a Conference on Contemporary Problems in the Technology of Concrete in the Aggregated Concrete Steel Industry, 1956.***

[4] P. B. Dempster and P. D. Ritchie, J. Appl. Chem. 3, No. 4, 182 (1953).

[5] S. Brunauer, The Adsorption of Gases and Vapors (in Russian), 1, Foreign Lit. Press, 1948.

[6] D. S. Sominskii and G. S. Khodakov, Scientific Reports, VNIITISM,* No. 29 (1957).

[7] N. I. Gludina and M. A. Matveev, Proc. D. I. Mendeleev Chem.-Tech. Ins. Moscow, vol. 21, 49 (1956).

[8] M. M. Piriutko and Iu. A. Shmidt, Bull. Acad. Sci. USSR, Div. Chem. Sci. 1953, 607.**

[9] R. Iler, The Colloid Chemistry of Silica and Silicates, 1955.

[10] M. Volmer, Kinetik der Phasenbildung, 1939.

[11] H. E. Buckley, Crystal Growth (in Russian), Foreign Lit. Press, 1954.

[12] A. D. Lesin, Scientific Reports, VNIITISM,* No. 25 (1957).

[13] Ia. L. Zabezhinskii, V. B. Ratinov and T. I. Rozenberg, Proc. Acad. Sci. USSR, 108, No. 6, 1137 (1955).

[14] V. B. Ratinov, Ia. L. Zabezhinskii and T. I. Rozenberg, Proc. Acad. Sci. USSR, 109, No. 5, 979 (1956).

[15] A. M. Smirnova, N. G. Zaitseva and P. A. Rebinder, Colloid J. 8, No. 1 (1956).**

[16] E. E. Segalova, V. N. Izmailova and P. A. Rebinder, Proc. Acad. Sci. USSR, 110, No. 5, 808 (1956).

The All-Union Scientific Research Institute for Fine Pulverization
The Academy of Builders and Architects of the USSR

Received July 23, 1958

*VNIITISM = All-Union Scientific Research Institute for New Problems of Building Materials in Connection with Fine Pulverization Methods.

**Original Russian pagination. See C. B. Translation.

***In Russian.

THERMODYNAMIC PROPERTIES OF ALLOYS OF COPPER AND PALLADIUM

A. A. Vecher and Corresponding Member Academy of Sciences USSR,

Ia. I. Gerasimov

We have used the electromotive force (EMF) method for determining the changes in free energy, heat content and entropy of mixing, for alloys of copper and palladium.

The EMF of the following galvanic element was measured –

$$Cu \mid Cu^{+} \text{ (fused halide)} \mid Cu - Pd \text{ (alloy)}.$$

The method has been described previously [1].

The electrolyte was either a fused eutectic mixture of potassium and lithium chlorides, or a mixture of sodium and potassium iodides of minimum melting point (about 590°). In the first case, about 1% of CuCl was added to the electrolyte, and , in the second case, CuI. Experiment showed that there was less scatter and improved reproducibility in the observed values of the EMFs when the iodide electrolyte was used. The fused mixture of the iodides of potassium, sodium and copper, of the stated composition, was therefore used in most cases.

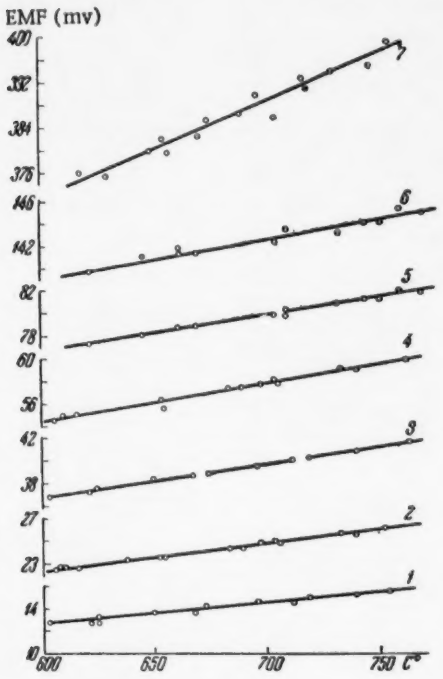

Fig. 1. EMFs of Cu-Pd alloys.
1) N_{Cu} = 0.887; 2) N_{Cu} = 0.835; 3) N_{Cu} = = 0.790; 4) N_{Cu} = 0.740; 5) N_{Cu} = 0.700; 6) N_{Cu} = 0.578; 7) N_{Cu} = 0.0809.

The alloys were prepared by mixing known weights of copper and palladium powders, followed by pressing and annealing at 900-1000°C for 200-250 hours. They were not analyzed. The leads were tungsten wires of diameter 1.2 mm. Shallow holes were drilled in the alloys after annealing, the leads were inserted in these holes, and the alloys were squeezed in normal clamps. Experiment showed that this treatment was quite adequate.

The experiments were carried out at 600-760°C, in an atmosphere of argon, purified by metallic sodium. Experiments lasted for 130-150 hours, since the first constant values of EMF were obtained after 30-40 hours, but subsequently, after altering the temperature, the EMF became constant relatively quickly (5-10 hours).

The experimental results for each composition are shown as EMF – temperature curves, which were found to be straight lines. The deviations of the individual EMFs from the straight lines did not exceed ± 0.5-1% (see Fig. 1). The subsequent method of treating the experimental data has been described previously [2].

Figure 2 shows the activities of copper and palladium in alloys at 1000°K, and Fig. 3 shows the integrated heats, free energies and entropies of formation of the Cu-Pd alloys at 1000°K.

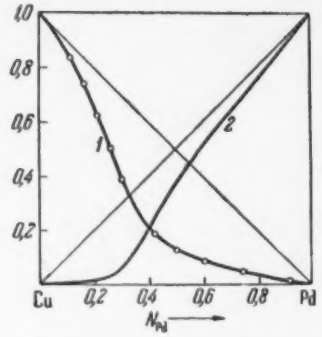

Fig. 2. Activities of copper and palladium in Cu-Pd alloys at 1000°K. Points – experimental results:
1) Activity of copper; 2) activity of palladium.

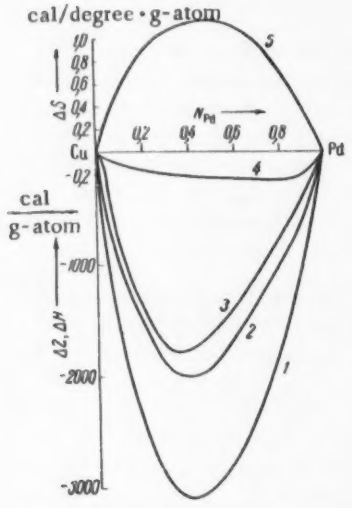

Fig. 3. Free energy, heat and entropy of mixing of Cu-Pd alloys at 1000°K:
1) ΔZ; 2) ΔZ^{exc}; 3) ΔH; 4) ΔS^{exc}; 5) ΔS.

There is adequate information in the literature (see, for example, [3-6]) on the degree of order of Cu-Pd alloys in the solid state. In all cases, in spite of some differences between the results of the various investigators on the temperature limits of the ordered states and the composition of the ordered alloys, it may be stated with certainty that we, and the other investigators working above 600°C, were dealing with disordered alloys. Moreover, it has been noted, that the process of ordering is extremely slow in Cu-Pd alloys [5].

However, a tendency to ordering at high temperatures was also clearly shown in our experiments by the negative deviations of the thermodynamic functions from ideality (Fig. 2 and 3), by the large negative heat of mixing (− 1780 kcal/g-atom at $N_{Cu} = 0.65$), and by the displacement of the minima of the heat of mixing and free energy towards the copper side (Fig. 3), where a greater tendency to ordering has been observed (in the references quoted, order has been observed in alloys of composition Cu_3Pd, Cu_3Pd, Cu_5Pd_3 and CuPd, but, so far no indication of order has been observed with alloys containing more than 50 atoms % Pd).

But, since there was only a low degree of order in the alloys, the excess entropy of mixing had a comparatively small negative value (of the order − 0.2 entropy units 1 g-atom) and did not alter much with composition. It is possible that the entropy of mixing was influenced by other factors.

Thus, the thermodynamic properties found for Cu-Pd alloys at 1000°K are consistent with the existence of a super-structure for the alloys at lower temperatures.

LITERATURE CITED

[1] A. A. Vecher and Ia. I. Gerasimov, J. Phys. Chem. 32, No. 12 (1958).

[2] Ia. I. Gerasimov, A. A. Vecher and V. A. Geiderikh, Proc. Acad. Sci. USSR, 122, No. 5 (1958).*

[3] A. A. Rudnitskii, Bull. Dept. Platinum 27, 227 (1952).

[4] F. Jones and C. Sykes, J. Inst. Met. 65, 419 (1939).

[5] A. H. Geisler and J. B. Newkirk, J. Metals, 6, 1076 (1954).

[6] D. Watanabe, M. Hirabayashi and S. Ogawa, Acta Cryst., 8, 510 (1955).

The M. V. Lomonosov Moscow State University

Received August 29, 1958

*Original Russian pagination. See C. B. Translation.

FORMATION OF FREE RADICALS IN BIMOLECULAR REACTIONS

REACTION BETWEEN TRIPHENYLCHLOROMETHANE AND ETHYLLITHIUM

F. S. D'iachkovskii, N. N. Bubnov and A. E. Shilov

(Presented by Academician V. N. Kondrat'ev, July 16, 1958)

In 1954 N. N. Semenov [1] advanced the hypothesis that the activation energy of the primary reaction between two molecules, with formation of free radicals –

$$R'X + YR'' \rightarrow R' \cdot + XY + \cdot R'' \qquad (1)$$

is primarily determined by the endothermicity of the process, while the activation barrier of such reactions must be small. Consequently, if compounds are chosen for which the sum of the energies of rupture of the bonds R'–X and R"–Y does not greatly exceed the energy of formation of the bond X–Y, or is even less than this (i.e., the process (1) is close to being thermally neutral or is exothermic), then reaction between these compounds should proceed with a small energy of activation. This condition is fulfilled by reactions between alkyl halides and organometallic compounds, examples of which are provided by the well-known Wurtz, Fittig and Grignard reactions. But the mechanisms of these reactions are far from clear. Zigler, Ochs, Hoffman and Gilman [2-4] investigated reactions between organometallic compounds and alkyl halides, and concluded that free radicals were formed in some cases, but their modes of formation remained unelucidated.

We have investigated the reaction between triphenylchloromethane and ethyllithium, the first stage of which, if it takes place according to scheme (1) –

$$(C_6H_5)_3CCl + LiC_3H_5 \rightarrow (C_6H_5)_3C \cdot + LiCl + C_2H_5 \qquad (2)$$

must clearly be exothermic.* The relatively small rate of dimerization of the triphenylmethyl radicals [7], formed in this reaction, enabled us to use the method of electron paramagnetic resonance for the identification of these radicals and for the determination of their concentration during the course of the reaction. The reaction was carried out in a thin-walled tube placed in the resonator of an EPR spectrometer. Toluene solutions of the reagents, separated by a membrane, were mixed when the latter was perforated by a fine glass tube. Radicals were indeed observed in the course of the reaction, by the EPR method, and their high resolution spectrum, shown in Fig. 1, agreed precisely with the previously recorded [8] absorption spectrum of the triphenylmethyl radical.

Figure 2 shows kinetic curves for change in concentration of the triphenylmethyl radical during the course of the reaction at –44, –54 and –80°. It is evident that, at all temperatures, the concentration of free radicals increased from the start of the reaction to a well-defined maximum, and then dropped off. The shapes of the curves indicated that the triphenylmethyl radicals, formed in the first stages, were recombining to give their $(2\,(C_6H_5)_3C \cdot \rightleftharpoons (C_6H_5)_3C - C\,(C_6H_5)_3)$ equilibrium concentrations, which were not very high at the temperatures used. The formation, at the start of the reaction, of triphenylmethyl radicals, at concentrations greatly exceeding the equilibrium values, clearly established that they were products of the primary reaction. If they

*In fact, D(C–Cl) in $(C_6H_5)_3CCl$ is 48 kcal [5] and D(LiCl) is 115 kcal [6]. Then the heat of reaction (2), q = = 115–48–D(Li–C_2H_5) = 67 – D(Li –C_2H_5). If, as may be supposed, D(Li–C_2H_5) < 67 kcal, then q > 0.

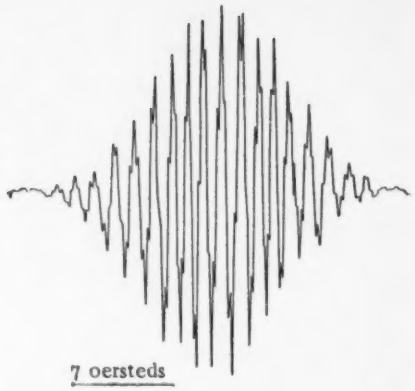

Fig. 1

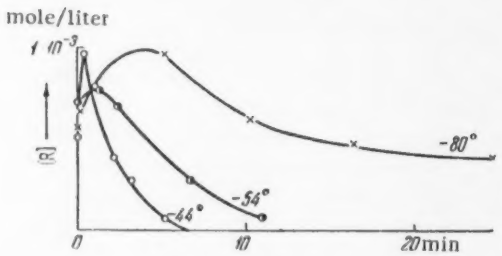

Fig. 2.

had been formed by the dissociation of hexaphenylethane, itself formed by some kind of primary process, we should have found a slow increase in radical concentration towards the equilibrium value. Special experiments showed that the existence of maxima in the kinetic curves was not due to dissociation of hexaphenylethane caused by a rise in temperature, since there was a negligible heating effect under the experimental conditions.

The nature of the kinetic curves of Fig. 2 corresponds to the build-up of an intermediate product with a subsequent bimolecular reaction. Using the formula derived for calculating the kinetics of this type of reaction [9], and from a knowledge of the velocity constants of the dimerization of triphenylmethyl radicals [7], it was possible to obtain from the above kinetic curves the velocity constants and activation energy for the reaction of formation of the radicals. Although it was impossible to avoid errors due to the very high rate of the primary reaction (close to the rate of mixing of the reagents), calculation led definitely to the conclusion that the activation energy of the primary reaction did not exceed 4-5 kcal.

Thus it may be reckoned as established that an elementary reaction of type (1), under suitable energy conditions, can take place with the formation of free radicals and with a neglible activation energy.

It was interesting to know what happened to the ethyl radicals, formed in accordance with Equation (2). Table 1 shows that the only gas-phase products of the reaction were ethane and ethylene, which might have been formed by disproportionation of ethyl radicals. But it was impossible to show the presence of ethyl radicals in the reaction mixture by any chemical method. It is known that ethyl radicals, formed in solution at near to room temperature, will abstract hydrogen atoms from hydrocarbon solvents to form ethane. In solution in aromatic hydrocarbons they can add on to solvent molecules, so that the yield of ethane is decreased [10]. If, indeed, disproportionation of ethyl radicals took place under the conditions chosen, then there should have been a simultaneous recombination, at higher speed, to form butane [12]. When we carried out the reaction in solvents labelled with deuterium (C_6D_6, $C_6H_5CH_2D$), the ethane formed contained no heavy hydrogen (mass spectrometry). The amount of ethane formed remained the same when the reaction was carried out in decalin, toluene or benzene, or in benzene with anthracene added. These results, together with the absence of butane in the reaction products, led us to the view that free ethyl radicals were not formed in solution in the case of this reaction. The explanation of this may lie in the fact that, as was shown recently [11], lithium alkyls in solution form complexes with themselves as the result of so-called lithium bonding. It is possible that an ethyl radical, formed in the reaction, would remain linked to a complex, and would then react to form only ethane and ethylene. The following hypothetical scheme is suggested:

$$(C_6H_5)_3CCl + LiC_2H_5 \cdots LiC_2H_5 \rightarrow (C_6H_5)_3C\cdot + LiCl + C_2H_5 \cdots Li - \dot{C}_2H_5;$$

$$\dot{C}_2H_5 \cdots Li - C_2H_5 \rightarrow \begin{matrix} HHH \\ | \\ C \\ | \\ H_2C\cdot Li \end{matrix} \quad \begin{matrix} \dot{C}H_2 \\ \| \\ CH_2CH_3 \rightarrow CH_2 \\ \\ Li \end{matrix} \quad C_2H_6;$$

$$Li + (C_6H_5)_3CCl \rightarrow LiCl + (C_6H_5)_3C\cdot$$

TABLE 1

Solvent	Reagent in mole · 10^4		Products in mole · 10^4			$[C_2H_4]/[C_2H_6]$
	C_2H_5Li	$(C_6H_5)_3CCl$	C_2H_4	C_2H_6	$(C_6H_5)_3C_2$	
Benzene	9,33	8,0	0,55	1,85		0,3
	10,5	4,0	0,36	1,10		0,32
	10,5	2,0	0,13	0,60		0,22
	12,6	24,90	1,23	3,00		0,41
	12,6	12,6	1,12	2,70	1,4	0,41
	12,6	11,6	1,02	2,44		0,42
	21,4	18,5	1,68	6,03		0,28
	21,4	18,5	1,40	5,83		0,24
Decalin	10,1	5,1	0,22	0,75		0,29
	6,1	8,5	0,20	0,64	0,4	0,31
	8,1	8,2	0,23	0,90	0,43	0,25
	21,3	10,0	0,56	1,85		0,30
	10,5	20,0	0,60	1,80	1,0	0,33
	21,3	20,0	1,55	3,05		0,38
	6,2	20,0	0,22	0,70		0,31
	18,0	21,1	0,86	2,53		0,34
	18,0	21,1	0,90	3,10	1,6	0,29

The large amount of ethane in comparison with ethylene may be the result of secondary reactions of ethyllithium – with the products of the primary reaction. In fact, it was found that ethyllithium readily reacted with separately prepared triphenylmethyl radicals to form ethane (this was clearly a reaction of metalation). It was also shown that, when the reaction of triphenylchloromethane with ethyllithium was carried out in the presence of previously added ethylene, there was a partial absorption of the latter, and this absorption would also affect the ratio of ethane to ethylene.

It follows, from the results shown in Table 1, that only a part (about 20%) of the triphenylmethyl radicals formed hexaphenylethane. The remaining radicals evidently reacted with ethyl radicals (possibly in cells) to form the products of their combination and disproportionation [$(C_6H_5)_3C - C_2H_5$, $(C_6H_5)_3CH$, C_2H_4].

We do not consider it possible, at present, to generalize the results, obtained on the formation of radicals, from the particular case investigated to all reactions between alkyl halides and organometallic compounds. It is possible that, in some cases, there may be a molecular or heterogeneous mechanism. But it should be noted that the absence of radicals from solution in similar reactions, for which there is some evidence, may be explained by the loss of radicals by reaction with the solvent (or by dimerization and disproportionation), or by intra-complex reactions, similar to the one proposed for the ethyl radical.

LITERATURE CITED

[1] N. N. Semenov, Some Problems of Chemical Kinetics and Modes of Reaction, M, 1954.*

[2] K. Zigler and C. Ochs, Ber. 55, 2257, 1922.

[3] C. S. Marvel, F. D. Hager and D. D. Goffman, J. Am. Chem. Soc. 49, 2323 (1927).

[4] H. Gilman and H. L. Jones, J. Am. Chem. Soc. 51, 2840 (1929).

[5] A. H. Schon and M. Szwarc, Ann. Rev. Phys. Chem. 8, 439 (1957).

[6] A. Gaydon, Dissociation Energies and Spectra of Diatomic Molecules, IL, 1949.**

[7] F. S. D'iachkovskii, N. N. Bubnov and A. E. Shilov, Proc. Acad. Sci. USSR, 122, No. 4 (1958).***

[8] H. S. Jarrett and G. I. Sloan, J. Chem. Phys. 22, 1783 (1954).

[9] A. D. Stepukhovich and L. M. Timonin, J. Phys. Chem. 25, No. 2, 143 (1951).

[10] J. Smid, A. Rembraum and M. Szwarc, J. Am. Chem. Soc. 78, 3315 (1956).

*In Russian.

**Russian translation.

***Original Russian pagination. See C. B. Translation.

[11] A. Rodionov, D. Shigorin, T. Talalaeva and K. Kocheshkov, Bull. Acad. Sci. USSR, Div. Chem. Sci. 1958, 120.*

[12] Y. Semerano, L. Riccomboni and F. Callegari, Ber. 74, 1297 (1941); M. H. J. Wijnen and E. W. R. Steacie, Canad. J. Chem. 29, 1092 (1951).

Institute of Chemical Physics of
the Academy of Sciences of the USSR

Received July 12, 1958

*Original Russian pagination. See C. B. Translation.

RETENTION OF LATENT IMAGE AND SENSITIVITY IN GRANULAR PHOTOGRAPHIC EMULSIONS STABILIZED WITH TRIETHANOLAMINE

A. P. Zhdanov, A. L. Kartuzhanskii, I. V. Ryzhkova and L. I. Shur

(Presented by Academician A. P. Vinogradov, July 17, 1958)

It has been shown [1-3] that treatment of granular photographic emulsions with triethanolamine (TEA) increases their sensitivity to any particles, including relativistic ones. Our investigation [4] of the mechanism of sensitization by TEA led to the conclusion that TEA reacts with Ag halide in the emulsion crystals to form subcenters of Ag in the sensitive centers, in the same way as, for example, by the action of light pulses. The transformation of subcenters in a center, under the subsequent action of a particle, occurs more readily than the transformation of a center in the absence of subcenters. This would also be expected to cause a reduction in regression of the latent image, i.e., the centers formed after sensitization with TEA should remain stable for a longer time. Further, since the subcenters themselves are known to be stable, it would be expected that the increase in sensitivity of emulsions, due to stabilization with TEA, would persist for some time, and this would reduce the fall in sensitivity (normally quite considerable for granular emulsions) during storage without exposure. Finally, it is known [5] to be possible for subcenters to reinforce each other to some extent during storage, and thus to form centers of development, and this might lead to an undesirable increase in background. The verification of these effects by experiment, in addition to its practical use, would be of value in confirming the theory of the formation of subcenters on sensitization with TEA. The relevant experimental results are presented below, together with the results of experiments designed to elucidate the individual details of the mechanism of sensitization by TEA.

The experiments were performed with various numbers of emulsion type R (NIKFI),* irradiated with relativistic electrons and stored in a refrigerator (temperature 5-6°, relative humidity ~ 50%). Some of the samples of each number of emulsion, after sensitization with TEA, were first irradiated and then stored for different times (to investigate regression of the latent image), while other samples were first stored for different times and then irradiated (to investigate retention of sensitivity); in addition, for the sake of comparison, samples of the same emulsion, not sensitized with TEA, were included in all the experiments, and stored and irradiated for the same times and under the same conditions. The development of all these emulsions was standardized.

Table 1 shows the data on regression and retention for two numbers of emulsion, one of them for two concentrations of TEA. In contrast to our previous results [1, 2], an increase in the concentration of TEA did not lead to any substantial increase in the density of the track, but did increase the background. Some (~ 10%) increase in the track density was observed on storage, both with irradiation before and after storage; this and the gradual, but not very pronounced, increase in background were attributed to regrouping of subcenters. The data on track density, for samples not sensitized with TEA, was only approximate, because the effect of storage on track density and sensitivity was to reduce not only the density of tracks, but also their number and length; it was, therefore, not always possible to find tracks of sufficient length, and the data, presented in this and the following tables, refers to the parts of tracks which were conserved. An important practical result, emerging from Table 1, is the complete retention of sensitivity and of the latent image in emulsions sensitized by TEA, within the limits of the storage times investigated and the precision of the measurements. This property of TEA is quite as important as its sensitizing action.

Table 2 shows data confirming our previous view [4], that sensitization by TEA is not associated with its presence in the emulsion at the time of irradiation and, in particular, is not connected with its acceptance of

*Motion Picture and Photography Scientific Research Institute– Publisher's note.

TABLE 1

Densities of Track (number of grains per 100 μ) and of Background (number of grains per 1000 μ^3)

Emulsion No.	TEA concentration, %	Storage time: 0 days, variants 1 and 2		10 (or 18) days* variant 1		10 (or 18) days* variant 2		30 days variant 1		30 days variant 2		90 days variant 2	
		density	background	density	background	density	background	density	background	density	background	density	background
3642	0	32±2	1,7	(31)	1,4	(32)	1,6	(27)	1,9	(29)	1,7	No tracks	2,9
	2	61±2	2,0	64±2	1,5	65±2	1,8	67±2	2,1	67±2	2,5	68±2	2,0
	6	63±2	4,7	65±2	3,3	66±2	4,0	68±2	4,7	69±2	5,5	66±2	6,8
3724	0	31±2	2,1	(33)	1,5	(33)	2,0	(30)	2,0	(30)	1,5	—	—
	2	65±2	4,0	69±4	4,4	65±3	2,7	69±2	4,4	67±3	3,2	—	—

*Storage time 10 days for emulsion 3642, 18 days for emulsion 3724.

**Variant 1 – storage after irradiation, Variant 2 – irradiation after storage.

TABLE 2

Densities of Track (number of grains per 100μ) and of Background (number of grains per 1000 μ^3)

Nature of treatment	Storage time: 0 days, variants 1 and 2		30 days variant 1		30 days variant 2		90 days variant 2	
	density	background	density	background	density	background	density	background
Without Treatment	32±2	1,7	(27)	1,9	(29)	1,7	No tracks	2,9
Immersion in 2% TEA	61±2	2,0	67±2	2,1	67±2	2,5	68±2	2,0
The same with subsequent washing out of TEA	63±2	2,2	66±2	3,6	63±2	3,3	60±2	3,9
The same with immersion in 1% $NaNO_2$ after washing	63±2	2,3	62±3	2,7	64±2	2,5	68±3	2,5
Immersion in 1% $NaNO_2$	32±3	2,4	(33)	1,8	(35)	1,2	(30)	2,5

halogen, liberated by the radiolysis of Ag halide, in spite of the opinion of Demers [6]. It may be seen that the considerable gain in sensitivity, freedom from regression and good storage life are not affected by washing out the TEA from the emulsion before irradiation; on the contrary, the addition to the emulsion of $NaNO_2$, which is known to be a good halogen acceptor, did not increase the sensitivity and storage life and did not reduce regression. The slight effect of washing out the TEA on the increase in background during storage shows that, from the moment of formation of subcenters, the presence of TEA in the emulsion had no significant influence, and that subsequent changes in the properties of the emulsion with time were determined by these same subcenters in the crystals.

The data in Table 3 shows that reduction of the alkalinity of TEA (by addition of an acid which does not react with Ag halide) decreased its sensitizing effect, as previously observed [4], but, as before, good retention of the latent image and sensitivity were provided. This indicated that, at lower values of the pH, the effect of TEA was also principally to form subcenters and the smaller increase in sensitivity must have been due mainly

TABLE 3

Densities of Track (number of grains per 100 μ) and of Background (number of grains per 1000 μ^3)

Form of sensitization	Storage time									
	0 days		18 days				30 days			
	Variants 1,2g		Variant 1. h		Variant 2. i		Variant 2. h		Variant 2. i	
	Density	background	Density	background	Density	background	Density	background	Density	background
Without sensitization	31±2	2,1	(33)	1,5	(33)	2,0	(30)	2,0	(30)	1,5
Immersion in 2% TEA	65±2	4,0	69±4	4,4	65±3	2,7	69±2	4,4	67±3	3,2
Immersion in 2% TEA, neutralized with HNO_3 to pH 7	45±5	3,5	46±3	9,5	49±2	8,1	40±3	4,4	40±2	5,2
Immersion in 2% TEA, neutralized with HOOC·COOH to pH 7	44±4	6,4	46±4	9,5	48±3	8,0	43±2	6,1	46±3	8,9
Immersion in NaOH (pH 9)	43±3	10,4	*	13,3	47±3	4,4	*	12,9	38±3	6,3

*The tracks present were only distinguishable with difficulty against the background.

to a reduction in the number of crystals in which TEA reacts to form subcenters. The slight regression in emulsions treated with NaOH (having the same pH as TEA, but differing in not being a reducing agent for Ag halide) suggests that in this case, subcenters were formed as the result of the consecutive reactions $AgHal \rightarrow AgOH \rightarrow Ag_2O \rightarrow Ag$. In any case, neither NaOH nor TEA affected processes occuring on irradiation and development of the emulsion, since the results of the action of NaOH did not alter when it was washed out of the emulsion before irradiation [4].

Since it had previously [2] been concluded that the sensitizing action of TEA was essentially the same for all forms of irradiation, we conducted experiments to investigate regression after exposure to low-intensity illumination for 45 seconds. The experiments were carried out with the same emulsions and according to the same scheme as in Table 3. After storage for 30 days, regression was so slight that it could not be definitely established even in control (untreated) samples. this was quite typical for illuminations of long duration [7]. After 75 days storage, there was an appreciable drop in the light sensitivity (approximately twofold for a blackening density of 1.0) of control samples, exposed before storage, a complete absence of such a drop with samples sensitized with TEA at pH 9, and some drop (~20-40%) with samples sensitized with neutralized TEA or with NaOH. These differences may be discerned in a less pronounced form in Table 3. The drop in light sensitivity was less for samples stored before exposure, and was only pronounced (~25%) in the case of control samples.

Thus, the experiments performed have been demonstrated the existence of both sensitizing and stabilizing effects by TEA, and are in complete agreement with the suggested mechanism for its interaction with the crystals of the photographic emulsion.

LITERATURE CITED

[1] A. P. Zhdanov, A. L. Kartuzhanskii, I. V. Ryzhkova and L. I. Shur, J. Sci. and Appl. Photography and Cinematography 3, 53 (1958).

[2] A. P. Zhdanov, A. L. Kartuzhanskii, I. V. Ryzhkova and L. I. Shur, Proc. Acad. Sci. USSR 118, 744 (1958).*

[3] K. S. Bogomolov, I. A Ruditskaia and A. A. Sirotinskaia, J. Sci. and Appl. Photography and Cinematography 3, 52 (1958).

*Original Russian pagination. See C. B. Translation.

[4] A. P. Zhdanov, A. L. Kartuzhanskii, I. V. Ryzhkova and L. I. Shur, J. Sci. and Appl. Photography and Cinematography 3, 4 (1958).

[5] P. C. Burton, Photogr. J. 86B, 62 (1946).

[6] P. Demers and J. Hebert, Sci. Ind. Photogr. 23A, 304 (1952).

[7] A. L. Kartuzhanskii, J. Sci. and Appl. Photography and Cinematography, 1, 321 (1956).

The V. G. Khlopin Radium Institute of
the Academy of Sciences of the USSR

Received July 12, 1958

THE EFFECTS OF ELECTRONEGATIVE ELEMENTS ON THE CATALYTIC ACTION OF SILVER ON THE OXIDATION OF ETHYLENE

A. I. Kurilenko, N. V. Kul'kova, V. E. Ostrovskii and M. I. Temkin

(Presented by Academician A. N. Frumkin, July 21, 1958)

Catalytic oxidation of ethylene to ethylene oxide

$$C_2H_4 + \tfrac{1}{2}O_2 = C_2H_4O \qquad (1)$$

takes place on the surface of silver at 200-300°. Small additions of chlorine compounds increase the selectivity of the catalyst, i.e., they reduce the role of the undesirable reaction

$$C_2H_4 + 3O_2 = 2CO_2 + 2H_2O, \qquad (2)$$

without reducing the degree of conversion of ethylene. Somewhat larger quantities of chlorine poison the catalyst [1]. There are indications of a similar action by sulfur [1, 2]. The interest aroused by these phenomena, in connection with the theory and practice of catalysis, provoked us to investigate them in more detail.

The method used for the kinetic measurements has been described previously [3]. The experiments were carried out by a flow circulation method at 1 atm and 218°. The ethylene-air mixture used contained 2.5 ± 0.2% by volume of C_2H_4. The space velocity ratio was about 1500 hours^{-1}; the degree of conversion of C_2H_4 over silver, without addition of Cl or S, was 50-60%. The concentrations of CO_2 and C_2H_4 were determined with a precision of 0.05% by volume, and that of C_2H_4O with a precision of 0.01% by volume.

In addition to the methods used previously [3] for purifying the reacting gases, the air was passed through a tube of zinc oxide at 400° to remove traces of organic sulfur compounds [4].

The sulfur compounds used were labelled with the radioactive isotope S^{35}. This made it possible to determine very small quantities of sulfur, and to follow its migration in the catalyst. The methods of preparing and metering H_2S were as previously described [5]. Sulfur was determined by dissolving the sample in nitric acid containing H_2O_2, and precipitating the sulfur as $BaSO_4$. The radioactivity of the $BaSO_4$ was determined with a layer equivalent to infinite thickness, using an end-window counter.

The catalyst consisted of spongy silver, made by the thermal decomposition of Ag_2CO_3 in a stream of a mixture of ethylene and air. The catalyst surface was measured by adsorption of nitrogen at low temperature. Most of the experiments were carried out with silver granules having a specific surface of about 1 m^2/g. Tablets were also used, 5 × 3 mm in size, with a specific surface of 0.3 m^2/g. The tablets differed from the granules in containing traces of chlorine, introduced during their preparation.

The activity of a catalyst was characterized by its velocity constant k_1 for reaction (1), which was calculated from the equation [6]:

$$\omega_1 = \frac{k_1 [C_2H_4]}{[C_2H_4O] + 0.3\,[CO_2]}, \qquad (3)$$

where ω_1 is the rate of reaction (1), measured as the ratio of the volume of C_2H_4O in ml at 0° and 1 atm, formed

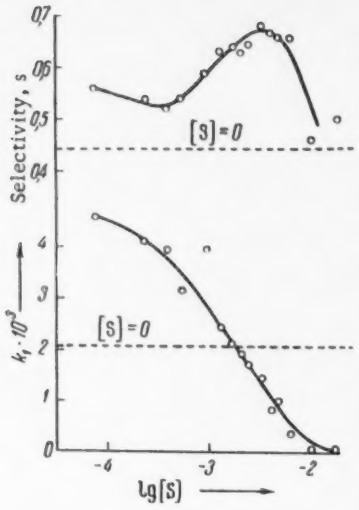

Fig. 1

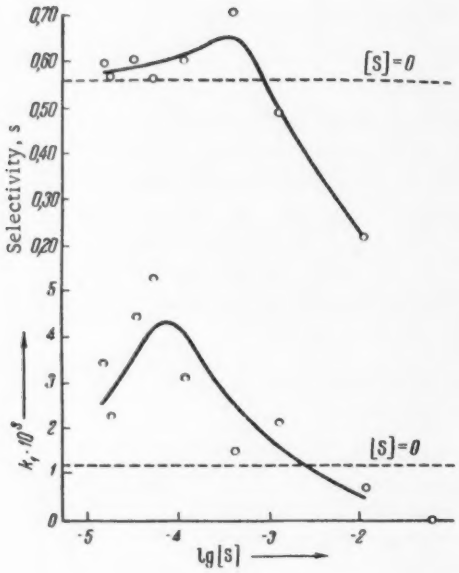

Fig. 2

in one second, to the surface of the catalyst in square meters. The selectivity s was given by the ratio of the rate of reaction (1) to the sum of the rates of reactions (1) and (2).

Experiments were first carried out with tabletted catalyst, and H_2S was added directly to the reaction mixture over a period of 20-30 hours. The concentration of H_2S was varied in different experiments from 0.1 to 50 mg/m^3. A small increase (10-20%) in the activity of the catalyst was observed after the addition of $3 \cdot 10^{-4}$ to $5 \cdot 10^{-4}$ atoms % of S (with respect to the silver). This was accompanied by an increase in the selectivity, s, from 0.70 to 0.77. Independently of the concentration of H_2S in the gas mixture, the oxidation of ethylene practically ceased after the addition of about 10^{-2} atoms % of sulfur to the catalyst. At this point, a dark stain appeared in the first tablets to be reached by the gas. Separate investigations of the catalytic activity of the silver layers showed that, in spite of the high linear speed of the gas in the flow-circulation system (about 1 m/second in the reaction zone), poisoning occurred principally in the first tablets to be reached by the gas. Measurements of the radioactivity of the tablets confirmed this and showed that the sulfur, originally picked up on the outer surface of a tablet, migrated into the interior under the conditions of the reaction. This may explain the slow change in activity and selectivity of catalysts, which was observed after the addition of H_2S to the reaction mixture had been discontinued.

The following methods were used to obtain an even distribution of sulfur on the surface:

1. Silver granules, of dimensions 0.1-0.2 mm, were treated as a "boiling bed," with hydrogen sulfide at room temperature (the granules stuck together at 218°).

2. Ag_2CO_3 and Ag_2S were coprecipitated and washed with hot water (only about 1/3 of the original sulfur remained in the silver after washing).

3. Silver carbonate was soaked in H_2SO_4 solution.

4. Silver powder (of particle size 0.05 mm) was soaked in Na_2SO_4 solution.

Independently of the method of introducing sulfur, it was found that after the catalyst had been used for some time for the oxidation of ethylene, the greater part of the sulfur added could be washed out of the catalyst with water at room temperature. Hence it may be concluded that, in the course of the catalytic process, the bulk of the sulfur was held by the silver in the form of a surface sulfate. This enabled us to calculate the degree of coverage of the surface, θ, from the total sulfur content, assuming that all the sulfur was on the surface. The values calculated in this way are shown below; it is clear that they may be overestimates, but not underestimates.

Figure 1 show the results of measurements of the catalytic activity and selectivity of silver granules pretreated with H_2S in a "boiling bed." Since a logarithmic scale is used in this and the following curves for the S concentration, the points representing the activity and selectivity without addition of sulfur cannot be plotted.

The corresponding values are shown by dotted lines. The catalysts were tested for about 10 hours. The points shown represent the mean operating characteristics of the catalyst during the period of test.

With sulfur contents up to $2 \cdot 10^{-3}$ atoms %, which corresponds to $\theta \leq 0.025$, the activity of the catalyst was greater than without addition of sulfur, but with greater sulfur contents the activity fell below its original value. At $2 \cdot 10^{-2}$ atoms % S, i.e., $\theta \sim 0.25$, the activity was 0.04 of the original. The selectivity, $\underline{s}$ without addition was 0.46. When sulfur was added the selectivity increased at first and reached its maximum value at $\theta \sim 0.03$. With $\theta \sim 0.1$, the selectivity had fallen again to its original value.

Figure 2 shows the results for catalysts obtained by coprecipitation of Ag_2CO_3 and Ag_2S. The values shown are the means for the activity and selectivity between the 44th and 54th hours of operation of the catalyst. The maximum activity was observed at $5.5 \cdot 10^{-5}$ atoms % of S, and was 4 times that of an unpromoted sample. The catalytic activity fell when the S content was further increased, but remained above that of the original sample up to $\sim 10^{-3}$ atoms % of S. The catalyst was almost completely poisoned by a sulfur content of 10^{-1} atoms %. The selectivity $\underline{s}$ increased from 0.57, for the original sample to 0.71 for a catalyst containing $4.2 \cdot 10^{-4}$ atoms % of S, and then decreased with further increase in sulfur content.

Experiments in which sulfur was introduced in the form of Na_2SO_4 and H_2SO_4 gave results agreeing with those described above which enabled us to attribute the activating and poisoning effects to SO_4^{2-} ions on the silver surface.

Experiments on the effects of adding Cl_2 and HCl to the reaction mixture were carried out with tabletted catalyst which already contained close to the optimum amount of chlorine. For this reason, only a reduction in catalyst activity was observed. Addition of Cl_2 or HCl, at a concentration of about 2 mg/m^3, reduced the activity by a factor of 5 since this corresponded to the introduction of $0.5 \cdot 10^{-2}$ atoms % of Cl with respect to Ag. At this point the selectivity had increased from 0.70 to 0.76-0.80. The poisoning was partially reversible. Higher concentrations led to irreversible poisoning.

The above results show that the increased selectivity of the catalytic action of silver, caused by sulfur (or chlorine), cannot be explained as due to partial poisoning of the catalyst with respect to the undesirable reaction (2). A small amount of sulfur increased the speeds of both reactions (1) and (2), but to different extents. An increase in the amount of sulfur led to poisoning. Thus it appears that we are here dealing with a phenomenon which has been described by S. Z. Roginskii, under the title "modification of catalysts" [7, 8]. It may be supposed that the surface of silver is modified by the action of various poisoning ions, particularly of SO_4^{2-} and Cl^-, the modification being dependent on the electronic state of the surface.

A. Kh. Breger and A. A. Zhukovitskii [9] established in principle the possibility of the existence of long-range forces between adsorbed atoms. Since oxygen is electronegative, it is natural to suppose that SO_4^{2-}, or other negative ions would decrease the adsorption energy of oxygen. There is obviously an optimum value of the oxygen-adsorption energy at which the catalytic activity will be at a maximum. The oxygen-adsorption energy is greater than the optimum on a clean silver surface; it decreases to the optimum value with increasing surface concentration of negative ions and then falls below this; this may explain why the reaction velocity passes through a maximum.

LITERATURE CITED

[1] V. A. Pokrovskii, Progress in Chemistry 21, 785 (1952).

[2] J. T. Kummer, J. Phys. Chem. 60, No. 5, 666 (1956).

[3] A. I. Kurilenko, N. V. Kul'kova, N. A. Rybakova and M. I. Temkin, J. Phys. Chem. 32, 797 (1958).

[4] Ia. D. Zel'venskii and S. Iu. Gerchikova, Trans. State Sci.-Res. and Planning Inst. Nitrogen Ind. 2, 132 (1953).

[5] Iu. I. Bulatnikova, L. O. Apel'baum and M. I. Temkin, J. Phys. Chem. 32, No. 12 (1958).

[6] A. I. Kurilenko, N. V. Kul'kova, N. A. Rybakova and M. I. Temkin, J. Phys. Chem. 32, 1043 (1958).

[7] S. Z. Roginskii, J. Phys. Chem. 15, 1 (1941).

[8] S. Z. Roginskii, Adsorption and Catalysis on Heterogeneous Surfaces, pub. Acad. Sci. USSR (1948) p. 511 [in Russian].

[9] A. Kh. Breger and A. A. Zhukhovitskii, J. Phys. Chem. 21, 423 (1947).

The L. Ia. Karpov Scientific Research
Institute for Physical Chemistry

Received July 15, 1958

INVESTIGATION OF FREE RADICALS FORMED IN SOLID BODIES IN THE PROCESS OF IRRADIATION WITH FAST ELECTRONS

Iu. N. Molin, A. T. Koritskii, N. Ia. Buben and Corresponding Member Academy of Sciences USSR V. V. Voevodskii

In recent years the method of electron paramagnetic resonance (EPR) has been widely used for investigating radicals in different materials exposed to the action of ionizing radiations. But as far as we know, there have not previously been any attempts to investigate radicals by the EPR method directly during the course of the action of ionizing radiations on the substance. Such an investigation offers considerable interest, since it is often suggested that radicals formed by the action of radiation may have a very short life and, consequently may only be detectable during the process of irradiation.

In our laboratory, attempts have been made to detect short-life radicals in some solid bodies during exposure to fast electrons. In this paper we present some results on the investigation of radicals with a life of the order of a few minutes.

An apparatus was constructed with which it was possible to record EPR spectra directly during irradiation of the sample. The EPR spectrometer used for recording the paramagnetic absorption signals, had a magnetic field modulated at a high frequency [1] of about 9400 Mc. The derived absorption signal was registered every 30 seconds by an EPP-09 recorder. The source of irradiation was a high-voltage accelerator giving a beam of electrons with energies up to 2 Mev. The current density to the sample could be varied within the limits 0.03-30 $\mu a/cm^2$ which corresponded approximately to a dosage of $6 \cdot 10^3 - 6 \cdot 1\ 0^6$ rads per second. A beam of electrons with an energy of 1.6 Mev was introduced into the region of the magnetic field through a cylindrical channel in one of the pole pieces of the magnet in a direction parallel to the lines of force of the magnetic field. The diameter of the channel at the outlet into the magnet gap was 6 mm. The presence of the channel caused a lack of uniformity of the magnetic field in the neighborhood of the sample of ~ 0.8 oersted/mm, in the direction of the channel axis. The samples investigated were prepared in the form of tablets of diameter 5 mm and thickness about 2 mm. They were inserted in the resonator on the end of a glass capillary. A thermocouple was pressed into the center of the sample for measurement of the temperature. A stream of heated or cooled air was passed round the sample so that its temperature could be varied within the limits + 150 to $-100°$.

Exploratory experiments were carried out at room temperature. EPR signals were observed during irradiation and after it had ceased. More than 20 different substances were investigated, including polymers (polyethylene, nylon, capron, polymethylmethacrylate, teflon and various types of rubber), solid organic acids and their salts (oxalic acid and its salts, succinic acid and its sodium salt, stearic and citric acids), aromatic compounds (naphthalene, α- and β-naphthol, benzoyl peroxide, metol).

With all the samples investigated the concentration of radicals reached saturation at doses of the order of a few tens of megarads. With the majority of substances, the radicals obtained were found to be fairly stable. They persisted for a few hours, and in some cases for longer. With naphthalene and α- and β-naphthol the signal intensity at comparable radiation dosages was considerably less than with the other substances. Radicals with relatively short lives at room temperature were recorded with polyethylene, oxalic acid, benzoyl peroxide and one sample of rubber. Only a few radicals were produced by irradiation of the two latter substances. In both cases one of the radicals was less stable than the others. With benzoyl peroxide the unstable radical

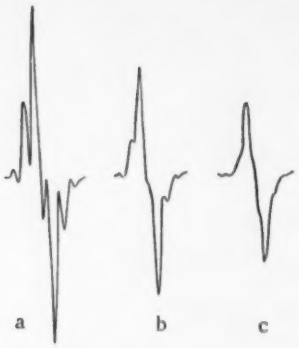

Fig. 1. EPR signals from polyethylene after shutting off electron beam.
a) Immediately after shutting off; b) 1 minute later; c) 4 minutes later.

disappeared within a few minutes and with the rubber it was observed only during irradiation, i.e., it had a life of less than 30 seconds. With oxalic acid the life of the free radicals was 2-3 minutes at room temperature which meant that it was possible to investigate the kinetics of recombination.

When polyethylene was irradiated we obtained a trace for the radical $-CH_2-\dot{C}H-CH_2-$, which is known to be unstable at room temperature [2]. The spectrum of this radical is shown in Fig. 1a, which was recorded immediately after shutting off the irradiation and lasted for a few seconds. Spectra b and c were recorded 1 and 4 minutes respectively after spectrum a.

Spectrum c hardly changed its shape with time, i.e., it represented a secondary more stable radical. Spectrum b was a combination of the spectra of the primary and secondary radicals. A comparison of spectra a, b and c showed that side by side with the conversion of one radical into the other, there was a decrease in the total concentration of radicals.

Observations made below room temperature showed that the rate of conversion of primary into secondary radicals decreased with fall in temperature. Thus, at $-18°$ there was only a slight change in the shape of the initial signal in 6 minutes, i.e., the secondary radical was not formed in appreciable quantities in this time. A comparison of these results with the previous data [2] showed that the formation of radical a was the primary chemical process when polyethylene was irradiated. Reduction of temperature prevented its conversion into radical c.

In conclusion it may be noted that appreciable concentrations of stable radicals in the majority of the solid substances investigated, may prevent the detection of radicals with lives of the order of seconds or less. We shall use the method of periodic modulation of the electron beam in order to observe the spectra of such molecules. It is also proposed to use an impulse method in order to register short life radicals in solid substances and particularly in liquids.

LITERATURE CITED

[1] A. G. Semenov and N. N. Bubnov, Apparatus and Technique of Experiments, No. 1 (1959).

[2] Iu. D. Tsvetkov and N. N. Bubnov, et al., Proc. Acad. Sci. USSR 122, No. 6 (1958).*

Institute of Chemical Physics of the Academy of Sciences of the USSR

Received August 11, 1958

*Original Russian pagination. See C. B. Translation.

OXIDATION OF DIVALENT VANADIUM AT A GERMANIUM ANODE

Iu. V. Pleskov and B. N. Kabanov

(Presented by Academician A. N. Frumkin, July 22, 1958)

The kinetics of electrochemical reactions at a semiconducting electrode were first investigated by Brattain and Garrett [1], who showed that the anodic process of dissolution of germanium took place at the expense of the holes. In germanium the p-type holes are not the primary current carriers and their concentration is small; for this reason the rate of dissolution of germanium electrons at a sufficiently positive potential is limited by the rate of diffusion of holes from the interior, where their concentration is constant to the interface between germanium and electrolyte, where they take part in the reaction. The mechanism of the process of anodic dissolution of germanium at the expense of the holes has been confirmed in a number of subsequent papers [2-4]. Although only the anodic dissolution of germanium was investigated in reference [1], the authors reckoned that it was possible to extend their conclusions on the hole mechanism to all oxidation processes at a germanium electrode. But the profound difference between the process of anodic dissolution of an electrode in which the crystalline lattice of the semiconductor participates, and processes of anodic oxidation of ions existing in solution, forced us to doubt the validity of this conclusion.* It was therefore of interest to investigate from this point of view some processes of the oxidation of ions in solution at a germanium electrode.

In this paper we describe an investigation of the oxidation of divalent vanadium ions at a rotating disc electrode made from monocrystalline germanium of the p-type with a specific resistance of 1.8 ohm · cm and a diffusion length of 0.3 mm. The germanium disc of diameter 7.75 mm and thickness 2 mm, was attached to a vertical axis, and the lateral surface of the disc and the axis were insulated by a teflon coating. The electrode was rotated by a synchronous motor, acting through a system of pulleys; the speed of rotation was measured with a strobotachometer.

The divalent vanadium solution was prepared by the reduction of a solution of V_2O_5 in H_2SO_4 with zinc amalgam. All the measurements were carried out in an atmosphere of purified nitrogen because V^{2+} ions are rapidly oxidized by atmospheric oxygen.

The rate of oxidation of germanium did not depend on the intensity of stirring, but beginning at a potential of 0.5 v, was limited by the rate of diffusion of holes from the interior of the sample to the surface ("saturation current") [1]. When divalent vanadium was introduced into the solution in which the germanium was dissolving at a positive potential of 0.5 v, then the current passing through the electrode at constant potential increased markedly; this increase ΔI was proportional to the concentration of V^{2+} and to the square root of the angular speed of rotation of the electrode ω, and in some cases exceeded the value of the "saturation current" for germanium (see Table 1).

Thus, V^{2+} ions were freely oxidized at a germanium anode (with simultaneous dissolution of germanium), in the same potential range in which the rate of dissolution of germanium alone (controlled by the rate of diffusion of holes) attained a limiting value. Under the given experimental conditions, the rate of oxidation of V^{2+} considerably exceeded the rate of diffusion of the holes. If follows that the holes were not necessary for the process of oxidation of V^{2+} at a germanium anode, i.e., the conclusions of reference [1] cannot be applied to all oxidation processes occurring at a semiconductor electrode.

*There is a similar uncertainty in the problem of the source of electrons in reduction processes at a germanium electrode, which is pointed out in the literature [7].

TABLE 1

Potential, v	Current, ma		ΔI, ma
	before addition of V^{2+}	after addition of V^{2+}	
0.72	7.3	12.3	5.0
0.92	7.4	20.0	12.6
1.22	15.5	20.0	4.5

Since the oxidation of V^{2+} at the germanium anode was always accompanied by dissolution of germanium itself, we used a previously [5] described method of separating processes occurring at a rotating disc electrode for determining the rates of each of the two processes. This method is applicable to cases where the rate of one process is proportional to $\sqrt{\omega}$, but the rate of the other does not depend on the stirring intensity (in our case, these were respectively, oxidation of V^{2+} and anodic dissolution of germanium). The total current density of these two processes at constant potential was a linear function of $\sqrt{\omega}$. By the use of the method referred to, it was possible to split up the experimental curve recorded with a germanium anode in a divalent vanadium solution (Fig. 1,1), into two separate curves: Curve 2 for the dissolution of germanium and Curve 3 for the oxidation of V^{2+}.

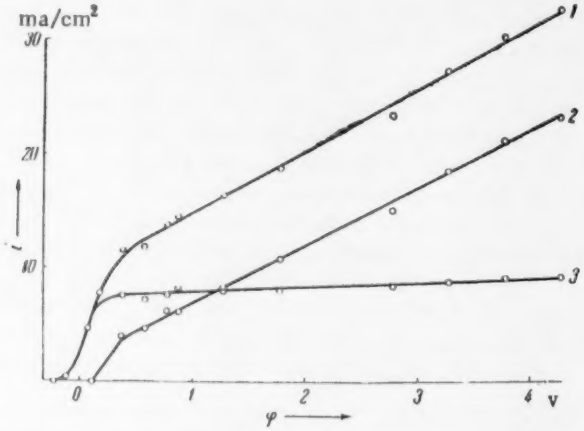

Fig. 1. Polarization curves for the oxidation of divalent vanadium at a rotating germanium disc anode in a solution of 2.2 M H_2SO_4 + 0.9 M $ZnSO_4$ + 0.067 M VSO_4. The speed of rotation was 2550 rpm.
1) Experimental curve; 2) calculated curve for anodic dissolution of germanium; 3) calculated curve for oxidation of V^{2+}.

Separate experiments showed that V^{2+} was oxidized to V^{3+} at a rotating platinum disc electrode and that the value of the limiting current was proportional to the concentration of V^{2+} and to the square root of the angular speed of rotation of the electrode ω. According to the theory of convective diffusion developed by V. G. Levich [6], a direct proportionality between the current and $\sqrt{\omega}$ shows that the rate of oxidation of ions is controlled by their rate of diffusion to the rotating disc electrode. It was found that the current density of the limiting current in Curve 3 was equal to that for the oxidation of V^{2+} on platinum. Consequently, the rate of oxidation of divalent vanadium on a germanium anode as on a platinum anode is determined by the rate of diffusion of V^{2+} ions from the body of the solution to the surface of the electrode. Thus the semiconductive character of a germanium anode is of no significance for the kinetics of the oxidation of divalent vanadium.

LITERATURE CITED

[1] W. H. Brattain and C. G. B. Garrett, Bell Syst. Techn. J. 34, 129 (1955).

[2] A. Uhlir, Bell Syst. Techn. J. 35, 333 (1956).

[3] D. Turner, J. Electrochem. Soc. 103, 252 (1956).

[4] E. A. Efimov and I. G. Erusalimchik, J. Phys. Chem. 32, 413 (1958).

[5] Iu. V. Pleskov, Proc. Acad. Sci. USSR 117, 645 (1957).*

[6] V. G. Levich, Physicochemical Hydrodynamics, pub. Acad. Sci. USSR (1958)[in Russian].

[7] H. Gerischer and F. Beck, Zs. Phys. Chem. N. F., 13, 389 (1957).

Institute of Electrochemistry of the
Academy of Sciences of the USSR

Received July 21, 1958

*Original Russian pagination. See C. B. Translation.

THE PROBLEM OF THE SEMICONDUCTIVE PROPERTIES OF IRON-COPPER SYNTHESIS CATALYSTS AND ACTIVATION BY THE ACTION OF ALKALINE PROMOTERS

I. B. Rapoport and V. N. Kulakov

(Presented by Academician B. A. Kazanskii, July 17, 1958)

One of the factors which most influences the increased activity of iron-copper catalysts used for the synthesis of oxygen compounds and promoters from CO and H_2, is promotion by alkaline addivives. The positive effect of alkali on the activity of iron catalysts was noted by the original investigators [1]; the question has since been more fully investigated in references [2-4] and others, and also by a number of Soviet scientists [5]. But, in spite of the fact that promotion with alkali is one of the most important steps in the development of iron synthesis catalysts the mechanism of the activation action has not yet been adquately explained.

Making use of present developments on the electronic mechanism of heterogeneous catalytic reactions [6, 7] and knowledge of semiconductors [8, 9], it seemed to propose a more probable theory of the action of alkaline promoters on iron-copper synthesis catalysts.

It is well known that active Fe-Cu catalysts are prepared by precipitation with soda from solutions of the nitrates of the respective metals. The precipitant (soda) is washed out and the product is activated (with KOH or K_2CO_3), shaped and reduced with hydrogen at low temperature up to 220-250°. Under these conditions the products are mainly FeO (not less than 50-60%), together with some compounds of the spinel type: $FeO \cdot Fe_2O_3$ ($Fe \cdot Fe_2O_4$), $CuO \cdot Fe_2O_3$ ($Cu \cdot Fe_2O_4$). If magnesium or manganese are included in the composition of the Fe-Cu catalyst then reduction of the sample leads also to the formation of $MgO \cdot Fe_2O_3$ or $MnO \cdot Fe_2O_3$. The content of metallic iron seldom exceeds 1.5-2.0%.

It may reasonably be supposed that Fe-Cu catalysts must have semiconductive properties, since it has been shown that after reduction they consist mainly of FeO and spinels, both of which belong to the class of semiconductors [10]. In this case, by analogy with other semiconductive materials, the action of alkaline promoters is presumed to be as follows. The crystalline lattice of FeO for example, is characterized by an excess of oxygen and, consequently shows hole type conductivity. The excess oxygen atoms (acceptors) draw off electrons from Fe^{2+} to a higher energy level, and the residual Fe^{3+} (holes) provides for the existence of a definite electrical conductivity characteristic of semiconductive materials. The addition of an oxide or salt of a metal, of valency less than that of Fe^{2+} (e.g., K_2CO_3), causes an increase in Fe^{3+}, since the absence of second positive charge on the potassium ion is compensated for in another part of the lattice. The increase in the number of holes causes an increase in the electrical conductivity.

N. P. Keier, S. Z. Roginskii and I. S. Sazonova [11], and also Hauffe, Werner and Wagner [6, 7], showed that for individual catalysts (e.g., NiO), there was a linear relation between electrical conductivity and activity. We presumed that there would also be a linear relation between electrical conductivity and catalytic activity for Fe-Cu catalysts for the synthesis of oxygen compounds and hydrocarbons from CO and H_2. In this case, the activating action of an alkaline promoter should be associated with an increase in the electrical conductivity of the catalyst. Experiments were undertaken to confirm these presumptions experimentally, and the results are described in the present paper.

EXPERIMENTAL

For measurement of electrical conductivity (or its reciprocal, electrical resistance) the catalyst was put in a hard glass vessel. In experiments with reduced samples the catalyst in the vessel was provided with an atmosphere of oxygen-free nitrogen. The height of the catalyst layer was 25 mm, and the distance between the electrodes sealed into the vessel was 33 mm. The catalyst was heated by an electric furnace fitted with an automatic thermoregulator. The catalyst temperature was measured by a thermometer, and its resistance by a universal Wheatstone bridge. The value of the resistance was determined from the formula $R = nr$, where $n = r_1/r_2$ was the ratio of the resistances in the reference arm of the bridge, and r was the resistance in the comparison arm. The catalyst resistance was measured for every 10-20° rise in temperature up to 200°, and then for every 5° up to 230°.

TABLE 1

The Electrical Resistance of Fe-Cu Catalysts Promoted with Different Amounts of K_2CO_3 (ohms · 10^{-3})

Temp. °C	Content of K_2CO_3, %					
	0,0	0,5	1,0	2,5	3,0	10,0
50	41,4	15,8	13,0	15,5	12,5	20,2
70	20,9	8,7	—	7,6	6,5	17,2
80	16,7	6,9	5,5	5,9	4,5	16,0
100	10,2	4,2	4,0	4,0	2,8	19,1
110	—	4,2	3,4	—	3,1	34,0
120	9,1	4,8	—	3,1	3,9	68,0
140	8,6	6,4	3,4	2,7	4,2	—
150	8,5	5,4	3,9	2,7	4,5	—
170	7,3	4,0	3,2	2,3	4,2	80,0
180	6,2	3,5	2,8	2,2	4,0	59,1
190	5,2	2,8	2,7	—	3,7	44 0
200	4,0	2,4	2,2	1,7	3,2	38,0
205	3,5	2,2	2,1	1,6	3,1	29,0
210	3,1	2,1	2,0	1,5	2,9	24,0
215	2,8	1,9	1,7	—	2,6	—
220	2,2	1,2—1,3	—	1,2	2,5	19,3
225	—	—	—	—	2,4	—
230	—	—	—	0,9	2,3	13,9

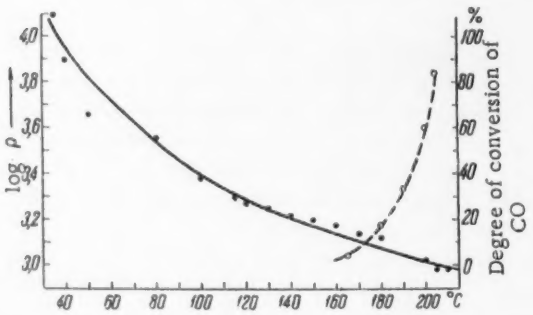

Fig. 1. Variation of the specific resistance and activity of an Fe-Cu catalyst with temperature: a) Logarithm of specific resistance; b) activity (degree of conversion of CO).

Six samples of unsupported Fe-Cu catalyst were prepared for the experiments. The first contained no alkali. The others contained 0.5, 1.0, 2.5, 3.0 and 10% respectively of K_2CO_3.

Experiments carried out with unreduced catalysts showed that these did not have any significant electrical conductivity even at 230°. Their resistances were greater than 1,000,000 ohms at all temperatures. But the reduced samples had quite different properties. The relation between their ohmic resistances R, and temperature is shown in Table 1, and is shown graphically for one sample in Fig. 1a. These results show that the ohmic resistance decreased exponentially with rise in temperature. This is characteristic of semiconductive materials, and showed that the reduced Fe-Cu catalysts were typical semiconductors. In proportion as the resistance dropped and therefore as the electrical conductivity increased, the catalyst gained in activity (Fig. 1b).

It should be noted that the starting temperature for the synthesis reaction was about 160-165° (5% degree of conversion of CO). At this temperature the specific resistance of the catalyst was 1400-1500 ohms ($\log \rho$ = 3.145-3.180). At about 205° the specific resistance was 980 ohms, which corresponded to normal activity of the catalyst with a carbon monoxide conversion of about 80%.

Thus, there was a linear relation between the electrical conductivity of an iron-copper catalyst and its activity for the synthesis reaction.

Characteristic of semiconductors is the dependence of the electrical conductivity on additives, and this was observed with synthesis catalysts. Figure 2 shows the variation of resistance with temperature for the 6 samples of catalysts.

The effects of potash content on the resistance and activity of the catalyst at 210°, are shown in Fig. 3. The catalyst sample which contained no K_2CO_3 had a specific resistance of 1880 ohms ($\log \rho$ = 3.275). Addition of a small amount of potash 0.5%, increased the conductivity by a factor of 1.5. A further increase in the K_2CO_3 content caused a decrease in the resistance and an increase in the activity of the catalyst.

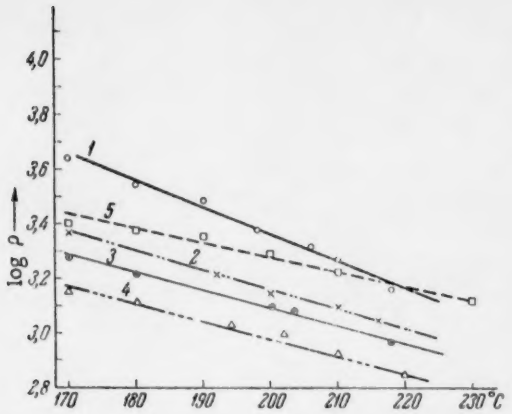

Fig. 2. Variation of specific resistance with temperature for samples of Fe-Cu catalysts containing different amounts of K_2CO_3:
1) 0.0%; 2) 0.5%; 3) 1.0%; 4) 2.5%; 5) 3.0% K_2CO_3.

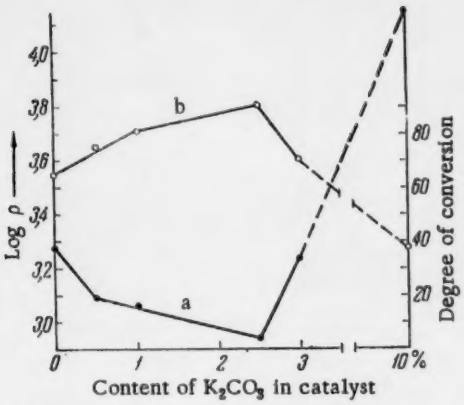

Fig. 3. Variation of specific resistance and activity of an Fe-Cu catalyst with K_2CO_3 content at the synthesis temperature.
a) Logarithm of specific resistance; b) activity (degree of CO conversion. t = 210°.

The promoting action of potash behaving as an acceptor additive, can be explained by its effect in increasing the electrical conductivity of the catalyst. The addition of 2.5% of K_2CO_3 to an Fe-Cu catalyst of given composition gave it the highest electrical conductivity and activity. But further addition of K_2CO_3, up to 3%, reduced both electrical conductivity and activity. The specific resistance was then 1750 ohms (log ρ = = 3.244), and the degree of CO conversion was just below 70%. The negative influence of more than 3% of K_2CO_3 is consistent with the effect of impurities on the electrical conductivity of semiconductors. A marked increase in conductivity occurs only with small concentrations of impurities, above which the conductivity falls [10]. Measurement of the electrical conductivity of the catalyst sample containing 10% of K_2CO_3 showed that even at 210°, it had the very high specific resistance of 14,500 ohms (log ρ = 4.161). The activity of this sample was very low. The degree of CO conversion was only 38% under the same conditions as before.

LITERATURE CITED

[1] F. Fischer and H. Tropsch, Ges. Abhandl. z. Kenntnis der Kohle, 10, 333 (1930).

[2] H. Kölbel and P. Ackerman et al., Chem. Ing. Techn. No. 7, 153 (1951); No. 8, 183 (1951).

[3] G. Storch, N. Golumbic and R. Anderson, Synthesis of Hydrocarbons from Carbon Monoxide and Hydrogen, IL (1954) p. 186.

[4] S. Kodama and K. Fujimura, Sci. Papers Inst. Phys. Chem. Res. 29, 272 (1936).

[5] B. P. Vainshtein, E. A. Plokhinskaia and I. B. Rapoport, Chem. and Technol. Fuels, No. 8, 31 (1956).

[6] K. Hauffe, Angew. Chem. 67, No. 7, 189 (1955).

[7] G. Schwab, Angew. Chem. 67, No. 17, 18, 433 (1955).

[8] M. S. Sominskii, Semiconductors and Their Uses (1955) p. 9.*

[9] A. F. Ioffe, Semiconductors and Their Uses, pub. Acad. Sci. USSR (1956) p. 6.*

[10] A. F. Ioffe, Physics of Semiconductors, pub. Acad. Sci. USSR (1957) p. 197, 201, 234, 330.*

[11] N. P. Keier, S. Z. Roginskii and N. S. Sazonova, Bull. Acad. Sci. USSR, Phys. Series, 21, No. 2, 183 (1957).

The All-Union Scientific Research Institute for the Treatment of Oils and Gases and for the Production of Artificial Liquid Fuels

Received May 23, 1958

*Russian translation.

THE NATURE OF THE ACIDITY OF ALUMINOSILICATE CRACKING CATALYSTS

K. V. Topchieva and I. F. Moskovskaia

(Presented by Academician V. I. Spitsyn, July 2, 1958)

The surface acidity of aluminosilicate catalysts has been investigated by many workers [1-7]. But the methods described in the literature give only a semiquantitative estimate of the acid strength [5, 6] or of the number of acid sites [7-10]. Unsatisfactory features of the methods used are the dependence of the results on the size of the basic neutralizing molecules, lack of precision in determining chemical and physical adsorption, and diffusion complications [11]. Also, none of the methods, including the spectroscopic method [12, 13], make it possible to determine the nature of the acid (proton or nonproton), so that it is impossible to derive any definite conclusions as to the role of either type of acid in the cracking reaction. The difficulties in defining the types of acid centers are associated with the lack of clear-cut methods for determining them and with their relatively low surface concentrations. Thus, the method of exchange adsorption allows preliminary hydration of the nonproton centers, and the other methods based on interaction of the acid sites with amine molecules, allow the possible formation of complexes (Catalyst. NR), both with proton and with nonproton centers.

As a possible way out of these difficulties we chose the method of successively excluding one type of center, and independent investigation of the other type. We showed previously [4, 8] that, by the method of exchange adsorption from salt solutions, it was possible to destroy independently the active centers of the aluminosilicate complex, practically without affecting the exchange centers of the oxides and thus together with the kinetic method to characterize precisely the catalytic activity of samples in terms of the deactivation of acid centers.

We have found that a combination of these two methods with a method for titrating nonproton acids is of value for the separate investigation of each type of acid for elucidating their roles in the cracking reaction.

For this investigation we took Al-Si* catalysts with increasing Al_2O_3 contents: 10/90, 30/70, 50/50, 80/20** prepared by simultaneous displacement, and also pure oxides of aluminum and silicon. The protonic acidity was determined by the reaction of exchange adsorption with solutions of the salts CH_3COOLi and CH_3COONa. Poisoning was produced by the method previously described [4, 8]. The activities of the initial and poisoned samples were determined by cracking cumene in a flow system at 475° [4]. Experimental kinetic data were treated in accordance with A. V. Frost's equation [14] for monomolecular heterogeneous reactions under flow conditions.

Figure 1 shows the relation between the velocity constant and the quantities of Li and Na cations introduced, and it is evident that for all the samples investigated, there was at first a linear decrease in activity with increasing quantities of the cation and then a break after which the activity altered very little, in spite of the addition of considerable amounts of the cation. In these experiments, the value of the proton acidity of the cracking catalyst was taken as the limiting acidity obtained by extrapolating the first linear portion of the curve (Fig. 1). This method of determination was equivalent to the belief in a strict proportionality between the quantity of metal cations introduced and the fall in activity. This proportionality broke down at the break in the curves; as stated above, considerable further exchange did not alter the velocity constant. We were inclined to think that the discontinuity in the straight line must be explained either by continuation of

*For the sake of brevity, Al-Si will subsequently be written to stand for aluminosilicate catalyst.

**The numerator of the fraction corresponds to the weight percentage of Al_2O_3, and the denominator to that of SiO_2 in the catalyst.

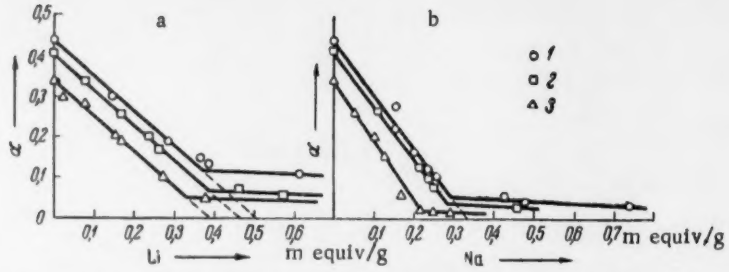

Fig. 1. Dependence of the velocity constant α, on the quantities of Li^+ (a) and Na^+ (b) ions introduced.
1) 30/70; 2) 50/50; 3) 80/20.

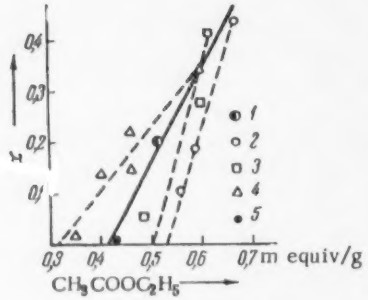

Fig. 2. Variation of the velocity constant α with the value of the nonproton acidity for initial (continuous line) and poisoned (dotted) samples of different composition.
1) 10/90; 2) 30/70; 3) 50/50; 4) 80/20; 5) Al_2O_3.

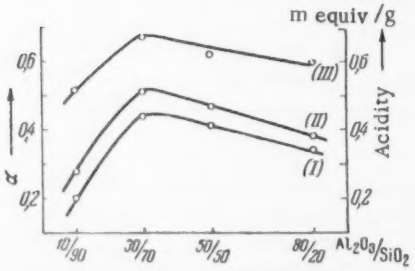

Fig. 3. Variation of velocity constant α (I), proton (II) and nonproton (III) acidity with catalyst composition.

exchange with only slightly catalytically active OH groups of the oxides Al_2O_3 and SiO_2, or by diffusion difficulties associated with the increased concentration of metal cations on the surface of the catalyst.

It is evident from Fig. 1 that proton acidity and activity were both a maximum for samples of composition 30/70, were somewhat less for 50/50 samples, and were still less for 80/20 and 10/90 samples. The variations in activity with the amount of adsorbed cations for the separate oxides are not shown in Fig. 1, because the velocity constants were less by an order of magnitude than for the Al-Si catalysts: 0.02 for SiO_2 and 0.01 for Al_2O_3. Ion exchange carried out with the original oxides was also not very great (0.025 m·equiv/g for Al_2O_3 and 0.070 m·equiv/g for SiO_2), and reduced the velocity constant for the cracking of cumene practically to zero. It may therefore be concluded that high exchange capacity and cracking activity are inherent in the Al-Si complex, but not in the component oxides.

It also follows from Fig. 1 that the slopes of the linear parts of the curves were different for samples poisoned with Li and Na. This difference is obviously associated with screening by the larger Na ions. In order to exclude the screening effect of the large ion, and to approach more closely to the true value of the limiting acidity use was only made in subsequent calculations of the experimental data obtained by exchange with lithium cations. It is interesting to note that the values of the exchange acidity, determined by extrapolation from Fig. 1 coincided with the values of the maximum exchange adsorption for the same samples, calculated by us from the E. N. Gapon equation for the exchange adsorption isotherm [15]. This agreement provided evidence of the validity of the use of the lithium cation for determining the true number of exchange centers. A similar conclusion, that a Li ion could only poison one active center, was reached by Danforth [9]. The data on exchange adsorption enabled us to determine the proportion of active surface, and was found to be 2% for the most active 70/30 catalyst. This value is in good agreement with that calculated from data on the reactivation of calcined catalysts by the introduction of small amounts of water [16].

In order to determine the nonproton acidity, the same samples and oxides were investigated by the

thermometric method, described by Trambouze [2]. The results, shown in Fig. 2, are the means of two repeated experiments. Figure 2 shows the variation of the velocity constant for unpoisoned aluminosilicate catalysts and aluminum oxide, with the value of the nonproton acidity. This variation was also linear and thus preserved the previous relation between activity and acidity. The sample of composition 30/70 had the highest acidity. The acidity of the original samples fell, with a corresponding drop in activity to the value of the nonproton acidity of pure aluminum oxide which showed a considerable Lewis acidity (0.43 m·equiv/g), while silicon dioxide was completely lacking in this type of acidity. The dotted lines in the same figure show the changes in nonproton acidity as the result of poisoning by lithium cations. The slight decrease in nonproton acidity as the result of poisoning (somewhat greater for the 80/20 sample), clearly shows up the selectivity of the given method with respect to nonproton centers. But it should be noted that the observed reduction in the value of the Lewis acidity with poisoning was not due to experimental error, but was associated with a lack of definition in the demarcation of the natures of the acid centers by this method, i.e., the proton sites of the aluminosilicate structure partially reacted on titration with a Lewis base (in this case ethyl acetate), and this was particularly noticeable with unpoisoned samples. If this were not so, the value of the Lewis acidity would not have altered with poisoning and the linear fall in activity would have been parallel to the ordinate axis.

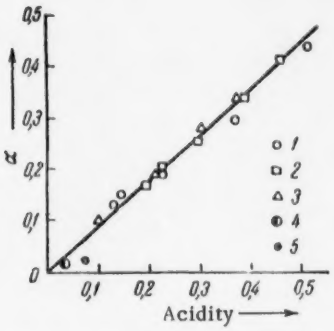

Fig. 4. Variation of the velocity constant for the cracking of cumene with proton acidity, as determined with Li^+.
1) 30/70; 2) 50/50; 3) 80/20; 4) SiO_2; 5) Al_2O_3.

Our experiments on the determination of nonproton acidity showed that it existed, and in considerable quantity both in aluminum oxide and in Al-Si catalysts. Figure 3 shows the variations of velocity constant for the cracking of cumene for the initial catalyst samples and also of the proton and nonproton acidities, as functions of composition. The nature of the curves shows that there is a definite relation between activity and both types of acidity. The close resemblance between the acidity curves suggests that either the acid centers are identical or that both forms of acidity are produced in the formation of aluminosilicate catalysts. The first suggestion must be rejected because the initial aluminum oxide and the poisoned aluminosilicates had a large remaining nonproton acidity with practically complete absence of activity for the cracking reaction. Between them the slight fall in Lewis acidity, when lithium cations were introduced and the nonproportional sharp fall in the velocity constant for the cracking reaction indicated that nonproton acidity appeared with proton acidity when aluminum was introduced into the silicon dioxide structure, but that, by itself, without protons (unhydrated), it played no part in the cracking reaction. On the other hand, the second supposition was confirmed by the existence of a high nonproton acidity in aluminum oxide and poisoned samples with a practically complete absence of cracking power.

The variation of activity with proton acidity, shown in Fig. 4, was linear in character. The straight line passed through the origin, which indicated that there was a direct and proportional connection between activity and proton acidity.

These results show definitely that the introduction of lithium cations into a catalyst lowers the cracking activity and that the number of cations which can be introduced is strictly proportional to the number of active sites and is not connected with adsorption on Lewis acid centers.

LITERATURE CITED

[1] T. H. Milliken, G. A. Mills and A. G. Oblad, Disc. Farad. Soc. 8, 279 (1950).

[2] V. Trambouze, J. Chim. Phys. 51, 723 (1954).

[3] K. G. Miesserov, Progress in Chemistry 22, 279 (1953).

[4] K. V. Topchieva, Sci. Trans. Moscow State Univ., No. 174, 75 (1955).

[5] Ch. Walling, J. Am. Chem. Soc. 72, 1164 (1950).

[6] H. A. Benesi, J. Am. Chem. Soc. 21, 5490 (1956).

[7] O. Johnson, J. Phys. Chem. 59, No. 9, 827 (1955).

[8] K. V. Topchieva and I. F. Moskovskaia, Proc. Acad. Sci. USSR 101, No. 3, 517 (1955).

[9] J. D. Danforth, J. Phys. Chem. 58, 1039 (1954).

[10] G. A. Mills, E. R. Boedeker and A. G. Oblad, J. Am. Chem. Soc. 72, 1554 (1950).

[11] R. L. Richardson and S. W. Benson, J. Phys. Chem. 61, No. 4, 405 (1957).

[12] J. E. Mapes and R. P. Eischens, J. Phys. Chem. 58, No. 12, 1059 (1954).

[13] E. I. Kotov, Optics and Spectroscopy 3, No. 2, 115 (1957).

[14] A. V. Frost, Moscow State Univ. Herald, No. 3-4, 11 (1946).

[15] E. N. Gapon, J. Gen. Chem. 3, 144 (1933).

[16] S. G. Hindin, A. G. Oblad and G. A. Mills, J. Am. Chem. Soc. 77, 535 (1955).

The Chair of Physical Chemistry of the
M. V. Lomonosov Moscow State University

Received June 28, 1958

THE EFFECTS OF IONS OF TETRAVALENT TITANIUM ON THE ELECTROCHEMICAL PROPERTIES AND CORROSION BEHAVIOR OF TITANIUM

V. V. Andreeva and V. I. Kazarin

(Presented by Academician A. N. Frumkin, July 25, 1958)

There are a number of papers [1-4] on the effects of the ionic composition of the electrolyte on the resistance to corrosion and electrochemical properties of titanium. It has been shown that the corrosion of titanium, in solutions of sulfuric and hydrochloric acids, is markedly reduced by the presence of various cations, such as Cu^{2+}, Pt^{4+}, Au^{3+}, Fe^{3+}, Al^{3+} and others. The retardation of corrosion has been explained as due to the adsorption of these ions on the surface of the titanium, with subsequent partial chemisorption.

The stability of titanium, both under atmospheric conditions and in liquid media, has been explained as due to the formation of a surface film of a different type. Evidently, in many cases, this protective film consists of titanium dioxide. This film has the following characteristics: it is insoluble in most electrolytes; it has semiconductive properties; and it is difficult to reduce (only by the most powerful reducing agents) to lower oxides.

The thickness of the "natural" film on titanium, obtained by evaporation of the metal in a high vacuum and condensation of the vapor on glass, was measured by an optical polarization method [5-7], and was found to be 12-25 A at the initial moment of contact between a clean titanium surface and atmospheric air. It was found to increase with time. After 75 days, the thickness was 50-55 A, and film growth had practically ceased. The process of formation of the surface film on titanium in an atmosphere of normal air is clearly associated with its hydration. The "natural" film on titanium is transparent, invisible (even to the aware eye), compact, and it also has good adhesive properties. It has good protective properties, since the process of diffusion through the film is extremely slow. The thickness of the film did not exceed 55 A after a very long time of storage (about 3 years), in an atmosphere of air (45-50% relative humidity). Under the same conditions of storage, samples of iron and copper were completely covered with corrosion products. From observations on corrosion, it is a known fact that there is an increase in the chemical stability of stainless steel, chromium, aluminum and other so-called autopassifying metals and alloys, if they are exposed to an atmosphere of air or oxygen for a definite time. The same thing happens with titanium. If titanium is subjected to the action of 40% sulfuric acid immediately after polishing or pickling, it becomes active in a few seconds, but if it is first exposed to air for a long time, it does not become active for about 2 hours.

We were interested in the cause of the increase in the corrosion resistance of titanium with increasing thickness of the surface film. It did not appear possible to use an optical method for measuring the thickness of a film forming on titanium at the time of polishing, since the initial values of the optical constants for a clean titanium surface were not known. In the given case, we could only follow the increase in thickness of an already existing film, using, for the initial optical constants, the values obtained immediately after polishing the titanium. The results showed that, in 180 days, the increase in film thickness only amounted to 17-22 A. Thus the process of formation of the natural film with time, evidently, mainly takes the form of a disappearance of the defects in the oxide lattice, and not of a growth in film thickness.

Granting that the high resistance to corrosion of titanium is explained by the existence on its surface of a protective film of titanium dioxide, whose solubility in sulfuric and hydrochloric acids is very small [8] (TiO_2 has a somewhat lower solubility in hydrochloric than in sulfuric acid), it may be presumed that, if the

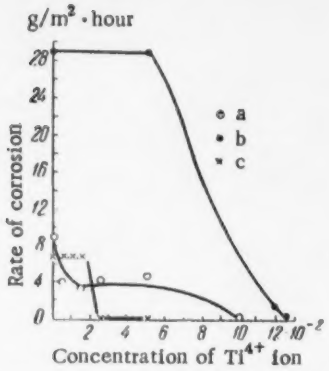

Fig. 1. Variation of the rate of corrosion of titanium with the concentration of $Ti^{4+} \cdot 10^{-2}$ (mole/liter) at 40°.
a) In 20% HCl; b) in 36% HCl; c) in 40% H_2SO_4.

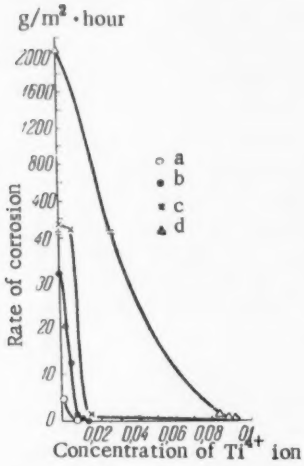

Fig. 2. Effect of the concentration of Ti^{4+} ions (mole/liter) in 40% sulfuric acid on the rate of corrosion of titanium, as a function of the solution temperature. a) 20°; b) 40°; c) 60°; d) 100°.

corresponding amount of tetravalent titanium ions is added to the solution of sulfuric or hydrochloric acids, then, in conformity with the law of mass action, a state of equilibrium could be created in which the corrosion of titanium would practically cease.

The equilibrium equation will have the form:

$$TiO_2 + 2H_2SO_4 \rightleftharpoons Ti(SO_4)_2 + 2H_2O$$

or

$$TiO_2 + 4H^+ \rightleftharpoons Ti^{4+} + 2H_2O$$

i.e.,

$$[Ti^{4+}] / [H^+]^4 = K.$$

An investigation was made with solutions of hydrochloric and sulfuric acids. The results showed that the amount of Ti^{4+}, necessary to render the titanium passive, depended on the concentration of acid and on the temperature of the solution.

Figure 1 shows the variation of the velocity of corrosion of titanium (produced by the iodide method, purity 99.8%) with the concentration of Ti^{4+} in 20 and 36% solutions of hydrochloric acid and in a 40% solution of sulfuric acid.

Figure 2 shows the variation of the rate of corrosion of titanium in 40% H_2SO_4 with the concentration of Ti^{4+} and with the solution temperature. In this 40% sulfuric acid solution, between 20 and 60°, 0.015 mole/liter of Ti^{4+} was sufficient to render the titanium passive; 0.1 mole/liter of Ti^{4+} was already required at higher solution temperature up to 100°. The higher solubility of TiO_2 in hydrochloric acid solutions meant that a higher concentration of Ti^{4+} was necessary (Fig. 1 and 2).

The change in electrode potential with time, of a sample of titanium (immediately after dressing) immersed in 40% sulfuric acid, showed progressive activation of the titanium as the potential acquired a steady value of −0.3 v. In the presence of 0.067 mole/liter of Ti^{4+} in the same solution, the potential rapidly altered from −0.22 to +0.1 v even in the first few seconds after immersion. When the titanium was allowed to remain in the solution, the potential shifted to the region of a positive value of +0.2 v, which demonstrated the process of formation and strengthening of the protective properties of the surface film.

In 40% sulfuric acid (without addition of Ti^{4+} to the solution) at room temperature, dissolution of titanium began after about two hours; during this period the potential gradually shifted to a negative value; activation occurred immediately when a cathode current of 10 $\mu a/cm^2$ was imposed. Under the same conditions, but with Ti^{4+} (0.14 mole/liter) present in the solution, activation was strongly retarded; it required about 200 $\mu a/cm^2$ (at 40°) to convert titanium from the passive to the active state, while at higher temperatures, up to 100°, activation of titanium only occurred with a cathode current density of 800 $\mu a/cm^2$; thus in spite of the higher temperature, activation of titanium, under these conditions, was not facilitated (Fig. 3), but on the contrary, was retarded.

Polarization curves obtained with titanium in 40% sulfuric acid in the presence of 0.14 mole/liter of Ti^{4+} at 40 and 60° (Fig. 4), showed that hydrogen was evolved on the titanium after activation, and this evolution did not cease when the cathode current was completely switched off, i.e., the titanium did not passify itself, once it had been made active. The initial shapes of the cathodic and anodic curves (from a potential

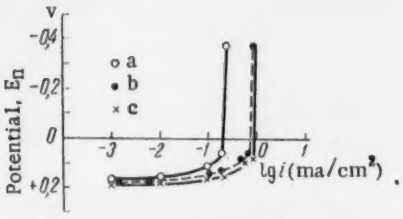

Fig. 3. Change in potential of titanium as a function of density of cathode current and of temperature, in 40% sulfuric acid with addition of 0.14 mole/liter of Ti^{4+} ion.
a) 40°; b) 80°; c) 100°.

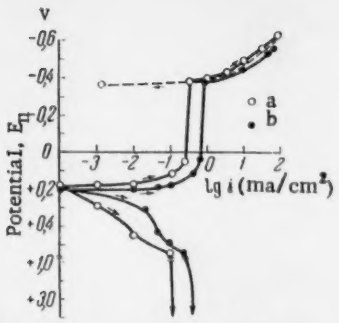

Fig. 4. Polarization curve for titanium in 40% sulfuric acid with addition of 0.14 mole/liter of Ti^{4+}.
a) 40°; b) 60°.

of + 0.2 v) showed the existence of oxidation-reduction processes. At potentials of ~ +0.04 v, and more negative, there was evidently a reduction of Ti^{4+} to Ti^{3+} ions, since both the electrolyte and electrode became violet colored. Marked anodic polarization was observed when a potential of ~ + 0.7 v was reached.

On the basis of the above, it becomes clear why hydrochloric acid pickling solutions for titanium, even when containing such powerful activators as derivatives of hydrogen fluoride, become less and less active with use, and why, finally, pickling of titanium practically ceases when the titanium content of the solution reaches a definite value. The fact is that titanium evidently originally goes into solution in the form of a divalent ion. With oxidizing agents, such as dissolved oxygen in the solution, because of the high affinity of titanium for oxygen, the divalent titanium ions lose electrons and are oxidized, first to Ti^{3+}, and then to Ti^{4+}, according to the equation:

$$Ti^{2+} - e \rightarrow Ti^{3+} - e \rightarrow Ti^{4+}.$$

Oxidation to Ti^{4+} occurs considerably more slowly than to Ti^{3+}. This explains why a pickling solution already containing a considerable amount of dissolved titanium, gradually loses its activity on standing in air. As the amount of Ti^{4+} ion in solution increases as the result of oxidation, the activity of the solution naturally falls.

LITERATURE CITED

[1] M. E. Straumanis and P. C. Chen. J. Electrochem. Soc. 98, 6, 234 (1951).

[2] H. H. Uhlig and J. R. Cobb, J. Electrochem. Soc. 99, 1, 13 (1952).

[3] H. H. Uhlig and A. Geary, J. Electrochem. Soc. 101, 5, 216 (1954).

[4] D. Schlain and D. J. Smatko, J. Electrochem. Soc. 99, 10, 10 (1952).

[5] V. V. Andreeva, Inst. Tech.-Econ. Inform. Acad. Sci. USSR, Subject 9, PS-55-503.

[6] V. V. Andreeva and V. I. Gavrilov, Trans. Inst. Phys. Chem. Acad. Sci. USSR, No. 3 (1951).

[7] V. V. Andreeva, Trans. Inst. Phys. Chem. Acad. Sci. USSR, No. 6, 79 (1957).

[8] Gmelins Handbuch der anorganischen Chemie. Titan. 1951.

Institute of Physical Chemistry
of the Academy of Sciences of the USSR

Received July 21, 1958

EFFECT OF CALCIUM CHLORIDE ON THE PROCESS OF STRUCTURE FORMATION IN AQUEOUS SUSPENSIONS OF TRICALCIUM ALUMINATES

E. P. Andreeva, E. E. Segalova and E. E. Volynets

(Presented by Academician P. A. Rebinder, August 4, 1958)

The mechanism of the effect of calcium chloride on the processes of setting and hardening of cement has not been completely explained, in spite of numerous investigations [1]. It has been shown by a number of authors that calcium chloride reacts chemically with the aluminate constituents of cement clinker, during the hydration process to form hydrated calcium aluminate chloride [2]. But it was still uncertain how the production of this compound affects the initial stage of the process of structure formation.

The suggestion has been made that the effect is connected with the chemical dispersion of a solid phase, and is the result of strains arising from the formation of the hydrated calcium aluminate chloride [3]. Dispersion does indeed increase the rate of setting and hardening, because of the increase of the specific surface of the cement. But it can hardly be supposed that dispersion is the sole cause of such a marked acceleration of setting and hardening, as is observed when a sufficient quantity of calcium chloride is added. Also, it does not explain why small or medium amounts of calcium chloride do not accelerate, but actually retard the setting process.

In order to elucidate the mechanism of the action of calcium chloride on Portland cement, it was first necessary to investigate its influence on the structure-forming process in suspensions of tricalcium aluminate (C_3A), an individual mineral in cement clinker, which controls the nature of the structure-forming process in the first stages of the interaction of cement with water. With this in view, we investigated the kinetics of structure formation and chemical interaction in suspensions of C_3A, and of its hydrate, $C_3A \cdot aq$ ($3CaO \cdot Al_2O_3 \cdot 6H_2O$), slaked with different-strength calcium chloride solutions.

Experiment showed that for a similar type of investigation it was most effective to use a mixture of 2 to 10% of cement with 98 to 90% of inert filler – ground quartz sand or calcite [4]. Concentrated suspensions were prepared from these mixtures by soaking, which prevented the possible destruction of the structure arising in the suspension immediately after slaking. The samples were preserved under water and under the various calcium chloride solutions. The process of structure formation was followed by the kinetics of the growth of plastic strength [5]. The results of these experiments are shown in Fig. 1-3.

The final amount of combined calcium chloride (Fig. 1) was the same for all the suspensions investigated and amounted to 0.75 mole $CaCl_2$ per mole of C_3A. X-ray and thermographic investigations showed that the same compound was formed in all the suspensions, in which there was sufficient calcium chloride to combine with all the C_3A or its hydrate. Debye diffraction patterns and thermograms of the product agreed with those given in the literature for the hydrated aluminate monochloride, and with those we obtained with hydrated calcium aluminate chloride, synthesized by Foret's [2] method.

The kinetics of the combination of calcium chloride depended very much on the composition of the suspension, and particularly on the concentration of calcium chloride. Chemical reaction began more slowly with suspensions of $C_3A \cdot aq$, than with C_3A, because of the lower solubility and rate of solution of the hydrated alumina [6], but the reaction subsequently speeded up, and was fully completed by the second day. With suspensions of C_3A in which, because of the high rate of solution and higher solubility a high supersaturation of the calcium aluminate chloride hydrate could occur, the formation of calcium aluminate chloride began very

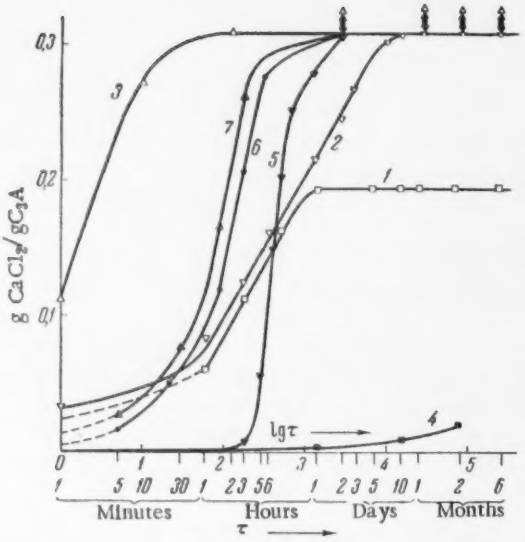

Fig. 1. Kinetics of the chemical combination of calcium chloride with suspensions of tricalcium aluminate and its hexahydrate, A) containing 3% C_3A + 97% finely ground quartz sand + 35 ml of calcium chloride solution per 100 g of dry powder, and B) 4.2% C_3A• + 95.8% finely ground quartz sand +33 ml of calcium chloride solution per 100 g of dry powder.
1) 0.31 N $CaCl_2$ solution, n = 0.5; (A); 2) 1.58 N, n = 2.5 (A); 3) 6.35 N, n = 10 (A); 4) 0.31 N, n = = 0.47 (B); 5) 1.58 N, n = 2.35 (B); 6) 3.17 N, n = = 4.7 (B); 7) 6.34 N, n = 9.4 (B).

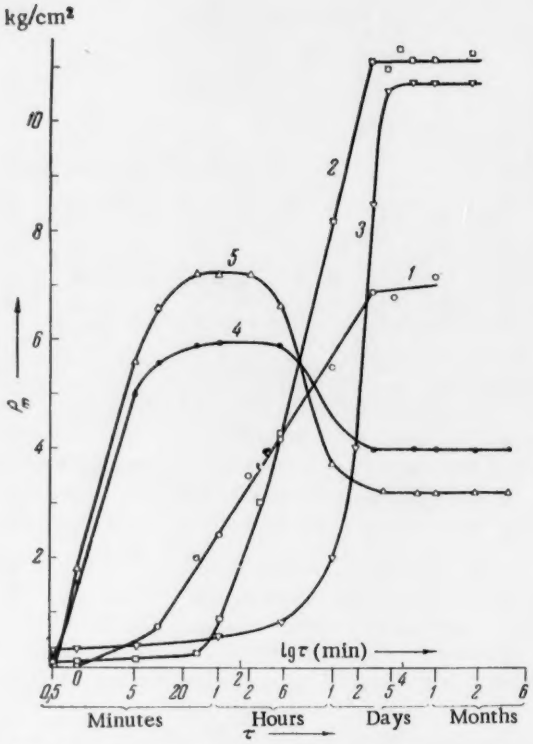

Fig. 2. Kinetics of structure formation in suspensions of tricalcium aluminate, containing 3% C_3A + 97% finely ground quartz sand +35 ml of calcium chloride solution per 100 g of dry powder.
1) H_2O; 2) 0.31 N $CaCl_2$ solution, n = 0.5; 3) 1.58 N, n = 2.5; 4) 3.17 N, n = 5.0; 5) 6.34 N, n = 10.0.

rapidly, but then with medium additions of $CaCl_2$ slowed up, and for example, in suspensions with a mole ratio (n) of $CaCl_2$: C_3A = 2.5, was only complete after 5-10 days. By analogy with the conditions for the formation of the hydrated aluminate sulfate [7], this could be explained by the retarding influence of hydrated aluminate chloride crystallites produced at a high degree of supersaturation, and forming a protective film over the surface of the original C_3A particles, thereby retarding their dissolution. With C_3A suspensions slaked with highly concentrated calcium chloride solutions(n = 5 and 10), the formation of hydrated aluminate chloride occured extremely rapidly and was almost complete in 30 minutes.

The special features of the kinetics of interaction of C_3A and its hydrate with calcium chloride were reflected in the processes of structure formation occurring in these suspensions (Fig. 2 and 3). Although with all suspensions in which $n \geq 1$, the amount of hydrated aluminate chloride formed was the same, yet the strength of the structures was different, which showed that there was a great dependence of the strength of the crystalline structure on the conditions of its formation.

With suspensions of C_3A containing small amounts of added calcium chloride ($n < 1$), the increase in strength was prolonged, and continued even after the $CaCl_2$ had been converted into calcium aluminate chloride, which indicated the subsequent crystallization of hydrated aluminate. The initial crystalline structure of hydrated aluminate chloride formed in these suspensions, had a very low strength, evidently because of the very fine state of division of the crystallites formed at very high supersaturation. The retarding effect of calcium chloride on the C_3A structure-forming process amounts to this—that together with the strong enough

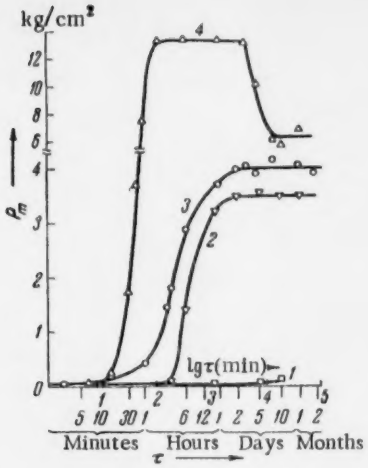

Fig. 3. Kinetics of structure formation in suspensions of tricalcium aluminate hexahydrate containing 4.2% C_3A·aq +95.8% finely ground quartz sand +33 ml of calcium chloride solution per 100 g of dry powder. 1) 0.31 N $CaCl_2$ solution, n = 0.47; 2) 1.58 N, n = 2.35; 3) 3.17 N, n = = 4.7; 4) 6.34 N, n = 9.4.

crystalline structure of hydrated aluminate, there also forms in the suspension an unstable fine crystalline structure of hydrated aluminate chloride, which is easily broken down by mechanical action. The same unstable structure arises in suspensions containing large amounts of added calcium chloride (n = 2.5). Three hours after slaking, the strength of this structure was 750 g/cm², although by this time the reaction of formation of hydrated aluminate chloride had already occurred to an extent of about 40%. Subsequently the hydrated aluminate chloride crystallized more slowly and covered over the original framework [8], so that the strength of the structure increased, and at the end of the process was higher than for suspensions slaked with water.

In the presence of large amounts of calcium chloride (n = 5 and 10), when the reaction of formation of hydrated aluminate chloride took place very intensively, there was a rapid growth of strength in the suspension up to a maximum value followed by a decrease (Fig. 2, Curves 4 and 5, and Fig. 3, Curve 4). The fall in strength was connected with the considerable expansion of the system. The increase in volume as the result of expansion was 20% for suspensions with n = 10.

LITERATURE CITED

[1] A. A. Baikov, Collected Papers, 5, 1948;* V. M. Moskvin, Additive-Accelerators for the Hardening of Cement (1938);* R. H. Bogue, The Chemistry of Portland Cement, N. Y., 1955.

[2] L. S. Wells, J. Res. Nat. Bur. Stand. 1, 4, 951 (1928); J. Foret, Recherches sur les combinaisons entre les sels de calcium et les aluminates de calcium, Paris, 1935; R. Nacken and R. Mosebach, Zs. anorg. u. allgem. Chem. 228, 19 (1936).

[3] Iu. A. Savina and N. N. Serb-Serbina, Building Industry, 9, 6 (1954); N. N. Serb-Serbina and Iu. A. Savina, Cement, No. 2, 3 (1955); N. N. Serb-Serbina, Iu. A. Savina and V. S. Zhurina, Proc. Acad. Sci. USSR, 111, No. 3, 659 (1956); V. V. Kind, E. V. Lavrinovich and P. E. Litvinova, Cement, No. 3, 7 (1955).

[4] E. E. Segalova, E. S. Solov'eva and P. A. Rebinder, Proc. Acad. Sci. USSR, 113, No. 1, 134 (1957).**

[5] E. E. Segalova, P. A. Rebinder and O. I. Luk'ianova, Moscow State University Herald, No. 2 (1954); P. A. Rebinder and O. I. Luk'ianova, Nature, No. 12 (1952).

[6] E. E. Segalova, E. S. Solov'eva and P. A. Rebinder, Proc. Acad. Sci. USSR, 117, No. 5, 841 (1957).**

[7] E. E. Segalova and P. A. Rebinder, Thesis. Proc. 4th All-Union Conf. Coll. Chem. Tiflis (1958), p. p. 130.*

[8] Tu Yu-ju, Thesis Proc. 4th All-Union Conf. Coll. Chem. Tiflis (1958), p. 133.*

Chair of Colloid Chemistry of the
M. V. Lomonosov Moscow State University

Received July 10, 1958

*In Russian.

**Original Russian pagination. See C. B. Translation.

KINETICS OF THE OXIDATION OF COAL WITH NITRIC ACID

V. S. Veselovskii and G. L. Orleanskaia

(Presented by Academician A. A. Skochinskii, June 24, 1958)

The oxidation of mineral carbon by aqueous media is of considerable interest as it often occurs in seams and in stored mined coal. Its investigation may also be useful for comparing the chemical activities of different coals, and particularly their tendencies to spontaneous combustion. The latter would be specially valuable because the existing method is not completely satisfactory. In view of these considerations, the work described below was carried out under the direction of A. A. Skochinskii, in the Institute of Fuel of the Academy of Sciences of the USSR. Nitric acid was used as an oxidizing agent. Its reduction by carbon may be expressed by the stoichiometric equation:

$$2HNO_3 = 3\,(O) + 2NO + H_2O.$$

Reduction of nitric acid takes place through several successive stages. Intermediate reduction products have a considerably greater oxidizing power than nitric acid itself. This is a disadvantage in the use of nitric acid for assessing the chemical activities of different coals, because the powerful oxidizing agents react almost equally easily with different substances, and it is therefore difficult to reveal differences between the oxidizabilities of the latter.

There is some work described in the literature on the oxidation of coal with nitric acid. H. H. Lowry [1], oxidizing different coals with 6.3% nitric acid, found that oxidation never began immediately after mixing the coal and acid, but after the elapse of some time. This phenomenon was investigated in detail by G. L. Stadnikov [2].

The apparatus which we used for the experiments consisted of a vessel of capacity about 200 ml. The vessel was closed by a rubber bung, with a gas outlet tube leading under a glass cylinder, which was calibrated to measure the volume of gas evolved. The experiments were carried out with Donetz coals of uniform petrographic structure.

In general the process began with a latent period,during which there was only a negligible evolution of gas. Then the velocity of gas evolution increased rapidly, soon reached its maximum and then decreased. Fig. 1 shows typical curves for the rates of oxidation of different coals by 5% nitric acid.

The experiments of this series showed the following:

1. No direct relation was found between the degree of metamorphosis of the coal and the length of the latent period or the maximum rate of oxidation.

2. On the average the longer the latent period the less was the subsequent rate of gas evolution. This certainly corresponded to a low chemical activity of the coal.

3. The greater the maximum rate of oxidation the more rapidly it declined.

During the latent period, it was impossible to detect any increase in the degree of oxidizability of the coal, even with such a sensitive index as the ignition temperature [4], and the content of material titratable with permanganate (mainly lower oxides of nitrogen) in the acid solution remained very small – of the order of 0.05 m equiv/liter. But the degree of oxidizability of the coal increased rapidly immediately after the

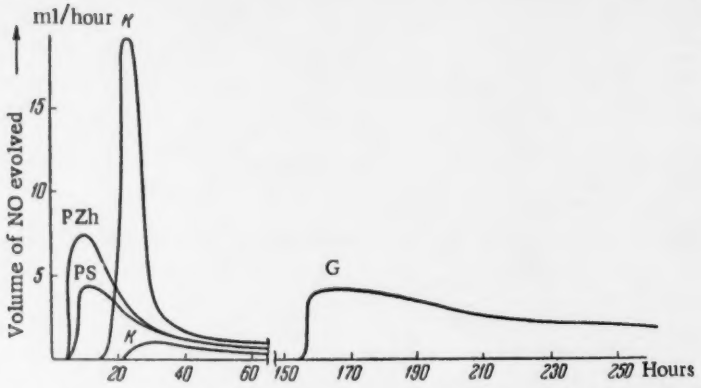

Fig. 1. Variation of the rates of oxidation of different coals with time.

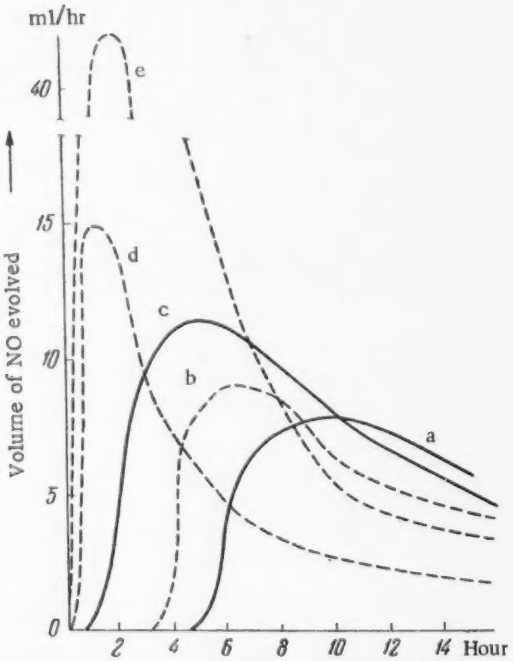

Fig. 2. Disappearance of the latent period as the result of addition of sodium nitrite:
a) 0%; b) 0.01%; c) 0.025%; d) 0.05%; e) 1%.

commencement of rapid gas evolution, and the content of titratable material in the solution increased by a factor of 10. Subsequently, the degree of oxidizability of the coal and the concentration of titratable material increased slowly. Humic acids extractable with aqueous alkali only appeared after prolonged oxidation.

It follows from these experiments that chemical interaction took place very slowly during the latent period. Rapid oxidation of the coal only began after a concealed preliminary process during the latent period.

The Donetz coal grade PZh, used in these experiments, had an oxidizability index $\Delta T_0 = 45°$, i.e., it must be reckoned as easily oxidizable. But a latent period of more than 5 hours was observed for its oxidation by 5% nitric acid, and the oxidizability index did not alter during this time. This meant that activation of the coal did not occur during the latent period. The existence of the latent period in the development of the process, and the subsequent rapid increase in the rate of the latter, must therefore be explained by the need for activation of the oxidizing agent. It is most natural to assume that the latter was activated by the presence of intermediate products. To test this assumption, a series of experiments was carried out in which sodium nitrite was added to the 5% nitric acid, i.e., lower oxides of nitrogen were present in the solution from the start. It is clear from Fig. 2 that the latent period was reduced, and the maximum rate of gas evolution increased with increasing addition of sodium nitrite. The total quantity of gas evolved in 50 hours did not alter appreciably. The latent period disappeared with a nitrite concentration of more than 0.05%. Hence it follows that an accumulation of a very small amount of active intermediate products was sufficient to transform the concealed preliminary process into a rapid reaction.

Subsequently, a mixture of 5% sulfuric acid with 1% of sodium nitrite was used instead of nitric acid. The curve obtained for the rate of evolution of gas was the same as for when 1% of sodium nitrite was added to nitric acid, i.e., without a latent period and with the same high maximum. Hence it follows that coal is oxidized primarily by lower oxides of nitrogen, and that nitric acid serves only as a source and reservoir of these oxides.

It should be noted that thermal autoacceleration did not occur in our experiments, and that the process should be regarded as isothermal.

The process occurred autocatalytically, and the course of the initial acceleration was determined by the function $e^{\varphi\tau}$, where φ is the chain branching velocity constant and τ is the time. But retardation soon began, and the velocity dropped after reaching its maximum value. This retardation cannot be explained by the decrease in concentration of nitric acid, as the latter was in great excess.

In order to explain the retardation mechanism, it is significant that the higher the maximum rate the sharper was the subsequent retardation. The total quantity of gas produced did not depend on the height of the maximum, and varied over a considerable range. It is obvious that, since the process slowed up to an almost constant rate, there must have been a uniform amount of material reacting. The simplest explanation is that the surface of the coal became covered by a layer of oxidation products, which obstructed the access of oxidizing agent. The formation of similar layers, which obstruct the process, has been observed in investigations of the kinetics of the low-temperature oxidation of coal by gaseous oxygen [3].

Since the rate of reaction is very high, all the oxidizing agents which penetrate the layer will be rapidly used up. Thus the rate of chemical conversion will be equal to the rate of penetration of the oxidizing agent:

$$kC = D(C_0 - C) \tag{1}$$

where C_0 is the concentration of oxidizing agent in the body of the solution, C is its concentration on the reacting surface of the coal, D is its penetration coefficient through the oxidized layer ("effective diffusion coefficient").

Hence

$$C = C_0 \frac{D}{D+k}. \tag{2}$$

It is evident from Equation (1) that the slower the penetration through the oxidized obstructing layer and the faster the reaction rate, the less will be the concentration of oxidizing agent on the reacting surface.

For the rate of evolution of gas we obtain

$$\frac{d[NO]}{d\tau} = kC = kC_0 \frac{D}{D+k} = C_0 \frac{1}{\frac{1}{k}+\frac{1}{D}} \tag{3}$$

The value of 1/D has the significance of a resistance opposed by the oxidized layer to the penetration of oxidizing agent.

The coefficient k cannot alter much with time, since it is mainly related to the reaction with fresh coal, which does not alter with time, so that the decrease in the rate of the process is mainly determined by the decrease in the penetrability D.

It is reasonable to suppose that the rate of penetration of oxidizing agent to the reacting coal surface will be inversely proportional to the resistance of the oxidized layer (V = 1/D), and that the rate of increase of this resistance will be proportional to the quantity Q, of reacted material:

$$\frac{dV}{d\tau} = \frac{Q}{V}. \tag{4}$$

If Q is taken as constant over a small time interval, then integration gives

$$V = \sqrt{2Q\tau}, \tag{5}$$

i.e., the retarding resistance of the oxidized layer is proportional to the square root of the time, and the quantity of oxidizing agent reacting (and consequently the rate of chemical conversion) is inversely proportional to V, i.e., to the square root of the time:

$$kC = \frac{d[NO]}{d\tau} = B\tau^{-1/2}$$

The results obtained provide material for developing a theory of coal storage and the effects of atmospheric oxides of nitrogen. They also show that nitric acid is unsuitable for estimating the tendency of coal to spontaneous combustion.

LITERATURE CITED

[1] H. H. Lowry, Fuel, 10, 291 (1937).

[2] G. L. Stadnikov, Spontaneously Combusting Coals and Ores, Their Geochemical Characteristics and Methods of Recognition (1956).*

[3] A. A. Skochinskii and S. Z. Makarov, Investigations on the Use of Antipyrogens, pub. Acad. Sci. USSR (1947).*

[4] V. S. Veselovskii and G. L. Orleanskaia, Bull. Acad. Sci. USSR, Div. Tech. Sci. No. 4 (1954).

Received June 6, 1958

*See C. B. Translation.

DIFFERENTIAL HEATS OF ADSORPTION OF WATER VAPOR ON SILICA GELS OF DIFFERENT DEGREES OF HYDRATION

T. S. Egorova, V. F. Kiselev and K. G. Krasil'nikov

(Presented by Academician M. M. Dubinin, May 28, 1958)

We have shown previously [1-3] that the values of the adsorption of the vapors of water and methanol, and also the heats of wetting by these liquids, bear a linear relation to the degree of hydration of the surface of the sample investigated. It appeared to be of interest to clarify the effect of hydration of the silica gel surface on the differential heat of adsorption, since the latter is determined by the interaction energy of the adsorbed molecules with the surface in different states of coverage, which is important for the study of the mechanism of the elementary act of adsorption. Differential heats of adsorption can be determined by direct calorimetric measurements, or by differentiating the curves relating the heat of wetting of samples to the amount of previously adsorbed vapor or, finally, can be calculated from the results of adsorption measurements [5].

The relation between heat of wetting Q_{wet}, and the amount of previously adsorbed vapor $\underline{a}$ is given [4] by the formula

$$Q_{wet} = \int_{a}^{a_s} (Q_a - L)\, da + \epsilon s'. \qquad (1)$$

Since the amount of vapor adsorbed at saturation a_s, is constant at a given temperature and since the surface energy of the film, $\epsilon s'$ (where ϵ is the surface energy of the liquid and s' is the surface of the saturated film) does not depend on $\underline{a}$, the differential heat of adsorption of the vapor is

$$Q_a = \frac{\partial Q_{wet}}{\partial a} + L.$$

The few quantitative investigations dealing with heats of adsorption on silica gel, containing previously adsorbed water (a critical review of these is given in [4]), were carried out with different samples, and the fundamental characteristics of these, in particular their specific surfaces, were unknown so that it is impossible to compare the results among themselves, or with the results of other measurements. The comparison actually made in [4], using values of the specific surface calculated from the "absolute" heat of wetting, may be in error, as was shown in [1]. Measurements were made in [4] of the relation between the heat of wetting of silica gel and the amount of previously adsorbed water, and the relation between the differential heat of adsorption and the amount of adsorbed water was calculated. But the initial region was not investigated. The values of the differential heats are shown in the table of [4], beginning with 2.5 μ mole/m^2 and above, but the corresponding heats of wetting were measured for considerably lower values of adsorption (from 0.24 μ mole/m^2 and above). We have calculated the initial part of the differential heat curve from the data given, and it lies considerably above the curve obtained in [4] by extrapolation. Direct calorimetric measurements of heats of adsorption of water vapor on silica gel were made in [6], but the authors only show the integral values of the amount adsorbed, and give no data on the specific surface of their samples. Thus it appears that there is no

TABLE 1

Adsorption Characteristics of the Silica Gels Used

Gel sample	Calcining temperature, °C	Specific surface, m^2/g	Heat of wetting, $ergs/cm^2$	Structural water $\mu mole/m^2$
K-2	300	695	141	3.01
K-2	700	550	108.7	1.17
K-2h	700	550	129.9	2.6
KSK-3	300	340	181	4.13

*Obtained by subjecting silica gel K-2 previously calcined at 700°, to the action of water for one month.

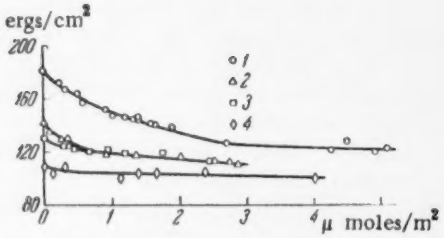

Fig. 1. Variation of specific heat of wetting with the amount of water previously adsorbed on silica gels: 1) KSK-3-300°; 2) K-2-300°; 3) K-2-700° h; 4) K-2-700°.

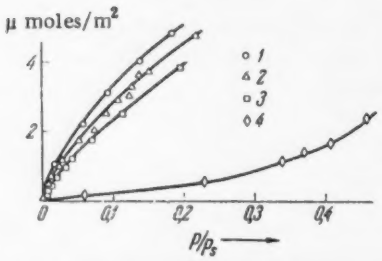

Fig. 2. The initial parts of the adsorption isotherms of water on silica gels: 1) KSK-3-300°; 2) K-2-300°; 3) K-2-700° h; 4) K-2-700°.

adequate data in the literature on the relation between differential heat of adsorption of water vapor and the degree of coverage of the surface.

In our work we used silica gels K-2 and KSK-3, the conditions for their preparation being the same as in [1, 2]. The adsorption characteristics of the samples are shown in Table 1. Heats of wetting were measured in a calorimeter with constant heat exchange [1]; heats of adsorption of vapors were measured in a calorimeter similar to one previously described [7]. The preparation of gel samples, containing different amounts of adsorbed water, was carried out in parallel with measurements of adsorption isotherms, for which purpose the fitting with the calorimetric ampule for measurement of heat of wetting was suspended from a spring balance in an adsorption apparatus. Adsorption of water vapor was conducted at constant vapor pressure obtained by means of a cryostat. The dosing of water vapor into the gas calorimeter was controlled by independent weighing [8].

We investigated the initial part of the isotherm and the differential heat of adsorption of water vapor on different silica gels, by two independent methods. Figure 1 shows heats of wetting, calculated for unit surface (i.e., specific values), as functions of the amount of water previously adsorbed. In the case of nonporous hydrophilic adsorbents with a practically uniform surface, the specific heat of wetting decreases with increasing amount of adsorbed water, and as a approaches a_s, tends to the value of the full surface energy of the liquid ϵ (118 $ergs/cm^2$ for water), as was shown in [9] for the system $TiO_2 - H_2O$.* With heterogeneous silica surfaces, the adsorption of water, as follows from [2], proceeds mainly on the silanol surface which may be considerably less than the total internal surface as determined for example, by adsorption of nitrogen. Since regions of different energies of wetting [1] exist on a silica surface, the values of the heats of wetting, according to Formula (1), will be different for them during the process of coverage. The heat of wetting of a siloxane surface will obviously increase with increase in a, as has been shown for hydrophobic surfaces [12], but will decrease for a silanol surface. In our experiments we determined the total heat over the whole heterogeneous surface, so

*Incorrect graphs are shown in [10, 11] to illustrate this data according to which the heat of wetting increases with the amount of adsorbed water).

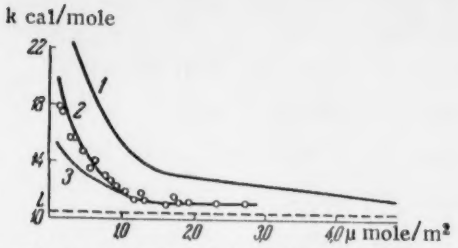

Fig. 3. Variation of the differential heat of adsorption of water with the amount previously adsorbed, for silica gels: 1) KSK-3-300°; 2) K-2-300°; 3) K-2-700°g; the continuous curves were obtained from the data of Fig. 1, the points of curve 2 were the results of direct measurements.

that the attainment by the heat curve (Fig. 1) of the value $\epsilon = 118$ ergs/cm² was no proof that the whole surface was covered with a saturated film of adsorbed water. In the case of porous adsorbents, it is also necessary to take into account the reduction of the surface film s', as the result of capillary condensation.

In our experiments, we were dealing with uniform, coarsely porous adsorbents and we were examining the region of adsorption up to the beginning of capillary condensation, when the surface of the film s', was practically equal to s [4]. It is clear from Fig. 1 that all the heat curves were of such a form that for a given previously adsorbed amount of water, the heat of wetting decreased with a decrease in the hydration of the surface of the original sample. A similar relation was also found for the initial parts of the adsorption isotherms for water vapor (Fig. 2). Although, when wetting the dehydrated silica gel K-2-700°, there was an additional heat of hydration [1] as well as the "physical" heat of wetting, yet because of the low hydration of the surface (Table 1), the total heat lay considerably below the heat curve for the rehydrated sample K-2-700° h.

The results of calculating differential heats of adsorption as functions of specific adsorptions are shown in Fig. 3. It is evident from the figure that the heats of adsorption on silica gel K-2-300°, obtained by direct calorimetric measurement, agreed well with the curves calculated from the data of Fig. 1. The initial value of the heat of adsorption of water on silica gel KSK-3 lay in the range 15-20 kcal/mole, so that evidently, at small degrees of coverage the adsorbed molecules formed 3 and 4 hydrogen bonds with the hydroxyl of the surface;* it is possible that in this region some of the molecules were adsorbed on centers of higher energy [3]. The heat of adsorption fell as the coverage of the surface increased, which could evidently be explained as the result of a decrease in the number of hydrogen bonds with the surface hydroxyl groups, arriving at an average of one adsorbed water molecule per group. No great part was played by repulsive forces between the dipoles of adsorbed molecules [4]. An estimate [13] of the energy of tangential interaction, for the idealized case of a completely filled, hydrated, surface monomolecular layer of uniformly oriented dipoles gave a value of less than 1 kcal/mole. In the case of a real, i.e., partly hydrated silica surface this value would be even less.

The value of the differential heat for a given degree of coverage decreased with decreasing degree of hydration of the sample surface (Table 1). On the other hand [4], we did not obtain one "absolute" relation for the differential heat of adsorption of water vapor in the case of the samples of coarsely porous silica gels investigated. The adsorption of water molecules on the silanol-covered part of the surface was evidently mainly dependent on the interaction of water molecules with two hydroxyl groups [2]. The probability of the formation of such paired interactions would decrease with a decrease in the concentration of surface hydroxyl groups, and the consequent increase in the mean distance between them; the adsorption interaction would then be determined by a single hydrogen bond from the adsorbed molecule to a single surface hydroxyl group. At relatively high pressures, as the result of gradual coverage of the siloxane part of the surface, the differential heat should approach the value of the heat of condensation. The investigation of adsorption and differential heats of adsorption in this pressure region, with appreciably dehydrated silica samples could only be carried out with nonporous or very coarsely porous material for which capillary condensation could be neglected, i.e., under the condition that $s' \approx s$.

Our estimate of the differential entropy of adsorption of water vapor ΔS, showed that it decreased with increasing hydration of the silica gel surface. Taking liquid as the standard state for water, the curves for the differential entropy lay in the region of negative values (for example at $a = 1$ μ mole/m², ΔS was -0.3 and -7.3 cal/mole respectively for K-2-300° and KSK-3-300°. The mobility of the adsorbed molecules increased with increasing dehydration of the surface, i.e., with decreasing number of adsorption centers, but for the samples investigated the mobility always remained below that of the molecules in liquid water, i.e., in this sense the surface became more uniform.

The authors' thanks are due to B. V. Il'in for his interest in this work and discussion of the results.

*Similar to what happens in the case of associated water molecules [14].

LITERATURE CITED

[1] M. M. Egorov, K. G. Krasil'nikov and E. A. Sysoev, Proc. Acad. Sci. USSR, 108, 103 (1956).

[2] B. V. Il'in, V. F. Kiselev and K. G. Krasil'nikov, Moscow State Univ. Herald, No. 6, 35 (1957).

[3] K. G. Krasil'nikov, V. F. Kiselev and E. A. Sysoev, Proc. Acad. Sci. USSR, 116, 990 (1957).*

[4] A. V. Kiselev and K. D. Krasil'nikov, et al., J. Phys. Chem. 26, 986 (1952).

[5] B. P. Bering and V. V. Serpinskii, Proc. Acad. Sci. USSR, 114, 1254 (1957).*

[6] W. H. Patrick and C. E. Greider, J. Phys. Chem. 29, 1031 (1925).

[7] A. V. Kiselev and V. F. Kiselev, et al., J. Phys. Chem. 23, 577 (1949).

[8] B. P. Bering and V. V. Serpinskii, Proc. Acad. Sci. USSR, 55, 741 (1947).

[9] W. Harkins and G. Jura, J. Am. Chem. Soc. 66, 919 (1944).

[10] A. V. Kiselev, Progress in Chemistry, 15, 456 (1946).

[11] A. V. Kiselev, Supplement to book by S. Brunauer, Adsorption of Gases and Vapors (1948), p. 714.**

[12] G. J. Joung, J. Chessick, E. H. Healy and A. C. Zettlemayer, J. Phys. Chem. 58, 313 (1954).

[13] J. Topping, Proc. Roy. Soc. A, 114, 67 (1927).

[14] D. Bernal and R. Fowler, Progress in Phys. Sci. 14, 586 (1934).

The M. V. Lomonosov Moscow State University

Received May 26, 1958

*Original Russian pagination. See C. B. Translation.

**Russian translation.

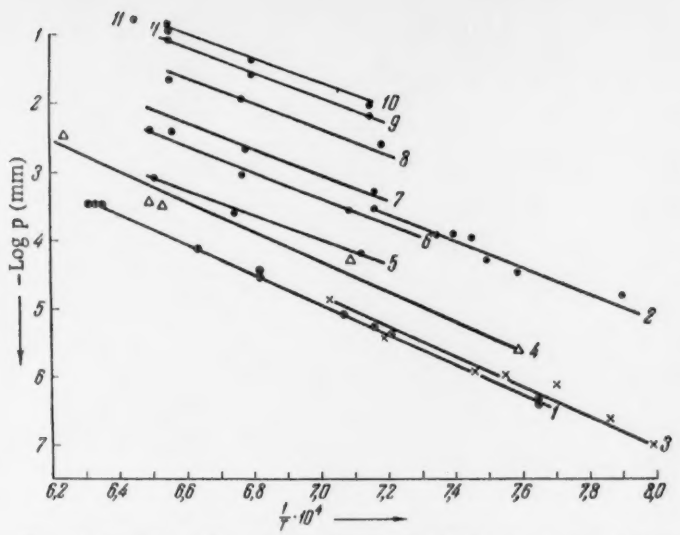

Fig. 1. Change in the vapor pressure of nickel with change in temperature.
1) From the data of [3]; 2) from [4]; 3) from [5]; 4) from [6]; 5-9) from our data, 5) with $a = 9.847 \cdot 10^{-3}$ cm^2, 6) with $a = 1.52 \cdot 10^{-3}$ cm^2, 7) with $a = 7.74 \cdot 10^{-4}$ cm^2, 8) with $a = 1.673 \cdot 10^{-4}$ cm^2; 9) calculated values of p_{equil}; 10) values of p_{equil} calculated from [3]; 11) from the results of our work with $a = 7.85 \cdot 10^{-5}$ cm^2.

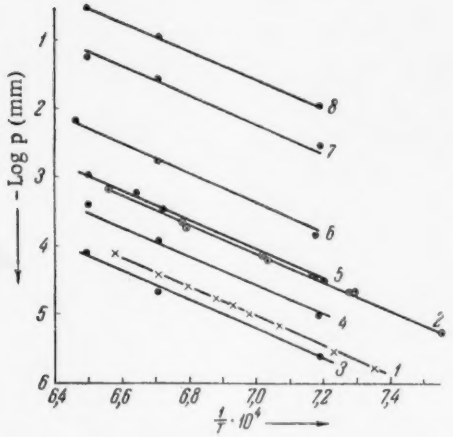

Fig. 2. Change in the vapor pressure of cobalt with change of temperature.
1) From the data of [1]; 2) from [2]; 3-7) from our data: 3) with $a = 9.847 \cdot 10^{-3}$ cm^2; 4) with $a = 1.884 \cdot 10^{-3}$ cm^2, 5) with $a = 9.847 \cdot 10^{-4}$ cm^2, 6) with $a = 7.74 \cdot 10^{-4}$ cm^2, 7) calculated values of p_{equil}; 8) values of p_{equil} calculated from [1].

the data of Johnston and Marshall [3] only differ by 20% from those calculated from our results. Thus the vapor pressures of nickel obtained by Langmuir's method are incorrect. They used evaporation utilizing the coefficient of Langmuir. From this point of view, the rate of evaporation of nickel can be correctly determined from our work and from that of Johnston and Marshall [3].

LITERATURE CITED

[1] J. W. Edwards, H. L. Johnston and W. E. Ditmar, J. Am. Chem. Soc. 73, 4729 (1951).

[2] Iu. V. Kornev and V. N. Golubkin, Proc. Acad. Sci. USSR, 99, 565 (1954).

[3] H. L. Johnston and A. L. Marshall, J. Am. Chem. Soc. 62, 1382 (1940).

[4] S. A. Vekshinskii and E. P. Pronov, J. Appl. Phys. 7, 109 (1930).

[5] G. Bryce, J. Chem. Soc. 1936, 1517.

[6] I. Langmuir and G. M. Mackay, Phys. Rev., 4, 337 (1914).

[7] An. N. Nesmeianov, L. A. Smakhtin and V. I. Lebedev, Proc. Acad. Sci. USSR, 112, 700 (1957).*

[8] M. G. Rossman and J. Yarwood, J. Chem. Phys. 21, 1406 (1953).

*Original Russian pagination. See C. B. Translation.

Received July 18, 1958

THE SURFACE ACTIVITIES OF LIQUID METALLIC COATINGS AND THEIR EFFECTS ON THE STRENGTHS OF METALS

N. V. Pertsov and Academician P. A. Rebinder

S. T. Kishkin and Ia. M. Potak and their co-workers [1, 2] investigated the drop in strength and emergence of brittleness of a number of high-melting and heat-resisting alloys, under the influence of liquid-metallic coatings and media, and explained this influence as an adsorption effect [3]. These effects were confirmed in our laboratory by the extension of monocrystals of different metals coated with thin films of more easily fusible metals in the liquid state [4, 5]. This phenomenon was explained as due to a reduction in surface energy of the deforming hard metal at surface cracks, arising at the starting points of defects, under conditions of adsorption from the liquid-metal coating, resulting in two-dimensional diffusion of the adsorbed (surface-active) material.

A detailed investigation of the effects of readily fusible coatings on the strengths of metals showed that the effects were highly specific, inasmuch as a given coating would reduce the strengths of some metals and have no effect on others while, on the other hand, a given metal would respond differently to different coatings.

It should be noted that the decrease in strength is not the result of a solvent action of the fusible coating, since the quantity of the latter is extremely small (less than 1%), and the solubility of the primary metal in the coating, as a separate phase is small, or in every case, limited. The existence of considerable effects in the case of metallic monocrystals shows that the effect of the liquid metallic medium cannot reasonably be associated with a selective action at the grain boundaries.

The experimental data on the effects of readily fusible metallic coatings on the mechanical properties of metals can be divided into two quite distinct groups: 1) there is a marked lowering in the strength of the metal investigated, and 2) there is no lowering of the strength (see Table 1).

A comparison of these results with the fusibility diagrams of the corresponding binary systems – metal-metal coating – clearly shows that reduction of the strength of the hard metal, under the influence of the liquid coating, always corresponds to the existence on the fusibility diagram of a narrow enough but quite definite region of formation of solid solutions. This naturally relates to the part of the diagram where the concentration of metal coating is small, and so answers to the case under consideration. On the other hand, the complete absence of a decrease in strength corresponds to a wide region of formation of solid solutions of the metal coating with the metal investigated.

The results obtained may seem trivial from this point of view. Actually, if the given film thickness (of the order of a micron) corresponds to the ratio of more- to less- easily fusible metal in the region of formation of solid solutions, the strength of the system metal + coating will not be less than that of the metal by itself, but usually somewhat higher (as the result of the introduction of impurities into the lattice). Certainly, impurity atoms diffusing in the solid-solution lattice may be adsorbed from the interior to surfaces developing at defect sites in the deformation process (if the impurities show some surface activity). But the effects of this are not large because of the small rate of volume diffusion as compared with two-dimensional surface migration, and also because of the low concentration of impurities. At high concentrations of these (corresponding to a high solubility) an increase in strength occurs, owing to actual formation of a solid solution.

If indeed the region of formation of solid solutions is so narrow that the system metal + coating lies outside the region, then deformation of the metal occurs in the presence of the liquid-coating phase, which is able

TABLE 1

Reduction in strength of metals under influence of molten coating		Absence of reduction in strength of metals under influence of molten coating	
metal investigated	metal coating	metal investigated	metal coating
Cadmium	Tin	Cadmium	Mercury
Zinc	Mercury	Lead	Mercury
Zinc	Gallium	Copper	Mercury
Zinc	Tin	Copper	Tin
Copper	Bismuth	Copper	Zinc
Iron	(Hydrogen)	Zinc	Lead

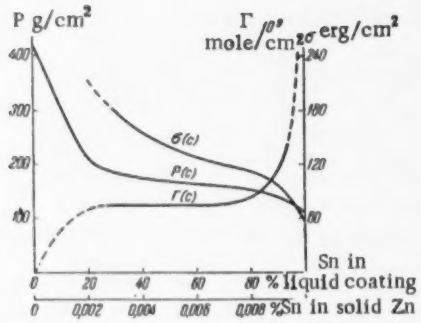

Fig. 1. P (c) is the experimental isotherm [4] for the reduction in strength of a zinc monocrystal as a function of the concentration of tin in a liquid coating of Pb + + Sn; σ (c) is the surface-tension isotherm, calculated from P(c) by the method of [6], for the region of brittle fracture; Γ (c) is the corresponding adsorption isotherm.

to become saturated with the substance of the distorting metal. When the alloy (metal + coating) crystallizes at this point, an equilibrium system is obtained consisting of separate crystallites of heavy metal phase separated by layers of the coexisting alloy, and this has either no strength or in any case the low strength corresponding to the formation of a coagulated structure. But, with the phenomena under consideration we are dealing not with equilibrium systems formed at temperatures above the melting point of the eutectic, but with the deformation behavior (mechanical properties) of a solid, originally-single component, metal, which may be a monocrystal covered with a thin film of a readily fusible metal.

The lowering of the strength of a solid body (metal) is explained by the ability of the fused metal coating to be adsorbed – its power to lower the surface or interfacial tension at the boundaries metal/gas or metal/thin film of liquid phase from σ_0 to σ, and to ensure a rapid penetration of the atoms of the readily fusible metal under the influence of the high two-dimensional pressure $\sigma_0 - \sigma$, into the conversion zone by a two-dimensional migration mechanism.

The relation between the reduction in the strength of a metal, as the result of the lowering of its surface tension, and its solubility in the metallic coating is completely analogous to the increase in the surface activity of an organic surfactant in aqueous solution with a decrease in its solubility in water. Liquid coatings which are only slightly soluble in the primary metal show a greater surface activity in the sense of a capacity to reduce the surface tension of the primary metal by formation of an adsorbed layer at the surfaces which are being produced. Indeed, the greatest reduction in surface tension and consequently in strength leading to rapid brittle fracture, corresponds to the formation of a new liquid phase, or of the conversion into the latter of a polymolecular layer.

Using the theoretical calculations of E. D. Shchukin [6] and the experimental relation between the strength of a zinc monocrystal, $P_c = f(c)$, and the concentration of lead in a tin/lead coating [4], it is possible to derive the function σ (c), for the region of brittle fracture; by application of the Gibbs equation, it is possible to evaluate the adsorption Γ and the course of the adsorption isotherm $\Gamma = \Gamma(c)$, on the surfaces which are being formed. Approximate calculations, the results of which are shown in Fig. 1, lead to the value $\Gamma_m = 1.3 \cdot 10^{-9}$ mole/cm², which corresponds well with a monoatomic layer of tin, and to the subsequent growth of Γ (c) in the region of polymolecular layers, which is well known to correspond to complete wetting, i.e., to the direct passage of liquid phase into the wetting layer.

In the case of a polymolecular layer, with the entry of liquid phase into the film at the interface (within the limits of formation by fracture of new interfaces between zinc and tin saturated with zinc), the work of formation of such interfaces by fracture (i.e., σ) will be less, the greater the mutual solubility (in the limit, $\sigma \to 0$ at infinite mutual solubility).

The absence of any significant reduction in strength when the coating is practically completely insoluble in the primary metal (zinc coated with lead) is associated with the retention of a sufficiently high value of the surface tension at the phase boundary.

Ia. M. Potak [2] pointed out that the decrease in the strength of iron (steel) under the influence of hydrogen, which is soluble in it, is also an adsorption effect (internal adsorption). The hydrogen in the metal, forming an embedded solid solution possesses a high mobility, and this together with the surface activity of atomic hydrogen with respect to iron [7], leads to the formation of a monoatomic hydrogen layer on the developing surfaces which causes a sharp fall in the surface tension of the iron and leads to hydrogen embrittlement [8].

Complex many-component alloys with higher concentrations of impurities at the grain boundaries show a much more complicated picture for the adsorptive effects of low-melting coatings (for example the strength reduction of heat-resisting alloys coated with a molten layer of tin [1]).

LITERATURE CITED

[1] S. T. Kishkin, Proc. Acad. Sci. USSR, 95, No. 4, 789 (1954); S. T. Kishkin and V. V. Nikolenko, Proc. Acad. Sci. USSR, 110, No. 6, 1018 (1956).

[2] Ia. M. Potak, Brittle Fracture of Steel and Steel Components (1955).*

[3] P. A. Rebinder, Z. Phys. 72, 91 (1931); P. A. Rebinder, Jubilee Coll. dedicated to 30th Anniversary of October Socialist Revolution, pub. Acad. Sci. USSR (1947);* P. A. Rebinder and V. I. Likhtman, Proc. 2nd Intern. Congr. Surface Activity London (1957);* V. I. Likhtman, P. A. Rebinder and G. V. Karpenko, Effects of Surface Active Materials on the Deformation of Metals, pub. Acad. Sci. USSR (1954).*

[4] P. A. Rebinder, V. I. Likhtman and L. A. Kochanova, Proc. Acad. Sci. USSR, 111, 1287 (1957).**

[5] V. N. Rozhanskii, N. V. Pertsov, E. D. Shchukin and P. A. Rebinder, Proc. Acad. Sci. USSR, 116, No. 5, 769 (1957).**

[6] V. I. Likhtman and E. D. Shchukin, Progress in Phys. Sci. 66, No. 2, 213 (1958).

[7] R. M. Barrer, Diffusion in Solid Bodies, IL (1948) [Russian translation].

[8] J. Helsop and N. J. Petch, Phil. Mag. 2, 649 (1957).

Chair of Chemistry of the Moscow Institute
for Machine Construction
Chair of Colloid Chemistry of the M. V. Lomonosov
Moscow State University

Received September 16, 1958

* In Russian.

** Original Russian pagination. See C. B. Translation.

INVESTIGATION OF THE SATURATION VAPOR PRESSURES OF SOME THALLIUM COMPOUNDS

M. G. Shakhtakhtinskii and A. A. Kuliev

(Presented by Academician V. N. Kondrat'ev, July 23, 1958)

In this paper we present the results of measurements of the saturation vapor pressures of thallous sulfide and oxide which are used in the preparation of thallium sulfide photocells [1, 2]. There is no data on their vapor pressures and thermodynamic functions in the literature.

Saturation vapor pressures were determined by Knudsen's method, using the apparatus shown diagrammatically in Fig. 1. The principle of the apparatus and the method of measurement were similar to those described previously [3]. But the present apparatus differed from that described previously [3] in that it was possible to alter the condensing bells 14, without breaking the vacuum; after carrying out an experiment the cooling system 13 was raised by the lever 15, operated by an electromagnet. In this way it was possible to carry out 10 experiments at different temperatures without breaking the vacuum.

We synthetized Tl_2S and Tl_2O_3 for use in the experiments. For the synthesis of Tl_2S [4], redistilled thallium and the stoichiometrically equivalent amount of thrice-sublimed sulfur were sealed in an ampule, which was evacuated to a pressure of the order 10^{-5} mm Hg. The ampule was then heated slowly to 450-460° C and held at this temperature for a long time. The conversion of metallic thallium to Tl_2O_3 was carried out in a stream of oxygen at 200° C. As a "tracer" for thallium in the sublimate, we used the radioactive isotope Tl^{204}, with a half life of 2.71 years which emitted electrons with an energy of 0.765 Mev.

In the case of Tl_2S, both components were made radioactive (Tl^{204} and S^{35}, emitting electrons with an energy of 0.169 Mev), so that the experimental arrangement made it possible to obtain the saturation vapor pressures by means of both components. Measurements of intensity of emission were carried out with a type B instrument, using an end-window counter with a thin mica window. Calculation of the saturation vapor pressure was carried out using the formula

$$P = 17.14 \frac{I}{KAtI_0}\sqrt{\frac{T}{M}}$$

where I is the intensity of the condensed material (counts/minute); I_0 is the specific activity of the evaporated material (counts/minute · degree); K is the Clansins coefficient; A is the orifice area (cm^2); t is the time of exposure (seconds); T is the absolute temperature; M is the molecular weight of the substance in the vapor state.

Extrapolation of log P vs reciprocal of temperature plot of the experimental data to 760 mm Hg gave a value for the boiling point, considerably below that of Tl_2O_3. The boiling point of the sublimed material was close to that of Tl_2O. This was evidence for the transformation of Tl_2O_3 into Tl_2O, which has been noted in the literature [5]. The values of the vapor pressures were therefore recalculated for Tl_2O.

The results for the measurement of the vapor pressures of Tl_2O are shown in Fig. 2. The value of the heat of sublimation, calculated from the slope of the cuves was 30.21 kcal/degree · mole.

Treatment of the experimental data by the method of least squares led to the following relation between log P and temperature:

$$\log P\,(mm) = 11.51 - \frac{6612}{T}.$$

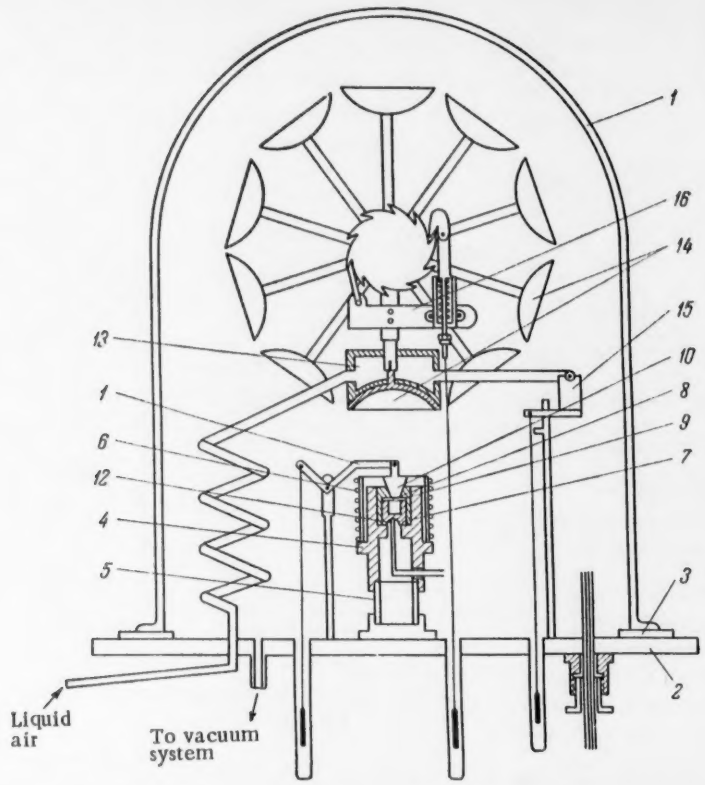

Fig. 1. Diagram of apparatus. 1) Glass bell jar; 2) iron plate; 3) rubber gasket; 4) source; 5) quartz tube; 6) furnace; 7) crucible; 8) platinum foil; 9) calibrated orifice; 10) cover; 11) lever; 12) thermocouple; 13) cooling system; 14) condensation bell; 15) lever for lifting cooling system; 16) mechanism for changing bells.

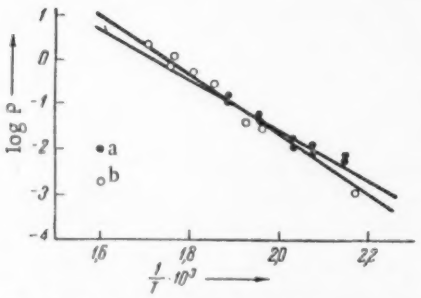

Fig. 2. Logarithms of the saturation vapor pressures of :
a) Tl_2S, and b) Tl_2O as functions of the reciprocal of the temperature.

Insertion of P = 760 mm in this equation gave T = 766°K, which agrees with the boiling point of Tl_2O given in [6]. The total intensity of emission from Tl_2S was measured with and without an Al filter. The intensities of emission of the components were then calculated as in [7]. This determination was possible because the energies of the electrons emitted by thallium and sulfur differ considerably.

The results of measurements of the vapor pressures of Tl_2S are shown in Fig. 2. The variation of log P with temperature for Tl_2S showed that the vapor pressures obtained with both components lay on the same straight line. This agreement showed that Tl_2S did not decompose on evaporation. The variation of log P with temperature could be expressed by the following equation:

$$\log P \text{ (mm)} = 7.354 - \frac{4484}{T} .$$

The sublimation energy was found to be 20.45 kcal/degree • mole.

The heats of sublimation of Tl_2S and of the components used in its preparation are very different. This suggests the possibility of purifying Tl_2S by vacuum sublimation.

In conclusion, the authors express their thanks to Corresponding Member of the Acad. Sci. Azerbaidzhan SSR G. B. Abdullaev for suggesting the subject and for his direction.

LITERATURE CITED

[1] B. T. Kolomnets, J. Tech. Phys. 17, 2 (1947).

[2] B. M. Gokhberg and M. S. Sominskii, J. Exp. Theor. Phys. 7, 9-10 (1937).

[3] A. A. Kuliev and M. G. Shakhtakhtinskii, Proc. Acad. Sci. USSR, 120, No. 6 (1958).*

[4] A. P. Obukhov and I. S. Bubyreva, Bull. Sect. Phys.-Chem. Anal. 19 (1929).

[5] B. V. Nekrasov, Course of General Chemistry (1953).**

[6] Selected Values of Chemical Thermodynamic Properties, Washington, 1952.

[7] V. I. Spitsyn and P. N. Kodochigov, et al., Methods of Working Using Radioactive Indicators, pub. Acad. Sci. USSR (1955).**

Institute of Physics and Mathematics of the
Academy of Sciences of the Azerbaidzhan SSR

Received July 21, 1958

*In Russian.

**Original Russian pagination. See C. B. Translation.

SPONTANEOUS THINNING OF THIN DOUBLE-SIDED LIQUID FILMS

A. Sheludko

(Presented by Academician A. N. Frumkin, July 26, 1958)

It is well known that two-sided liquid films usually thin themselves spontaneously under the influence of the suction pressure from their thickened and concave extremities. Our investigations [1, 2] of comparatively thick films, of thickness greater than 0.2 μ, showed that when the film had flat parallel sides the flow of solution from it was of the same form as that through a slit and was in accordance with the Reynolds relation:

$$\frac{d(1/h^2)}{dt} = \frac{2}{3\eta}\,\frac{b^2+c^2}{b^2c^2}\,P_0, \qquad (1)$$

where η is the viscosity of the solution, b and c are the semiaxes of an elliptical film, h is its thickness, t is the time of thinning and P_0 is the capillary pressure producing thinning. The solutions investigated contained 0.1 mole/liter of KCl to depress the Gouy diffuse electrical layers. In the absence of electrolyte or when there was very little of it, thinning was slowed to a standstill evidently because of electrical repulsions between the Gouy layers [3].

In the present paper we have investigated the spontaneous thinning of thinner two-sided liquid films for the range of thickness between 0.2 and 0.03 μ. The thickness of the film as a function of time was recorded automatically with a specially constructed interference microphotometer [2]. The investigation was carried out with microscopic ($\sim 2 \cdot 10^{-2}$ cm) two-sided liquid films of aniline with 0.5% of $C_{12}H_{25}OH$ as a foam stabilizer, and of water containing 0.1 mole/liter of KCl and 0.01% of stabilizer OP10 or 0.0056 mole/liter of sodium oleate. The stabilizer concentration was kept to a minimum (so that the film ruptured at a thickness of about 0.03 μ), to prevent the possibility of the film's properties being affected by adsorbed layers and to eliminate rheological changes during the thinning process.

Figure 1 shows the variation of film thickness with time in terms of the coordinates $\frac{1}{h^2} - \frac{1}{h_0^2}$, $t - t_0$ (where h_0 is the thickness at the moment of time t_0), for aniline and water (with OP10 and sodium oleate), respectively. The dotted lines correspond to Equation (1). The results showed that beginning approximately at a thickness of 0.1 μ, the rate of thinning increased from the value corresponding to Equation (1), and that the difference steadily grew larger in proportion to the thinning of the film.

We did not see any reason why the nature of the flow of solution out of the film as calculated by Equation (1), should alter for a thickness less than 0.1 μ. An estimate of the thinning attributable to evaporation caused by the difference in pressure and corresponding difference in vapor pressure between the film and its thickened extremities, showed that this did not play any part in the case of aniline and only a very minor one in the case of aqueous films. An estimate of the effect of diffusion of the surface-active stabilizer from the interior of the film to the surface on the rate of slip of the adsorbed layer showed that this factor was very small and also, could not explain the deviation of the rate of thinning from the value corresponding to Equation (1). Finally, the fact that we were observing an increase in the rate of flow out of thin films clearly excluded the effect of an increase in the rheological characteristics of the film, as, for instance, an increase in viscosity as compared with the bulk properties of the liquid.

These considerations led us to the view that the increased rate of thinning of thin double-sided liquid

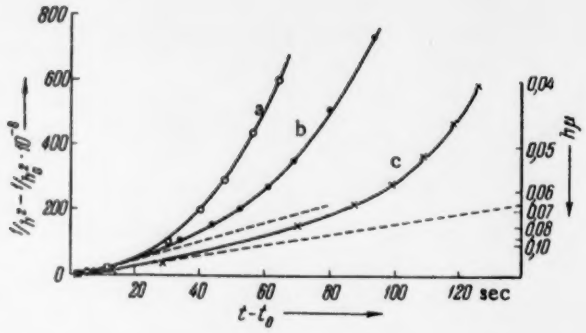

Fig. 1.

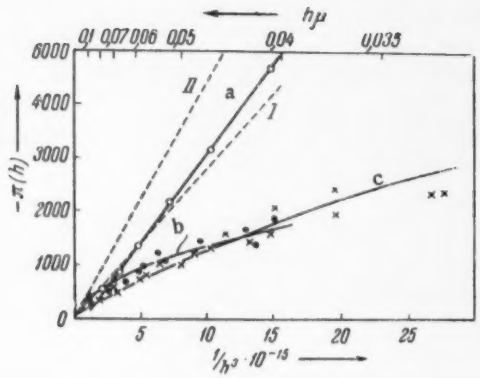

Fig. 2.

films, above that corresponding to (1), was due to the appearance of an additional pressure attributable to long-range intermolecular forces, i.e., according to Deriagin, a loosening pressure which is negative in the present case. According to Frenkel [4], an approximate calculation of this pressure, π, for a two-sided liquid film leads to the equation:

$$\pi = -\frac{4\sigma\delta^2}{h^3}, \qquad (2)$$

where σ is the surface tension of the liquid, and $\delta = \sqrt{\frac{v}{N_A}}$ (v is the molecular volume and N_A is Avogadro's number) is the molecular diameter. The third power of h in Equation (2) corresponds to a London intermolecular interaction. This law was used in the present case, since the thickness of a film was of the same order as λ, and particularly for approximate calculations, it was not yet necessary to take into account electromagnetic screening. It is clear from (2) that Frenkel's calculation corresponds to the sign of the observed effect.

If the additional negative pressure, $-\pi$, appears in the film, then it follows that P_0 in Equation (1) should be replaced by $P_0 - (-\pi)$, whence we obtain for $-\pi$:

$$-\pi = \frac{3\eta}{2}\frac{b^2c^2}{b^2+c^2}\frac{d(1/h^2)}{dt} - P_0, \qquad (3)$$

where $\frac{d(1/h^2)}{dt}$ for different values of h may be obtained by graphical differentiation of the experimental curves of Fig. 1 and P_0 can be determined in the form $2\sigma/R$ (where R is the radius of curvature of the concave edge of the film, in our case 0.2 cm, the radius of the tube in which the microscopic film was formed). The curves for $-\pi = f(h)$, obtained in this way, are shown in Fig. 2, with coordinates $-\pi$ and $1/h^3$, for the aniline and water (OP10 and sodium oleate) films, respectively. It is clear that for aniline (Fig. 2a), good agreement was obtained with the relation $-\pi \sim 1/h^3$. For different measurements the slope of this line varied within 10% of a mean value of $3.7 \cdot 10^{-13}$, close to the theoretical value calculated from Frenkel's Equation (2), of $4\sigma\delta^2 = 4.8 \cdot 10^{-13}$ ($\sigma = 43$ and $\delta = 5.3 \cdot 10^{-8}$ for aniline). For water (Fig. 2b, c) the curves of $-\pi = f(h)$ * did not

* In view of the large variations, curves b and c for aqueous films were drawn on the basis of a number of measurements.

agree with the theoretical curves (the dotted lines in Fig. 2, I and II for OP10 and sodium oleate). The values obtained for $-\pi$ were below the theoretical and with thinning of the film clearly increased more slowly than $-\pi \sim 1/h^3$.

All the measurements were made at room temperature (20°). The values of surface tension and viscosity used were determined in the normal way. The dimensions of the films (the semiaxes b and c) were determined photographically.

LITERATURE CITED

[1] A. Sheludko, G. Desimirov and K. Nikolov, Sofia Univ. Herald, 49, No. 2, 127 (1954-1955).

[2] A. Sheludko, Koll. Zs. 155, 39 (1957).

[3] B. V. Deriagin and A. S. Titievskaia, Coll. J. 15, No. 6, 416 (1953).*

[4] Ia. I. Frenkel, Kinetic Theory of Liquids, Moscow (1945), p. 305 [in Russian].

Institute of Physical Chemistry
of the Sofia State University, Sofia
Bulgaria

Received June 26, 1958

* In Russian.

MISSING PAGES ARE INDEX PAGES
WHICH HAVE BEEN PHOTOGRAPHED
AT THE BEGINNING OF THE VOLUME(S)